1-2022

Functional role of PPAL and potential for moss in industrial applications.

Susana Perez Martinez
University of Louisville

Recommended Citation

FUNCTIONAL ROLE OF PPAL AND POTENTIAL FOR MOSS IN INDUSTRIAL
APPLICATIONS

By

Susana Perez Martinez

M.Sc., Biology, University of Louisville, 2019

B.A., Biology, University of Louisville, 2017

A Dissertation

Submitted to the Faculty of the

College of Arts and Sciences of the University of Louisville in

Partial Fulfillment of the Requirements for the Degree of

Doctor of Philosophy in Biology

Department of Biology

Division of Molecular, Cellular and Developmental Biology

University of Louisville

Louisville, Kentucky

May 2022

FUNCTIONAL ROLE OF PPAL AND POTENTIAL FOR MOSS IN INDUSTRIAL
APPLICATIONS

By

Susana Perez Martinez

M.Sc., Biology, University of Louisville, 2019

B.A., Biology, University of Louisville, 2017

A Dissertation Approved on

April 25th, 2022

By the following Dissertation Committee:

_____

Dr. Mark P. Running, Principal Advisor

_____

Dr. Michael H. Perlin

_____

Dr. Lisa L. Sandell

_____

Dr. David J. Schultz

_____

Dr. Dae-Sung. Hwangbo

ACKNOWLEDGMENTS

I am also thankful to Dr. Sarah Emery and Dr. Perri Eason for their indispensable help, support, and encouragement, including acceptance into the program, orientation, answers to all my questions and concerns, for nominating me for the McSweeny Fellowship (which I am grateful to have been awarded), for their advice throughout the program, for graduation formalities and deadlines, among others. I want to thank Doris Meadows and Terri Norris for their immense kindness, support, and help with order requisitions, handling grant funds, package labeling and shipments, traveling, hiring process, and helping figure out any problems.

A special thanks goes to my dearest and beloved husband Luis. There are no words to express my gratitude to you, my love. You have been there for me through my achievements and failures. Your motivation, support, encouragement, love, admiration, honesty, and positive criticism has been the foundation I needed to become a better person and to achieve my career goals for us and our family. Thank you for being my rock and inspiration. Another special thanks go to my beloved parents Maria and Antonio. They have been my role models and the best parents you could hope and wish for. Being an adolescent at 16 years old and coming to this country with my parents from Cuba was a tremendous challenge. By itself been an adolescent is insufferable even when you are around your family and friends, living in your native country, speaking your native language and accustomed to your culture.

Imagine that all the sudden everything changes, and now you find yourself in a new everything: country, language, culture, no friends, or acquaintances. All I really had when I came to this country was my parents and their exceptional support and unconditional love. We faced multiple obstacles together and no matter the circumstances

they were always there for me. Therefore, although I love science and research, I truly chose to do a PhD to follow my parents' footsteps and to make them proud. This was the best way I found to honor them, because not every person successful in their country-of-origin leaves everything that they have achieved behind, to give their children a better life. I am eternally grateful for their love and courage. I also want to thank my wonderful brother Juan Pablo and his fantastic wife Yanara, for their infinite love, encouragement, and support.

DEDICATION

This work is dedicated to my beautiful family:

My extraordinary husband, my exceptional parents, amazing brother and sister-in-law.

ABSTRACT

FUNCTIONAL ROLE OF PPAL AND POTENTIAL FOR MOSS IN INDUSTRIAL
APPLICATIONS

Susana Perez Martinez

April 25th, 2022

This dissertation is an examination and characterization of the functional roles of PPAL. *PROTEIN PRENYLTRANSFERASE ALPHA SUBUNIT-LIKE* (*PPAL*) is a recently discovered gene. *PPAL* homologs are present in all plants and many animals, where its function is largely unknown. It is possible that PPAL could participate in prenylation processes since it shares similarity to the α subunits of known prenylation enzymes. Prenylation is a post-translational modification of proteins that involves the addition of a lipid moiety to proteins to facilitate membrane targeting and association and promote protein-protein interactions. Prenylation has important roles in plant growth and development, including cell elongation, cell differentiation, and cell identity determination.

In moss there are two *PPAL* homologs, *PpPPAL1* and *PpPPAL2*, and the disruption of either results in lethality. To study the functional role of PpPPAL, we used targeted gene knockdown through artificial miRNA followed by genotypic and developmental studies in *Physcomitrium patens*. First, we found that PpPPAL has roles in cell differentiation, cell expansion, polar cell elongation, organization of the cytoskeleton, and response to hormones and external stimuli. Plant growth and development must be continuously adjusted to respond to available resources. The ability to sense the

resources require the integration of signals conveying the plant metabolic status, its growth and developmental stage, and hormonal balance. Sugar sensing and signaling is vital to integrate internal regulators and environmental cues to govern and sustain plant growth and survival.

We studied the ability of PpPPAL to sense and respond to external stimuli. We showed that PpPPAL is a potential glucose sensor and/or regulator in the plant glucose signaling network as well as a potential overall energy sensor. Environmental concerns surrounding the overuse of natural gas and petroleum, the excessive greenhouse gas (GHG) emission, and global warming has led to the search for sustainable bioenergy sources, such as biomass feedstock, for creating profitable biorefineries and facilitating bioeconomy. We characterized and proposed the moss *Physcomitrium (Physcometrilla) patens* as a potential biomass feedstock for biofuel production. These studies help elucidate some of the functional roles of PpPPAL in plant biology and development and suggest ways to use moss biomass in the emerging economy.

TABLE OF CONTENTS

LIST OF TABLES

LIST OF FIGURES

MANUSCRIPT 1 FIGURES:

INTRODUCTION

The evolution of early plants included the development of multicellularity, which resulted in differentiated cell types, and facilitated the transition of plants from water to land by permitting the production of specific tissues and structures that have specialized roles in nutrient uptake, anchoring, spreading, reproduction and photosynthesis (Antimisiaris & Running, 2014; Galichet & Gruissem, 2003; Kramer, 2009; Maurer-Stroh et al., 2003; Thole et al., 2014). The vegetative growth cycle of the moss *Physcomitrium patens* serves as a model for the understanding of how early land plants utilized differentiated cell types for specialized roles (Cove, 2005; Cove et al., 2006; Decker et al., 2006; Rensing et al., 2020; Thole et al., 2014).

P. patens has become a powerful model system in plant molecular genetics as it allows for a high frequency of homologous recombination, which makes gene targeting possible (Cove et al., 2006; Decker et al., 2006; Nishiyama et al., 2003; Rensing et al., 2020; Schaefer, 2002; Schaefer & Zryd, 1997; Schumaker & Dietrich, 1997; Thole et al., 2014). The germination of *P. patens* spores leads to the formation of protonema, filamentous rows of cells that elongate solely by polar tip growth of the apical cell (Menand, Calder, et al., 2007; Menand, Yi, et al., 2007; Pressel et al., 2008). Chloronema and caulonema are the two types of protonemal cells. Chloronema are rich in chloroplasts, possess a relatively slow growth, and is the first cell type present following spore germination or from regeneration from protoplasts. Caulonema cells are the result of a transition from select chloronemal apical cells, divide and grow quickly (facilitating

colonization and spreading), contain fewer chloroplasts and cytologically resemble root hairs and pollen tubes of Angiosperms (Cove et al., 2006; Decker et al., 2006; Jang & Dolan, 2011; Pressel et al., 2008; Prigge et al., 2010; Rensing et al., 2020; Thole et al., 2014).

Plants, like other eukaryotes, must coordinate nutrient availability with metabolism and growth functions. Plant growth and development are driven by the intricate interaction between energy availability, environmental cues, genetic programs, phytohormones, and the cross talk between actin and tubulin cytoskeleton (Jaeger & Moody, 2021; Sheen, 2014; Thelander et al., 2018; Thelander et al., 2005; Thole et al., 2014), which makes the sensing, signaling, and response to these programs crucial for the function of both individual cells and the organisms (Rolland et al., 2006).

The three master metabolic sensors and regulators are hexokinase, TOR complex kinase and the plant Snf1-related kinase (SnRK1) (Baena-Gonzalez et al., 2007; Claeyssen & Rivoal, 2007; Granot et al., 2013; Jang et al., 1997; Kim et al., 2013; Lastdrager et al., 2014; Nilsson et al., 2011; Roth, Westcott, et al., 2019; Sheen, 2014; Thelander et al., 2004; Tsai & Gazzarrini, 2014; Wurzinger et al., 2018; Xiao et al., 2000; Xiong et al., 2013). Glucose occupies a central role in plant metabolism by acting as a metabolic substrate, a signaling molecule, and inducing biological changes at all levels of cellular activity (Jang & Sheen, 1994; Li & Sheen, 2016; Rolland et al., 2006; Sakr et al., 2018). The glucose signaling network modulates the regulatory mechanisms and functions of the three master regulators, to induce biological changes from transcription and translation to protein stability and activity (Jang et al., 1997; Kushwah & Laxmi, 2014; Moore et al., 2003;

Nilsson et al., 2011; Olsson et al., 2003; Sheen, 2014; Thelander et al., 2004; Tsai & Gazzarrini, 2014; Wurzinger et al., 2018; Xiao et al., 2000; Xiong et al., 2013).

Post-translational modifications are critical for the regulation, intracellular targeting, localization, and functional activation of biological macromolecules, such as proteins. A common modification is prenylation, the addition of a lipid moiety to proteins to facilitate membrane targeting and association and promote protein-protein interactions. Prenylation has important roles in growth and development. including cell elongation, cell differentiation, and cell identity determination (Antimisiaris & Running, 2014; Charng et al., 2014; Galichet & Gruissem, 2003; Maurer-Stroh et al., 2003; McTaggart, 2006; Nguyen et al., 2010; Palsuledesai & Distefano, 2015; Pereira-Leal et al., 2001; Running, 2014; Thole et al., 2014).

Protein prenylation is conserved among eukaryotes and involves the transfer of a 20-carbon geranylgeranyl or a 15-carbon farnesyl moiety to one or two cysteines near the C-terminus of target proteins. The known enzymes responsible for carrying out prenylation are protein farnesyltransferase (PFT), protein geranylgeranyltransferase-I (PGGT), and Rab geranylgeranyltransferase (Rab-GGT, also called Geranylgeranyl transferase-II). PGGT and PFT share a common α subunit but have distantly related β subunits. Rab-GGT α and β subunits share only 20-30% similarity to the PGGT/PFT α and β subunits respectively.

These enzymes are essential for the prenylation of a vast variety of vital signaling proteins (Antimisiaris & Running, 2014; Charng et al., 2014; Galichet & Gruissem, 2003; Maurer-Stroh et al., 2003; McTaggart, 2006; Nguyen et al., 2010; Palsuledesai & Distefano, 2015; Pereira-Leal et al., 2001; Running, 2014; Thole et al., 2014). While

studying the components involved in the prenylation process, we came across an additional gene that contains prenyltransferase α-subunit repeats. We named this gene *PROTEIN PRENYLTRANSFERASE ALPHA SUBUNIT-LIKE (PPAL)* (Thole et al., 2014). *PPAL* homologs are present in plants, mammals, and other animals, where their function is largely unknown, and they have not been identified in fungi (Thole et al., 2014).

   PPAL shares weak similarity with the α subunits of the prenylation enzymes and binds specifically to one of the *Arabidopsis* Rab-GGT β-subunits (Thole et al., 2014). Most animals and plants, like *Arabidopsis*, harbor either zero or one copy of the *PPAL* gene; interestingly, the moss *P. patens* contains two copies of the *PPAL* gene, *PPAL1* and *PPAL2* (Thole et al., 2014). The knockout or complete loss of the *PPAL* gene in *Arabidopsis* produce viable mutants with various growth and developmental defects. However, in *P. patens* the loss of either of the two *PPAL* homologs is lethal, suggesting that they are both essential for survival (Thole et al., 2014).

   In my thesis, we investigate the biological, developmental, and metabolic function of PPAL in the moss *P. patens.* Gene knockdown approaches were used to study the functional role of PPAL, followed by phenotypic, genotypic, growth, metabolic, and development studies. The hypothesis we are working with is that at least some of the roles of *PPAL* are conserved among plants, although it is possible to find both similarities and differences (Thole et al., 2014). Because of the role we found for PPAL in carbohydrate metabolism and energy sensing, we initiated an investigation of the biochemical composition of moss, finding that it has many potential significant advantages as a biofuel feedstock. This research has implications in genetics and biology as well as application in the industry specifically using moss for biofuel production.

MANUSCRIPT 1

THE BIOLOGICAL AND DEVELOPMENTAL ROLES OF PPAL IN THE MOSS

PHYSCOMITRIUM PATENS

1. INTRODUCTION

Post-translational modifications are critical for the regulation, intracellular targeting, localization, and functional activation of biological macromolecules, such as proteins. A common modification is prenylation, the addition of a lipid moiety to proteins to facilitate membrane targeting and association and promote protein-protein interactions. Prenylation involves the transfer of a 20-carbon geranylgeranyl or a 15-carbon farnesyl moiety to one or two cysteines near the C-terminus of target protein (Galichet & Gruissem, 2003; Maurer-Stroh et al., 2003; Thole et al., 2014). The known enzymes responsible for carrying out prenylation include protein farnesyltransferase (PFT), protein geranylgeranyltransferase-I (PGGT), and Rab geranylgeranyltransferase (Rab-GGT, also called Geranylgeranyl transferase-II). The three heterodimeric enzymes contain both α and β subunits. PGGT and FPFT share a common α subunit but have distantly related β subunits, which have approximately 35% sequence identity at the amino acid level (Leung et al., 2006; Maurer-Stroh et al., 2003; McTaggart, 2006; Thole et al., 2014). Also, Rab-GGT α and β subunits share only 20-30% similarity to the PGGT/PFT α and β subunits, respectively (Leung et al., 2006; Thole et al., 2014). These enzymes are essential for the

5

prenylation of a vast variety of vital signaling proteins, including most members of the Ras superfamily of small GTPases, some classes of protein kinases, Rab GTPases (CC/C*X*C or CAAX motifs), a family of Ras-related small GTPases, and heterotrimeric G protein subunits, among others (Leung et al., 2006; McTaggart, 2006; Nguyen et al., 2010; Thole et al., 2014).

Prenylation of eukaryotic proteins allows for the proper activity and localization of various proteins that have vital functions in development and regulation (Palsuledesai & Distefano, 2015; Ramazi & Zahiri, 2021). The process of prenylation is highly conserved among eukaryotes, indicating the evolutionary and biological importance of this lipid modification pathway (Galichet & Gruissem, 2003; Palsuledesai & Distefano, 2015; Thole et al., 2014). Studies on *Arabidopsis thaliana* and the moss *Physcomitrium paten*s (*P. patens*) have demonstrated that prenylation has major roles in plant growth and development, including polar cell elongation, cell differentiation, and cell identity determination (Antimisiaris & Running, 2014; Running, 2014; Thole et al., 2014). Our lab has identified an additional gene that contains prenyltransferase α-subunit repeats. We named this gene *Protein Prenyltransferase Alpha subunit-like (PPAL)* (Thole et al., 2014). *PPAL* homologs are present in plants, mammals, and other animals where their function is largely unknown, and they have not been identified in fungi (Thole et al., 2014). Known protein prenyltransferases are all cytosolic proteins, and sequence analysis of PPAL protein showed that there are no specific motifs for any subcellular organelle or membrane targeting (Thole et al., 2014). In addition, the construct expressing the green fluorescent protein-tagged *PPAL* (GFP-*PPAL*) was detected in both cytosol and nucleus, suggesting that PPAL is a cytosolic protein (data not shown).

PPAL shares weak similarity with PGGT/PFT α subunit (28%) as well as similarity with the two Rab-GGT α subunits *RGTA1* (25%) and *RGTA2* (28%) at the amino acid level. PPAL has also been shown to bind specifically to one of the *Arabidopsis* Rab-GGT β-subunits (Thole et al., 2014). In addition, the *Drosophila melanogaster PPAL* homolog, Tempura, has been shown to be a Rab-GGT α subunit involved in Notch signaling by promoting the prenylation of Rab11 and Rab1 (Charng et al., 2014). Most animals and plants, like *Arabidopsis*, harbor either no or only one copy of the *PPAL* gene; interestingly, the moss *P. patens* contains two copies of the *PPAL* gene, *PPAL1* and *PPAL2* (Thole et al., 2014). PPAL knockouts in *Arabidopsis* are gametophytic lethal and partial loss of function mutant results in extremely slow seedling growth, anther dehiscence defects, delayed cell separation processes in flower organ abscission, hypersensitivity to glucose and ABA treatment, and increased carbohydrate accumulation (data not shown). However, in *P. patens* the loss of either of the two *PPAL* homologs is lethal (Thole et al., 2014). One explanation could be that *PPAL1* and *PPAL2* have diverged in function, both becoming essential for survival, or that both homologs have the same function and are required at such a high level that the loss of one homolog kills the moss.

The moss *Physcomitrium patens* has become a powerful model system in plant molecular genetics as it allows for a high frequency of homologous recombination, which makes gene targeting possible (Nishiyama et al., 2003; Schaefer, 2002; Thole et al., 2014). The germination of *P. patens* spores leads to the formation of protonema, filamentous rows of cells that elongate solely by polar tip growth of the apical cell. Chloronema and caulonema are the two types of protonemal cells. Chloronema are rich in chloroplasts, possess a relatively slow growth, and is the first cell type present following spore

germination or from regeneration from protoplasts (Menand, Calder, et al., 2007; Menand, Yi, et al., 2007; Pressel et al., 2008). Caulonema cells are the result of a transition from select chloronemal apical cells, divide and grow quickly (facilitating colonization and spreading), contain fewer chloroplasts, and cytologically resemble root hairs and pollen tubes of angiosperms (Menand, Calder, et al., 2007; Pressel et al., 2008; Thole et al., 2014). Like higher plants, growth and development in *P. patens* is regulated by phytohormones including auxin and cytokinin, environmental factors such as the quantity and quality of light, and the cross talk between actin and tubulin cytoskeleton (Cove et al., 2006; Decker et al., 2006). Here, we investigate the biological and developmental function of *PPAL* in the moss *P. patens.* To study the functional role of *PPAL*, we implemented gene knockdown approaches followed by genotypic and developmental studies. It is crucial to study the functional role of *PPAL* homologs in *P. patens* to learn about their biological and developmental function and to see if some of the roles of *PPAL* are conserved among plants.

2. MATERIALS AND METHODS

2.1 Plant Materials and Growth Conditions

Normal growth conditions of P. patens

Protonemal tissue of wild type and *Ppppa*l mutants in the wild type background were subcultured using a Polytron homogenizer T20B.S1 (IKA) and grown on BCDAT medium (https://moss.nibb.ac.jp/protocol.html) with cellophane for 5 days. Knockdown mutant lines were then grown in both 1μM Beta Estradiol/DMSO/BCDAT inducible medium and DMSO/BCDAT control medium for 7 days. Plants were grown at 25°C under continuous light at 50 μmol m^{-2} s^{-1} intensity.

Arabidopsis growth conditions

Arabidopsis wild type (Col-0), loss of function mutant *ppal-1* in the Col-0 background, and *ppal-1* and Col-0 lines transformed with *PpPPAL* genes from *P. patens* were planted in Sungro Horticulture propagation mix soil (Premium Horticultural Supply, Louisville, KY, cat no.5232601). The propagation mix soil was presoaked overnight in gnatrol (WDG organic BTI fungus gnat control, eBay) and then seeds were sowed the next day. All trays were stratified at 4⁰C for 5 days and then moved to the growth chamber at 22 ⁰C, with 60-70% relative humidity (RH) and light intensity 90 μmol m-2 s-1 with continuous light. Plants were watered and fertilized as needed. *ppal-1* (Salk_045793) was obtained from the *Arabidopsis* Biological Research Center (http://www.biosci.ohio-state.edu/~plantbio/Facilities/abrc/index.html).

2.2 Phenotypic Analysis of Protonemata

For hormone morphological studies, small pieces of fresh protonemal tissue (approximately 2 mm in diameter) were inoculated on BCDAT plates without cellophane, with different additives 1-Naphthaleneacetic acid synthetic auxin (NAA) and 6-Benzylaminopurine synthetic cytokinin (BAP). For colony growth assays, representative 18-day old colonies were photographed using a dissecting microscope with a 20w LED fiber optic dual gooseneck lights microscope illuminator and the diameters of four independent colonies were measured. In the caulonemal filament induction assay, the numbers of caulonemal filaments clearly protruding from the edge of an 18-day old colony were counted using a dissecting microscope. Moss colonies grown under these standard conditions have a closely connected edge in the wild type, and even more so in the *Ppppal* mutants. This made it possible to define a filament extending beyond the rim of the colony as a protruding filament. Such protruding filaments were counted for four colonies in each case.

2.3 Hormone Treatment in *P. patens*

Knockdown mutants in the wild type background and wild type moss were grown in normal growth conditions for 5 days. Samples were then treated with 1 μM, 10 μM, and 100 μM of auxin (NAA) and cytokinin (BAP) hormones for 18 days. Mutants were transferred to both 1 μM Beta Estradiol/DMSO/BCDAT inducible medium and DMSO/BCDAT control medium with the different concentration of hormones. Wild type was grown on BCDAT with the different concentration of hormones. Plants were grown at 25°C under continuous light at 50 μmol m^{-2} s^{-1} intensity.

2.4 Genotyping of *Arabidopsis* PPAL-1

Salk T-DNA mutant and wild type lines were obtained [Colombia (Col-0)], Salk_045793 (*ppal-1*) from the *Arabidopsis* Biological Resource Center (ABRC). *ppal-1* genotyping primer sequences LBa1, RP and LP were obtained from the SALK website (http://signal.salk.edu/tdnaprimers.2.html) and are listed in Table 1. Wild type with no insertion gives a product around 1100 bps (amplifying the fragment from LP to RP). *ppal-1* homozygous lines with insertion in both chromosomes amplified a band 910 bps (LBa1+RP) and for *ppal-1* heterozygous lines with one of the chromosomes with insertion, both bands of 1100 and 910 bps were amplified. LP +RP was best amplified at 60⁰C and LBa1+RP at 58⁰C.

2.5 Transformation

Transformation of *Physcomitrium* was done by Polyethylene glycol-mediated transformation of protoplast performed following standard procedures (https://moss.nibb.ac.jp/protocol.html). Briefly, moss protoplasts were mixed with linearized plasmid DNA, MMM solution, PEG solution and heat shocked at 45°C for 5 min followed by incubation at 20 °C for 10 min. 8 % mannitol was used to wash the protoplasts, which were then mixed with PRM/T and spread onto PRM/B medium to regenerate for 10 days. Regenerated plants were transferred onto BCDAT selection medium with 100 µg/l zeocin (Alfa Aesar) or 30 µg/l hygromycin (Invitrogen). The selection lasted 10 days and was followed by a 7-day release period on BCDAT without antibiotic. Then a second selection was conducted after the release. Plants surviving the second round of selection were screened by fluorescence microscopy or PCR. Transformation of *Arabidopsis* followed Agrobacterium-mediated transformation using the floral dip method (Zhang et al., 2006).

2.6 Plasmid Construction

The design of amiRNAs followed (Khraiwesh et al., 2010). All primer sequences are listed in Table 1. Ideal amiRNA sequences targeting *PpPPAL1, Pp PPAL2 and PPAL1,2* genes were identified using Web MicroRNA Designer (http://wmd3.weigelworld.org/). The amiRNA sequences were obtained by using plasmid pRS300 containing the (*Arabidopsis thaliana* miR319a precursor) which served as a template to amplify each amiRNA fragment through site directed mutagenesis using PCR. The resultant PCR fragment was cloned into pENTR/D-TOPO (Invitrogen, K240020) and introduced into the destination vector PGX8 to construct PGX8-PpPPAL-amiRNA plasmids by the LR reaction using LR clonase II (Invitrogen, 11791020). To construct the vector for expressing YFP-AtRabA4d in *Physcomitrium*, YFP-AtRabA4d was amplified by PCR using 35S:eYFP-AtRabA4d (a gift from Dr. E. Nielsen) as a template. The PCR fragment was then cloned into pENTR/D-TOPO and introduced into pT1OG12 destination vector to construct T1OG-YFP-AtRabA4d by LR reaction. The pMDC32 plasmid was ordered from ABRC (CD3-738, donor Mark Curtis and Ueli Grossniklaus). *PpPPAL1* and *PpPPAL2* CDS were amplified and cloned into pENTR/D-TOPO and introduced into pMDC32 destination vector to construct pMDC32-PpPPAL by LR reaction. The Lifeact-mEGFP probe in the PTZ-UBI overexpression plasmid (a gift from Dr. M. Bezanilla) were used to study the cytoskeleton in moss.

2.7 RNA Extraction and Quantification

qPCR analysis of *Ppppal* knockdown mutants' expression was achieved by growing homogenized *Ppppal* mutants on BCDAT supplemented with 1 μM β-estradiol and wild type in BCDAT for 7 days. 100 mg of tissue was ground in liquid nitrogen, total RNA was extracted with the RNeasy plant mini kit (Qiagen, 74904) and treated with RNase-free DNase

I (Qiagen, 79254) to remove genomic DNA. ImProm-II Reverse Transcription System (Promega, A3800) was used to reverse transcribe 0.5 µg of total RNA in a 20-µL RT first-strand synthesis reaction that contained oligo(dT) primers. 2µl from 10 ng cDNA template was used in a 20 µl reaction using BlasTaq™ 2X qPCR MasterMix (Cat. G891) on the BioRad® CFX96. The PCR conditions were as follows: 95°C for 5 min, followed by 35 cycles of 95°C for 30 sec and 60°C for 45sec, and ending with a melting curve analysis. The PCR and the average CQ values were calculated. A relative normalization Bar chart was produced normalized to UBQ10 (internal control) and WT set to 1.

2.8 Gel Electrophoresis and Visualization of PCR Product

All PCR products were run for 30 mins at 157 V using 1.2% agarose gel with 2 µl of loading dye in 0.5X TBE buffer. The gel was stained using ethidium bromide with a working concentration of 0.625 mg/ml and visualized under a UV transilluminator.

2.9 Immunostaining

Immunostaining was performed by growing homogenized *Ppppal* mutants on BCDAT supplemented with 1 µM β-estradiol and wild type in BCDAT for 7 days. The procedure for immunostaining (Sato et al., 2001) was slightly modified. Briefly, protonemata samples were fixed in PME (100 mM PIPES, 5 mM EGTA, and 2 mM MgSO4, pH 6.8) with 1% (v/v) DMSO, 0.01% (v/v) Nonidet P-40 and 8% (w/v) paraformaldehyde for 1 h. After three washings in PME supplemented with 0.01% (v/v) Nonidet P-40 (PMEN0.01), protonemata were attached to polyethylene-imine-coated cover glasses. The attached protonemata were treated with an enzyme solution containing 0.4 M mannitol, 2% (w/v) driselase and 1× proteinase inhibitor (Complete Mini EDTA-free; Roche Diagnostics) for 10 min.

Protonemata were soaked in cold methanol for 10 min at –20°C after washing with PMEN0.01 three times. After three rinses with PMEN0.01, protonemata were treated for 10 min with 0.05% (w/v) BSA and 0.05% (v/v) Triton X-100 for further permeabilization. The protonemata were incubated with anti-α-tubulin monoclonal antibody (Ab-1; Oncogene Research Products) diluted 100-fold in PBS overnight at 4°C. After three rinses in PBS, protonemata were treated with Alexa Fluor 488 rabbit anti-mouse IgG (Invitrogen) for 3 h at 37°C. An additional two rinses in PBS were followed by staining with 0.2 mg/L DAPI for 10 min. Samples were visualized with an epifluorescence microscope equipped with DAPI, 488 nm (FITC), and 547 nm (TRITC).

2.10 Phototropic Analysis

To examine the differential cell elongation exhibited by protonemata in response to directional blue light, protoplast samples were suspended in PRM/T, poured onto a 9-cm Petri dish containing PRM/B medium overlaid with cellophane and incubated at 25˚C for 3 days under continuous polarized white light (60 µmolm-2sec-1). A fluorescent light (lamp: FL20SD) through a red plastic plate (Shinkolite A, #102; Mitsubishi Rayon Co., Tokyo) was used as a red-light source. Plants were imaged using a Nikon TE200 microscope equipped with a DS-U3 camera according to protocol (https://moss.nibb.ac.jp/protocol.html).

2.11 Gravitropic Response of Caulonemata

Mutants and wild type protonemata were inoculated on agar plates and cultured for 2 weeks under normal light conditions. Then the plates were placed at the bottom of a light-tight box and wrapped with aluminum foil to completely exclude light. The box was placed vertically

and cultured for 3 weeks. Samples were imaged using a Nikon TE200 microscope equipped with a DS-U3 camera according to protocol (https://moss.nibb.ac.jp/protocol.html).

2.12 Actin Microscopy

Lifeact- mEGFP probe was imaged using an epifluorescence microscope. 488 nm (FITC) laser illumination was used for excitation of Lifeact-GFP. Emission filters were 525/50 nm for GFP.

2.13 Calcofluor White Microscopy

Calcofluor white (Sigma, 18909-100ML-F) was filter sterilized with a 0.22 μm filter and stored at 4°C before use. About 3 mm diameter of a colony of samples protonemal tissue were mixed with 10 μl of the sterilized calcofluor white for 2 min. A Nikon TE200 microscope equipped with a DS-U3 camera with the 418 nm laser.

3. RESULTS

3.1. Utilizing artificial microRNA (amiRNA) for conditional knockdown in *P. patens*

To study the functional role of *PPAL* in moss, we used an inducible knockdown system combining the advantage of artificial miRNA (amiRNA) and inducible expression method using the XVE system (Khraiwesh et al., 2010; Zuo et al., 2000). β-Estradiol treatment activates the XVE transcriptional factor, which binds to the LexA operator and recruits RNA Pol II to the CaMV m35S promotor to induce the transcription of the downstream gene, in this case the amiRNA construct targeting *PPAL* homologs. The amiRNAs regulate the expression of *PpPPAL1* and *PpPPAL2* through mRNA degradation. Effects of artificially constructed miRNA on knocking down a target gene have been examined in *Physcomitrium* and *Arabidopsis* (Khraiwesh et al., 2008; Schwab et al., 2005). Six amiRNAs were designed to knockdown the expression of the *PPAL* homologs in *P.patens*: two targeting *PPAL1*, two targeting *PPAL2*, and two targeting both *PPAL1* and *PPAL2* (Supplementary material: Fig. S1). Microscopy and gene expression studies were used to select the most severe knockdown lines.

3.2 Quantifying gene expression levels in the knockdown lines

Gene expression levels of knockdown lines were analyzed with real time-PCR. Wild type moss was grown in BCDAT medium, and the mutants were grown in both the inducible medium (β-Estradiol /DMSO/ BCDAT) and in control (DMSO/BCDAT) medium. A relative normalization Bar chart was produced normalized to UBQ10 (internal

control) and WT set to 1. The data show that all three knockdown mutants' gene expression is downregulated compared to both control and wild type (Figure 1). The ami*Ppppal2* construct shows the most downregulation, the ami*Ppppal1* construct leads to slightly less downregulation than the ami*Ppppal2* construct, and ami*Ppppal1,2* is the construct that causes the least downregulation (Figure 1).

Significant ($P < 0.01$) differences in expression levels between the controls and the knockdown lines were observed. The ami*Ppppal1,2* construct was significantly ($P < 0.01$) less downregulated than the ami*Ppppal1* and ami*Ppppal2* constructs. An explanation could be that, since the knockout of either *PPAL1* or *PPAL2* genes in moss is lethal, the downregulation of both genes cannot be at levels that are too low. We could expect *PpPPAL1* and *PpPPAL2* genes to function similarly and or to have some overlapping functions and others that are different. Viable *Ppppal1*, *Ppppal2*, and *Ppppal1,2* knockdown mutants were used for phenotypic and developmental studies in moss.
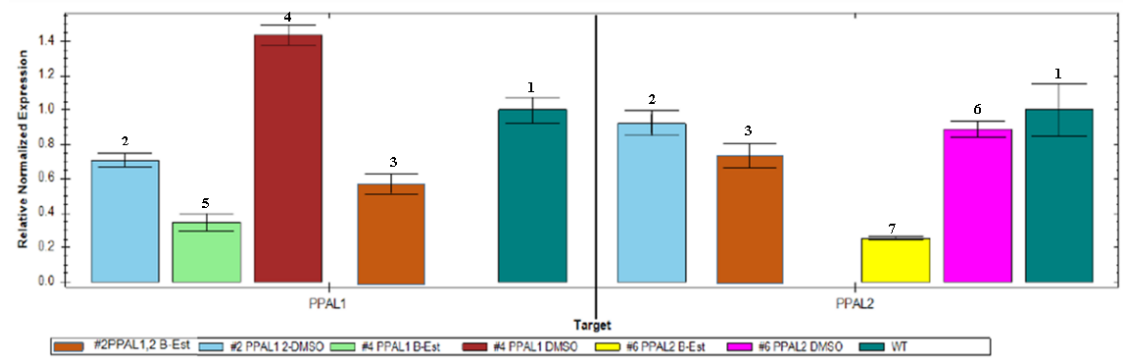
Figure 1. Gene expression results - Bar Chart Data (Normalized to UBQ10 and WT set to 1). The chart shows the gene expression for *PPAL1* (Left) and *PPAL2* (Right) gene

targets. The left shows, wild type (1) grown on BCDAT and *Ppppal1,2* (2) and *Ppppal1* (4) knockdown lines grown on DMSO control medium. Also on the left side, *Ppppal1,2* *(*3) and *Ppppal1* (5) knockdown lines grown on β-Estradiol inducible medium. On the right there is wild type (1) grown on BCDAT and *Ppppal 1,2* (2) and *Ppppal2* (6) knockdown lines grown on DMSO control medium. Also on the right, *Ppppal1,2* (3) and *Ppppal2* (7) knockdown lines grown on β-Estradiol inducible medium. Error bars indicate standard errors of the mean. The significances of the observed differences between samples were tested using a two-tailed two-sample *t*-test assuming unequal variances.

3.3 Microscopic analysis of mutant morphological properties

We used light microscopy to analyze the knockdown mutants' protonemata phenotype (Figures 4 and 3B), and a dissecting microscope was utilized to study colony growth and development (Figures 2 and 3A). The amount of caulonemal filaments protruding the colony edge was counted for 4 colonies per sample. We found that knockdown mutants exhibited inhibition of both caulonema cell formation, with less than 26 caulonema filaments formed on average, and bud development, with less than 5 gametophores formed on average (Figures 2 and 3A). Thus, mutants display a smaller colony diameter, always below 8 mm, compared to wild type, always above 15 mm (Figures 2 and 3A). Wild type also formed an average of 100 caulonemal filaments (Figures 2 and 3A). Significant ($P < 0.01$) differences in caulonema formation, gametophore number, and colony growth were observed between wild type and the mutants (Figure 3A). In addition, significant differences ($P < 0.01$) in caulomema formation were observed between *Ppppal1,2* and *Ppppal1*, and *Ppppal1,2* and *Ppppal2* mutants (Figure 3A).

Ppppal1 and *Ppppal2* mutants also showed significant (P <0.05) differences in caulomema formation (Figure 3A). Significant differences (P <0.05) in gametophore number were found between *Ppppal1,2* and *Ppppal1*, and *Ppppal1,2* and *Ppppal2* mutants (Figure 3A).

We quantified an average of 100 protonema filaments from 4 colonies per sample. In *Ppppal* mutants, an average of 24 protonema filaments showed misdirection of growth, an average of 37 protonema cell tips are curved instead of straight, and all filaments exhibited reduced expansion of apical cell tip growth (Figures 3B and 4). In mutants, an average of 55 protonemata cells exhibited swelling at the apical and subapical tip with an average of 27 cells forming extra tips (Figures 3B and 4). In wild type an average of 2 protonema filaments exhibited curved tips and misdirection of growth, no filaments were found showing protonema tip swelling nor formation of extra tips (Figures 3B and 4). Significant (P <0.01) differences were observed in protonemata growth and developmental defects between wild type and mutants (Figure 3B). *Ppppal 2* and *Ppppal 1,2* mutants also showed *s*ignificant (P <0.01) differences in protonemata growth and developmental defects (Figure 3B). In addition, significant (P <0.01) differences in the number of curved tips, extra tip formation, and tip swelling in protonemata were observed between *Ppppal 2* and *Ppppal 1* mutants (Figure 3B). Significant (P <0.05) differences in misdirection of growth were found between *Ppppal 2* and *Ppppal 1* mutants (Figure 3B).

Calcofluor-white (CFW) fluorescent blue dye and a fluorescent microscope were utilized to observe cell expansion of mutants through cell wall labeling (Figure 5). Wild type protonemata develop through filamentous tip growth, with the growing point localized to the tip region of apical cells. Cell expansion only occurs at the tip of apical cells and branching apical cells (Wu & Bezanilla, 2018). However, knockdown mutants exhibit

uncoordinated cell expansion, forming truncated cells defective in tip growth and cell polarity (Figure 5). Cell expansion is controlled by various factors including hormones, like auxin and cytokinin, and changes to cytoskeleton organization (Decker et al., 2006; Wu & Bezanilla, 2018). The above phenotypic changes were observed in all three mutants with a difference in degree of inhibition and morphological changes. The ami*Ppppal2* construct exhibited the most severe phenotypic changes, followed by the ami*Ppppal1* construct; the ami*Ppppal1,2* construct phenotypic changes were less severe. Based on the phenotypic characterization, it appears that both that actin and tubulin cytoskeleton as well as certain responses to hormones may be affected in the mutants.

Figure 2. *Ppppal* knockdown mutants' colony morphology. (A) Wild type, *Ppppal1,2* (B), *Ppppal1* (C), and *Ppppal2* (D). Wild type shows elongated caulonema cells protruding the colony. Wild type colony size is very large compared to the mutants and multiple gametophores are formed. Mutants displayed inhibition of growth, as shown by small colony diameter, and reduced formation of both caulonema cells and gametophores. (E) Zoomed-in pictures of mutants show similar colony diameter, with almost no caulonema and gametophore formation. Scale: 4 mm.
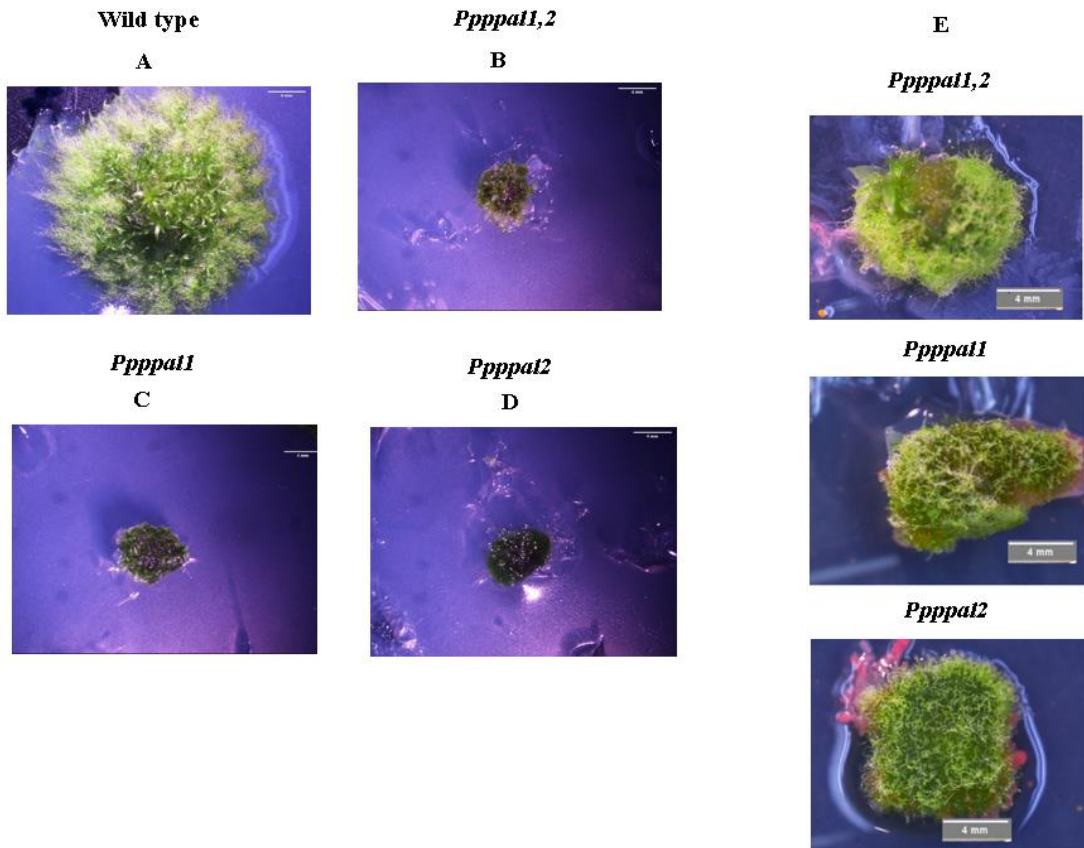
Figure 3. Quantification of wild type and *Ppppal* mutants' growth and development. Samples were grown on BCDAT/1μMB-Estradiol medium for 18 days. (A) Quantification of colony diameter, the number of protruding caulonemal filaments per colony, and gametophore formation. Quantification of the number of protonemata growth and developmental defects (B). The histograms show the average ±SEM of four colonies, error bars indicate standard errors of the mean. The significances of the observed differences between samples were tested using a two-tailed two-sample *t*-test assuming unequal variances.

A
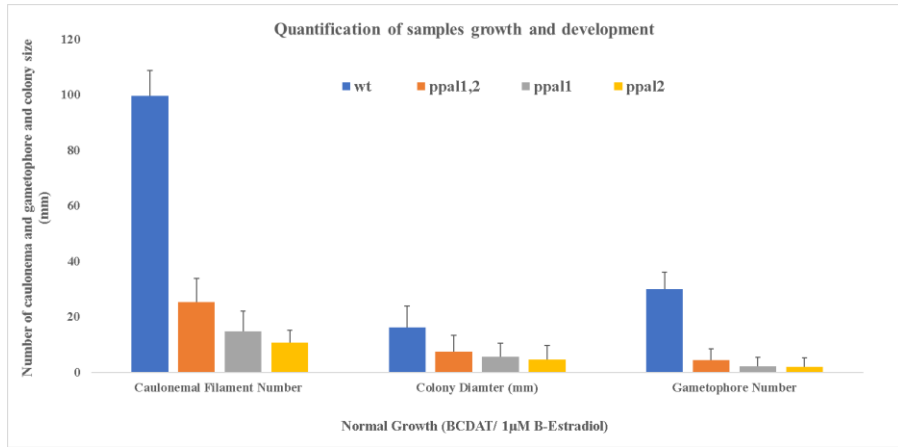
B
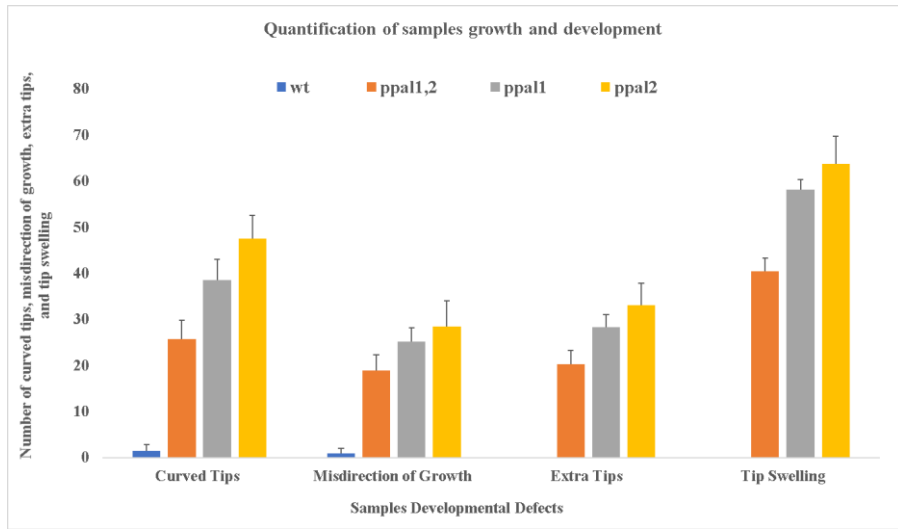
Figure 4. Phenotype of mutants' protonemata. Below are representative protonemata for mutants and wild type. In contrast to wild type (A) and (B), *Ppppal* mutants exhibited reduced filamentous growth and expansion (C, D, E and F), apical and subapical cell tip swelling (C), curving of cell tips (D), formation of extra tips (E), and misdirection of tip growth (F). These phenotypic changes were observed in all three mutants with a difference in degree of inhibition and morphological changes, *Ppppal2* mutant showed the highest inhibition followed by *Ppppal1* and *Pppal1,2*. Scale: 50 μm (A and B) and 10 μm (C-F).
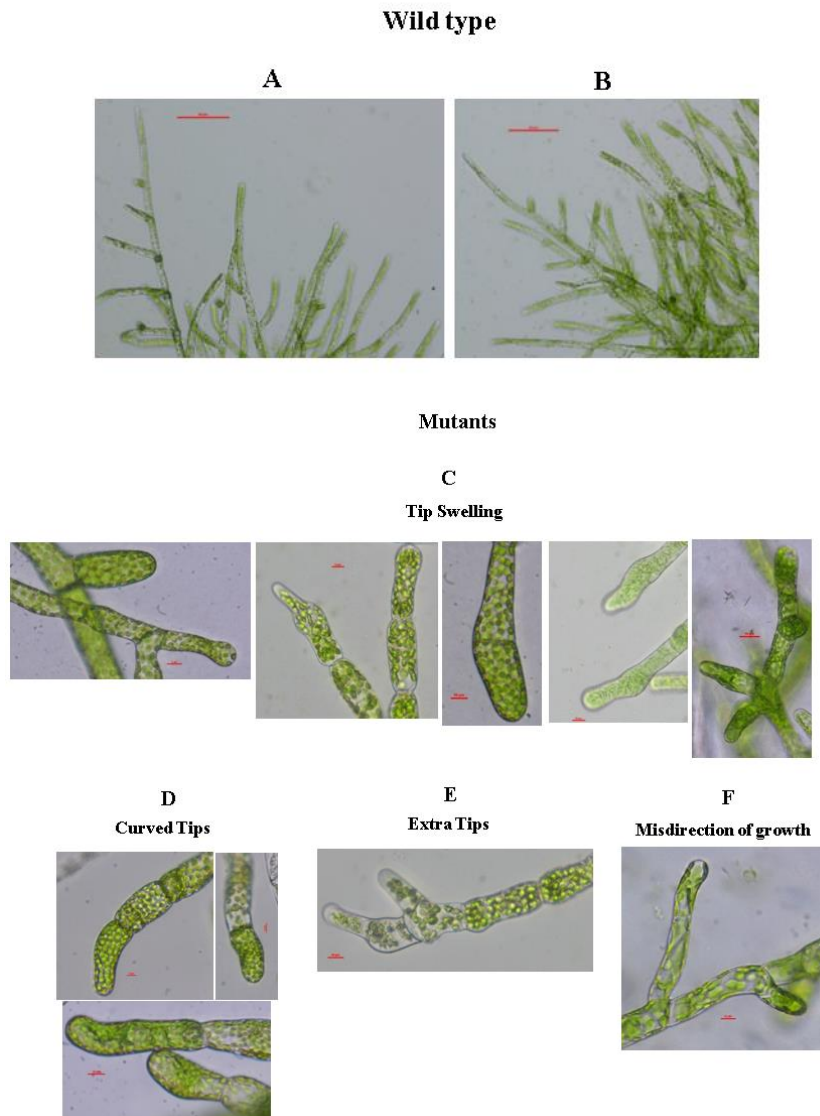
Figure 5. Knockdown mutants cell expansion. (A) Cell wall staining with calcofluor shows normal cell expansion and polarized cell growth in wild type (Illustrated by arrows). (B) *Ppppal* mutants show inhibition of polarized cell growth and uncoordinated cell expansion with growing points localized at cross cell walls and peripheral regions (Illustrated by arrows and circle). Scale: 50 μm and 10 μm.

(A)
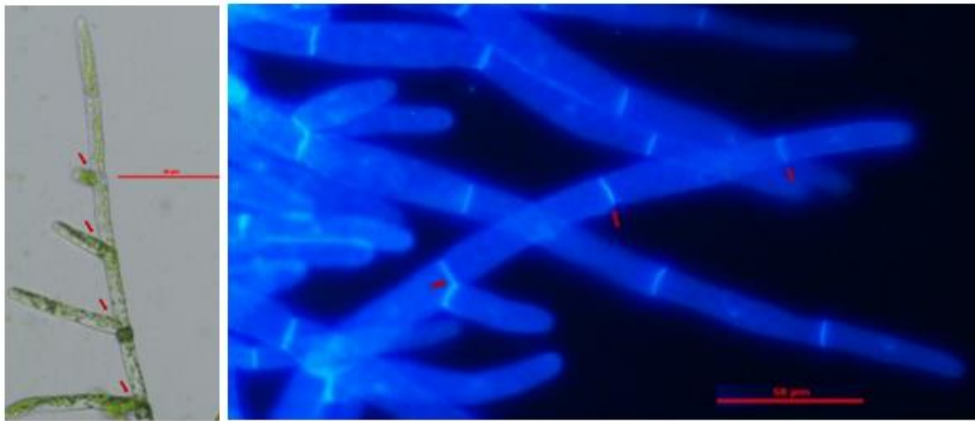
(B)
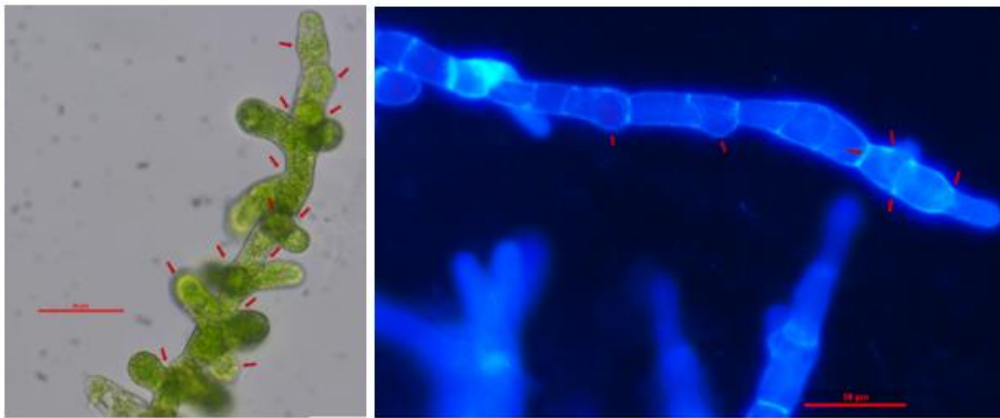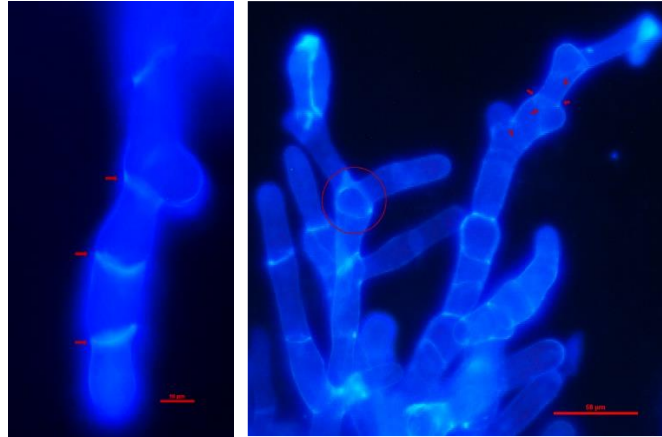
3.4 Complementation experiment with *Arabidopsis* and moss

To investigate conservation of PPAL gene function in the plant kingdom, a complementation experiment with *Arabidopsis* and *Physcomitrium* was implemented. *Arabidopsis ppal* knockouts are gametophytic lethal and *ppal* partial loss of function mutant (*Atppal-1*) phenotype included extremely slow seedling growth, anther dehiscence defects, and delayed cell separation processes in flower organ abscission (data not shown). *Atppal-1* mutant was transformed with both *PPAL1* and *PPAL2* wild type genes from moss to see if one or both *PPAL* homologs from moss can rescue the *Arabidopsis ppal-1* mutant phenotype. The pMDC32 destination vector for constitutive (CaMV 35s promoter gateway system) gene expression in plants was utilized. The vector has been used with other genes and had no effect on its own on growth or development (Curtis & Grossniklaus, 2003).

CDS of *PPAL1* and *PPAL2* from wild type moss were amplified and the genes were cloned into pENTR vector and subcloned into pMDC32. pMDC32 containing either *PPAL1* or *PPAL2* was used to transform Arabidopsis through Agrobacterium-mediated transformation using the floral dip method. Both *PpPPAL1* and *PpPPAL2* from *Physcomitrium* recovered the *Arabidopsis ppal-1* partial loss of function mutant phenotype, further confirming PPAL function in plants (data shown in the supplemental material, Fig. S4).

3.5 *Ppppal* mutants and wild type response to auxin (NAA) treatment

Auxin has a central role in mediating developmental decisions and environmental responses in plants. Studies on the effects of auxin on moss growth and development, especially the stimulatory effect of auxin on the chloronema to caulonema transition and bud induction for gametophore development, suggest that the core auxin machinery could be conserved among plants (Prigge et al., 2010; Rensing et al., 2008; Thelander et al., 2018). Mutants and wild type were treated with increasing 1-Naphthaleneacetic acid (NAA) amounts of 1 μM, 10 μM and 100 μM. The effects of auxin are dose dependent. Production of caulonemata is increased by higher concentration of auxin. Also, as auxin concentration increases, inhibition of chloronemata growth increases, resulting in a reduction in colony size (Thelander et al., 2018).

At 100 μM NAA was when inhibition of chloronemata growth and the induction of chloronema to caulonema transition and bud development was most apparent in wild type (Figures 6 and 7). The mutants' phenotype stayed the same at NAA concentrations of 1 μM and 10 μM. However, the mutants' colony diameter decreased to less than 5 mm

when grown in 100 µM NAA (Figure 6 and 7). In addition, the amount of caulonemal filaments protruding the colony was reduced to less than 7 and no gametophores formed when grown in 100 µM of NAA (Figure 6 and 7). Significant differences (P <0.01) in caulonema formation, colony growth, and gametophore number were observed between wild type and mutants in NAA (Figure 7). These results suggest that the stimulatory effects of auxin on the chloronema to caulonema transition and bud development are blocked in the mutants. But the mutants do appear to respond to NAA in some ways, as treated mutants showed increased growth inhibition, resulting in reduced colony diameter.

Figure 6. Auxin treatment of wild type and *Ppppal* mutants. Wild type colony (A) and protonema cell (B). Wild type responded normally to NAA treatment as shown by induction of caulonema filaments and gametophore formation and inhibition of chloronemata growth. *Ppppal1*,2 colony (C) and protonema cell (D). *Ppppal1* colony (E) and protonema cell (F). *Ppppal2* colony (G) and protonema cell (H). Mutants were insensitive to NAA induction of chloronema to caulonema transition and bud induction but seemed to respond to NAA inhibition of chloronemata growth. Scale: (colony) 4 mm and (protonema cell) 100 μm.
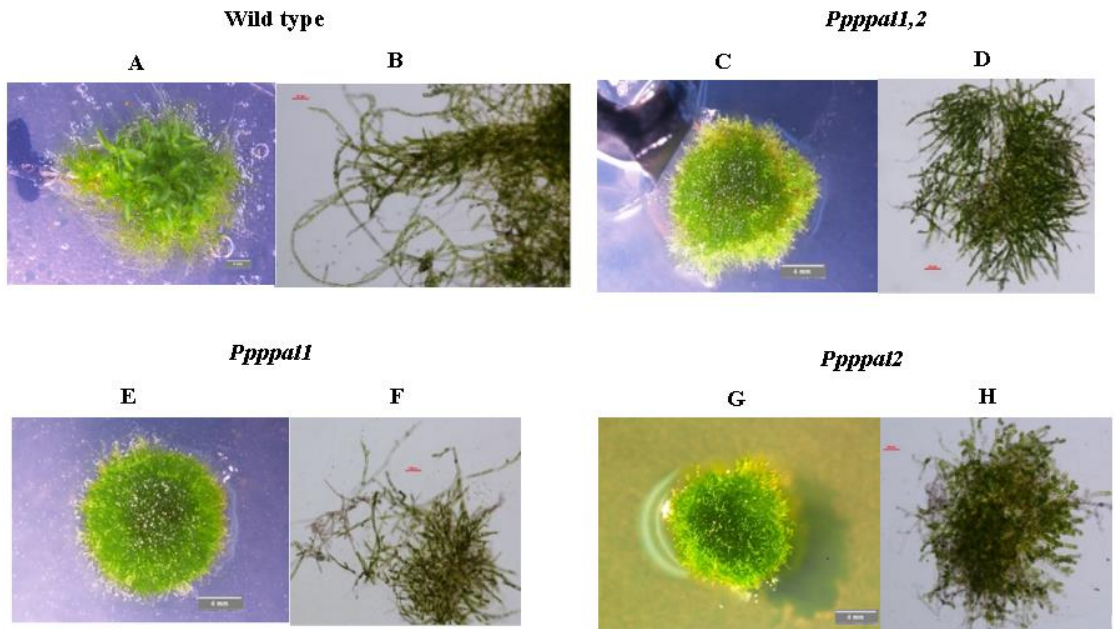
Figure 7. Quantification of caulonema formation and colony growth. Wild type and *Ppppal* mutant colonies were grown in induction medium normal growth conditions or induction medium supplemented with 100 µM NAA for 18 days. The number of protruding caulonemal filaments per colony, the number of gametophores, and colony diameter of samples in millimeters was quantified. The histograms show the average ±SEM of four colonies, error bars indicate standard errors of the mean. The significances of the observed differences between samples were tested using a two-tailed two-sample *t*-test assuming unequal variances.
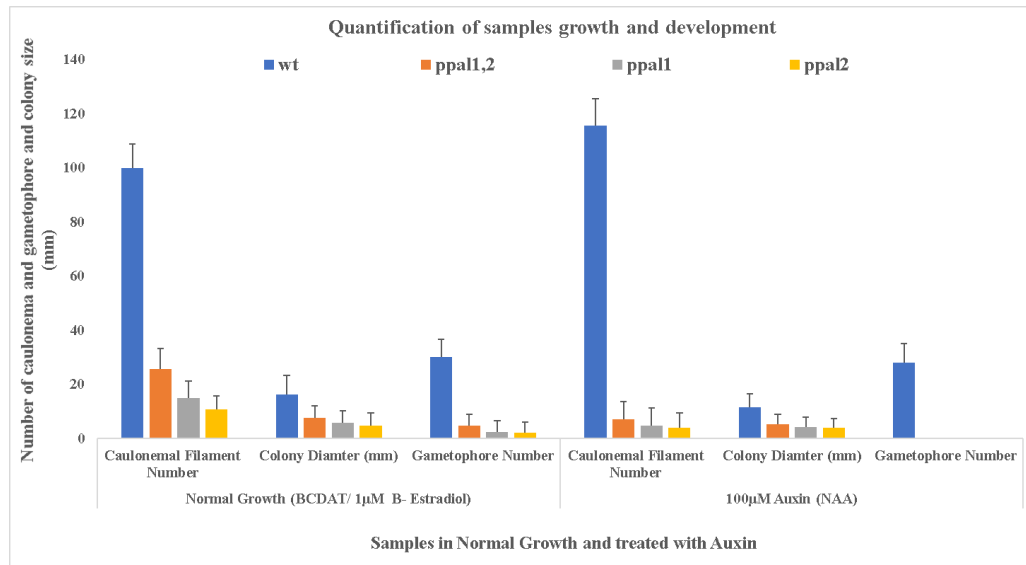
3.6 Response of *Ppppal* mutants to cytokinin (BAP) treatment

Cytokinin plays important roles as a growth-regulating compound in plants (Ashton et al., 1979; Hutchison & Kieber, 2002; Kieber, 2002). Cytokinin inhibits growth and development by suppressing both the formation of chloronemata, particularly secondary chloronemata, and of caulonemata (Ashton et al., 1979; Hutchison & Kieber, 2002; Kieber, 2002). Wild type and mutants responded to the growth inhibition induced by BAP, as shown by highly reduced colony diameter of less than 4mm and inhibition of caulonema filament formation (Figure 7). BAP treatment in wild type also induced the formation of callus and clusters of bud-like cells (Figure 8). The inhibitory effects of BAP in both wild type and mutants increased with increased concentration (1 μM, 50 μM, and 100 μM) with the highest inhibition at 100 μM BAP. Mutants, however, showed fewer bud-like cells and less callus formation, and a greener coloration compared to wild type even at 100 μM BAP (Figure 8).

Ppppal1,2 mutant developed some buds and callus formation but much less compared to wild type. *Ppppal2* and *Ppppal1* mutants are less responsive to the inhibitory effects of BAP compared to the *Ppppal1,2* mutant, as shown by fewer bud-like cells and no callus formation (Figure 8). Significant differences in bud-like cell formation ($P <0.01$) were observed between wild type and mutants (Figure 8 I). *Ppppal1,2* and *Ppppal1* mutants showed significant differences ($P <0.01$) in bud-like cell formation (Figure 8 I). *Ppppal1,2* and *Ppppal2* mutants also showed significant differences ($P <0.01$) in bud-like cell formation (Figure 8 I). Moreover, significant differences ($P <0.05$) in bud-like cell formation were found between *Ppppal1* and *Ppppal2* mutants (Figure 8 I). It seems that mutants respond to BAP inhibition of growth but are less sensitive to BAP induction of

clusters of bud-like cells and callus formation even at high concentrations compared to wild type.

Figure 8. Cytokinin treated mutants and wild type. Samples were grown in induction medium supplemented with 100 μM of BAP for 18 days. Wild type colony (A) and protonema cell (B) show that wild type is more sensitive to BAP treatment as shown by increased bud-like cells and callus formation. *Ppppal1,2* colony (C) and protonema cell (D). *Ppppal1* colony (E) and protonema cell (F). *Ppppal2* colony (G) and protonema cell (H). mutants responded to BAP growth inhibition but were less sensitive to the other effects of BAP. (I) Quantification of the number of bud-like cells formation. The histogram shows the average ±SEM of four colonies, error bars indicate standard errors of the mean. Scale: (colonies) 2 mm and (protonema cells) 100 μm. The significances of the observed differences between samples were tested using a two-tailed two-sample *t*-test assuming unequal variances.
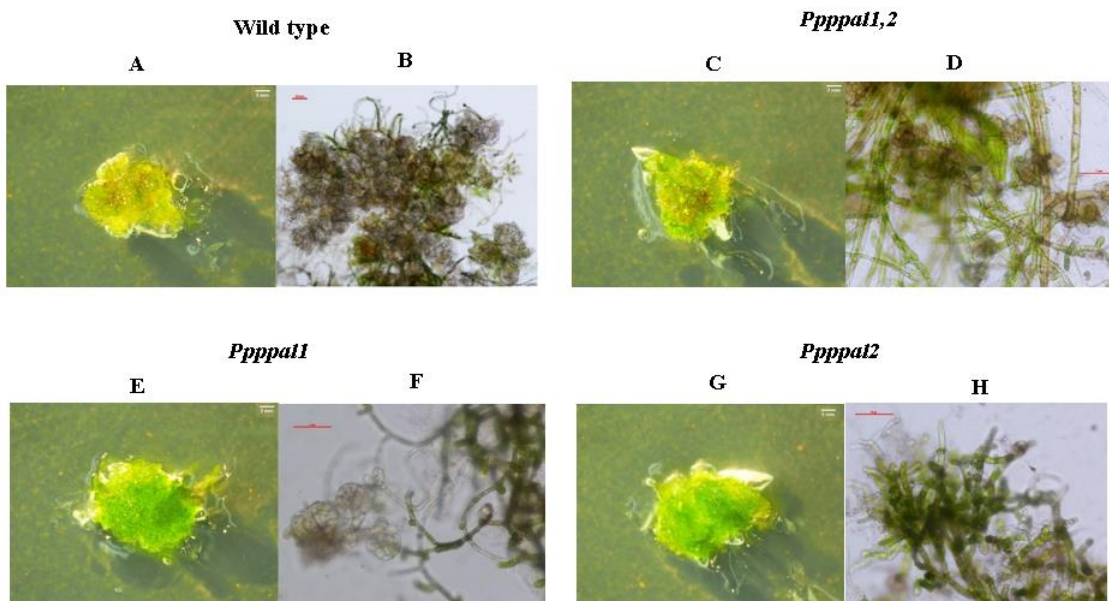
(I)
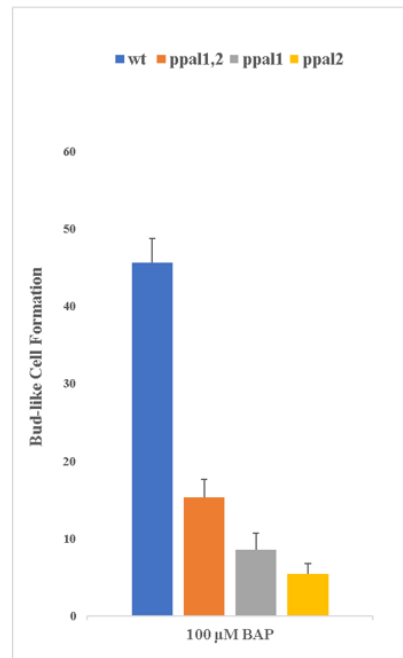
3.7 Phototropic and gravitropic response in mutants and wild type

Phototropism is a growth movement induced by a light stimulus, and the direction of growth is related to the direction of the incident light; the cells can either grow towards the light or away from it (Bao et al., 2015, 2019). In *P. patens*, at low light intensities chloronema filaments exhibit positive phototropism; that is, they grow towards the light. The response of caulonemal cells can be somewhat complex, as there are filaments that grow toward and others that can grow away from the light; however, at low light intensities the majority grow away from light. Intermediate light intensities induce a positive response in most filaments, and under strong light negative phototropism dominates. Moss filaments grow in a negatively gravitropic fashion, for example, upward when grown in dark. Phototropism dominates in the light, masking the gravitropic response (Bao et al., 2015, 2019; Jenkins et al., 1986). Phototropic protonemata growth is mediated by phytochrome

and occurs under unilateral red light. To study phototropic response in mutants and wild type, a fluorescent light through a red plastic plate was used as a red-light source (Bao et al., 2015, 2019; Jenkins et al., 1986). Both wild type and mutants displayed positive phototropism, growth towards a light source (Figure 9 B, D, F, H, and I).

For gravitropic response measurements, protonemata of mutants and wild type were grown two weeks under normal light conditions. After two weeks, the plates were placed on the bottom of a light-tight box wrapped with aluminum foil to completely exclude light. The box was placed vertically and protonemata was grown for three weeks. Negative gravitropism, growth against the force of gravity (upwards), was observed in both mutants and wild type (Figure 9 A, C, E, G, and I). Although mutants have fewer and less elongated caulonema cells and generally a smaller colony size compared to both wild type and DMSO/BCDAT control (Figure 9), the mutants showed normal phototropic and gravitropic responses when compared to wild type. In the phototropic response, *Ppppal1,2* mutant showed more inhibition of growth and much fewer caulonemal cells than *Ppppal1* and *Ppppal2* mutants (Figure 9 D, F, H, and I). For gravitropism *Ppppal1,2* and *Ppppal1* mutants showed more inhibition and less caulonemal formation than *Ppppal2* (Figure 9 C, E, G, and I). Significant differences ($P < 0.01$) in caulonema formation for both gravitropism and phototropism were observed between wild type and mutants (Figure 9 I). Also, significant differences ($P < 0.05$) in colony growth during gravitropism were observed between wild type and mutants (Figure 9 I). The components needed for processing of light cues to derive proper adaptive phototropic and gravitropic responses appear to not be affected in the knockdown mutants.

Figure 9. Gravitropic and Phototrophic response in wild type and mutants. All samples showed normal gravitropic and phototrophic response. However, the samples differed in the formation and elongation of caulonemata and colony size. For both gravitropic (A, C, E, G, and I) and phototrophic (B, D, F, H, and I) responses wild type formed large amounts of very elongated caulonema filaments compared to mutants. *Ppppal1,2* gravitropic (C) and phototrophic (D) response. *Ppppal1* gravitropic (E) and phototrophic (F) response. *Ppppal2* gravitropic (G) and phototrophic (H) response. Mutants exhibited reduced caulonema filaments formation that were very short. Both *Ppppal1,2* and *Ppppal1* mutants formed fewer caulonema filaments than *Ppppal2*. (I) Quantification of caulonemal filament number and colony size. The histograms show the average ±SEM of four colonies, error bars indicate standard errors of the mean. The significances of the observed differences between samples were tested using a two-tailed two-sample *t*-test assuming unequal variances. Scale 50 μm.
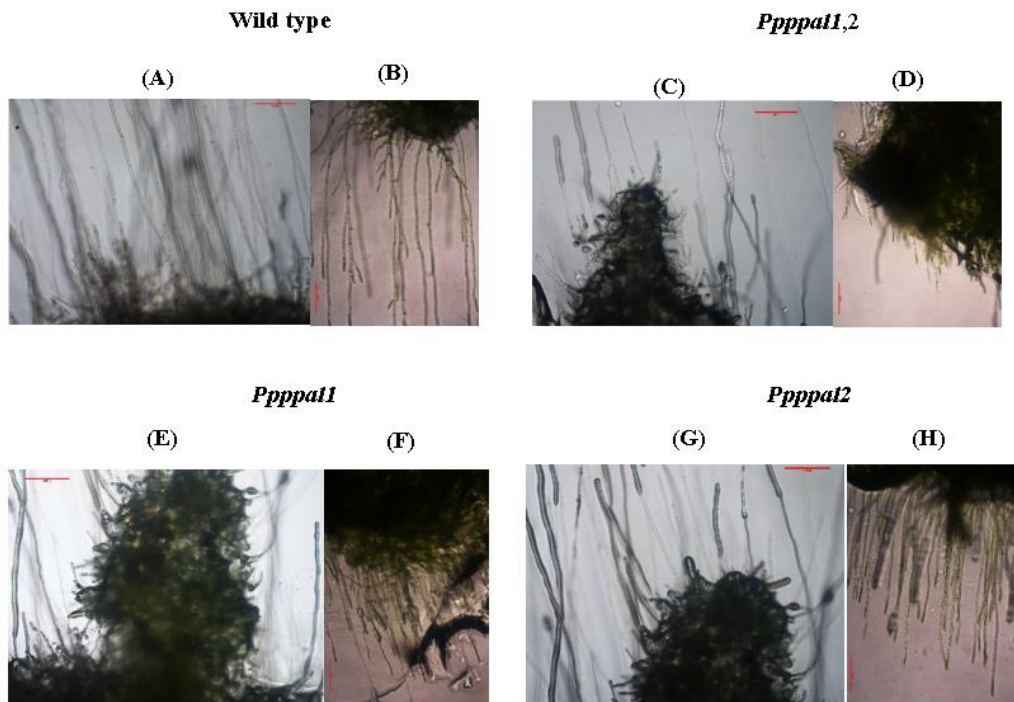
(I)
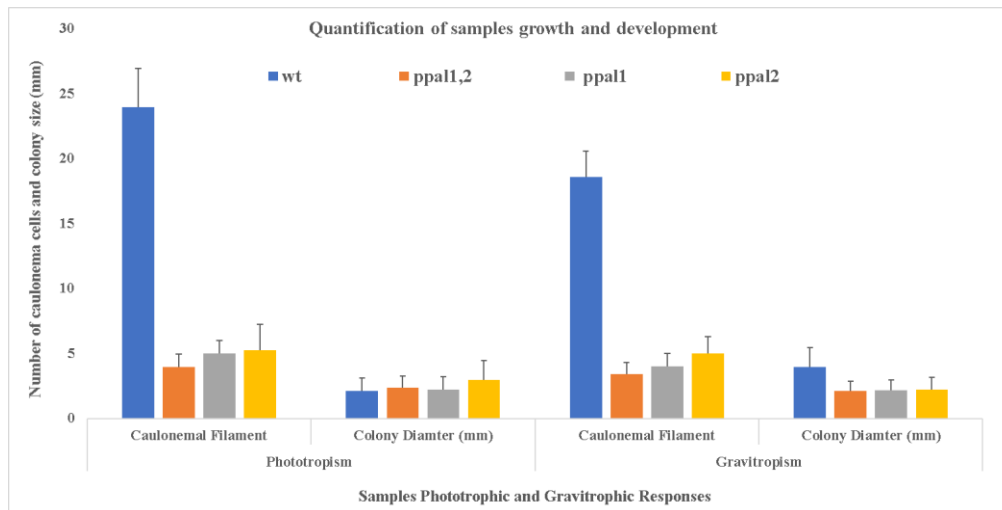
3.8 Tubulin and actin cytoskeleton analysis in mutants and wild type

The actin and microtubule cytoskeletons are crucial for various cellular processes. In plants, actin is required for cell expansion in tip growing cells, and microtubules are needed to guide the orientation of cell expansion (Wu & Bezanilla, 2018). In *Physcomitium,* the actin cluster near the cell apex dictates the direction of rapid cell expansion. The formation of the actin cluster is dependent on microtubule convergence near the cell tip. The coordination between both networks results in persistent polarized growth (Wu & Bezanilla, 2018). Phenotypic analysis of the protonemata in the knockdown mutants revealed misdirection of filamentous growth, swelling at the cell tips, formation of extra tips, and cell tips with curved shapes (Figure 3 B and 4). These phenotypic changes are often induced by disruption in microtubule assembly and organization, which also perturbs the actin cytoskeleton. To analyze the architecture and organization of the

cytoskeleton in the *Ppppal* mutants and wild type, live imagining and immunostaining approaches were utilized.

For live imaging, zeocin-resistant lines expressing Lifeact-mEGFP were generated using the overexpression vector pTZUBI::Lifeact-mEGFP (Vidali, Rounds, et al., 2009; Wu & Bezanilla, 2014). The vector contains the maize ubiquitin promoter used for transient overexpression or for generating a stable line, targeting a redundant copy of the ARPC3 gene in *Physcomitrium* (Vidali, Rounds, et al., 2009; Wu & Bezanilla, 2014*)*. The Lifeact-mEGFP probe does not affect the dynamics of actin and robustly labels actin microfilaments specifically in the cell apex (Figure 10 C). In moss Lifeact-mEGFP also labels filamentous actin structures in other cell types, including cells of the gametophore (Vidali, Rounds, et al., 2009). Another probe used for live imaging is the pT10G-YFP-RabA4d construct. RabA4d is a Ras-related protein responsible for intracellular vesicle trafficking, protein transport, and regulation of tip growth. YFP-RabA4d protein localizes specifically at the tip of the apical cell in *P. patens* protonemata, showing growth points of the apical cells (Figure 10 A) (Szumlanski & Nielsen, 2009). The pT10G-YFP-RabA4d vector allows for constitutive expression using the 35S promoter from the plant pathogen Cauliflower Mosaic Virus (CaMV), targeting a redundant copy of the PTA1 gene in *P. patens*. Lastly, immunostaining of protonemata was done using the anti-α-tubulin monoclonal antibody to bind tubulin and the rabbit anti-mouse IgG secondary antibody for visualization (Sato et al., 2001).

Figure 10. Wild type and knockdown mutants expressing YFP-RabA4d and GFP-Lifeact, and immunostaining of microtubules. (A) Shows wild type expressing and accumulating RabA4D at the cell apex. Mutants exhibited scattered expression and accumulation of RabA4d in places other than at the cell apex (B). (C) Wild type expressing Lifeact shows the accumulation of apical actin filaments at the cell apex to create the actin cluster. Mutants showed disruption in apical actin cluster formation (D). Yellow arrows point to an actin cluster forming (C). Green arrows show waves of actin bundles migrating and accumulating throughout the cell body (D). White arrows show abnormal apical actin accumulation at the cell tip (D). Blue arrow shows low actin abundance near the cell apex (D). (E and F) Immunostaining of samples show microtubule distribution in the cell. Microtubules are distributed from the nucleus to the cell apex, with an apical focus of microtubule plus ends at the cell tip in wild type (E). Immunostaining of mutants show random microtubules distribution, with a spread-out distribution at the cell apex, cell regions lacking microtubules, and no apical focus of microtubule plus ends at the cell tip (F). Yellow arrows show the nucleus, red arrow shows apical focus of microtubule plus ends at the cell tip, and ⌐ shows lack of apical focus of microtubule plus ends at the cell tip. Scale: 100 px (A-D) and 10 μm (E and F).

(A)

(B)

(C)

38

(D)

(E)

(F)

39
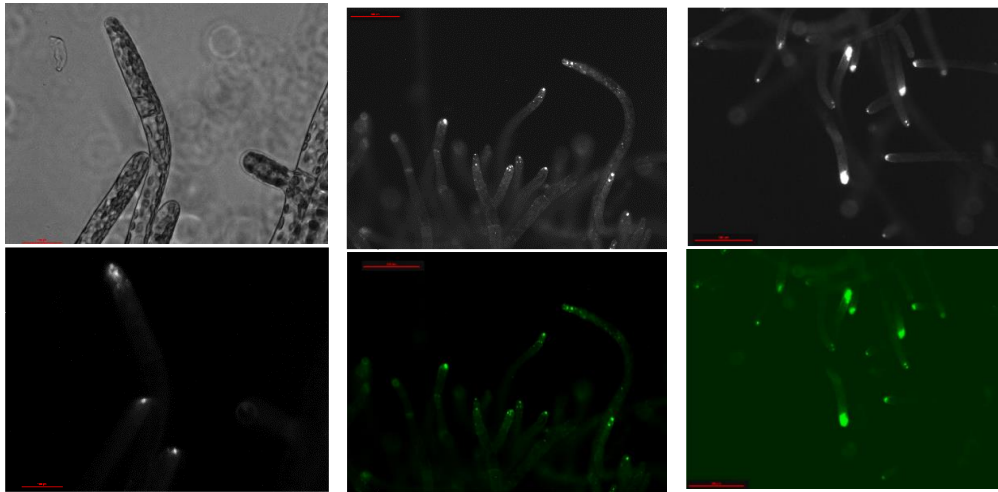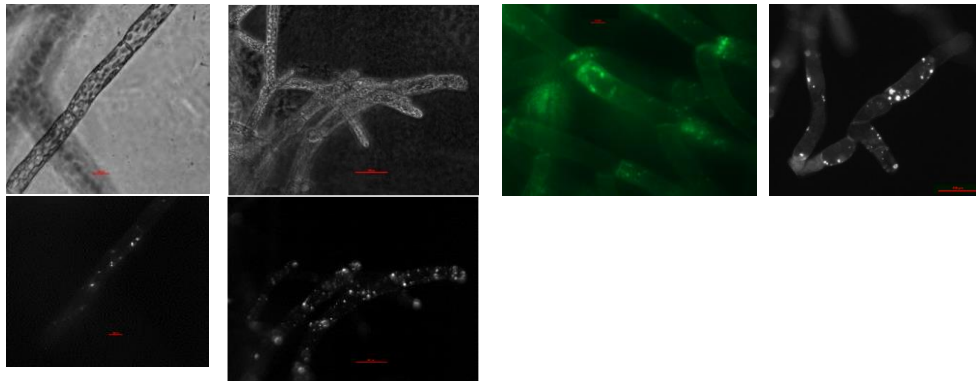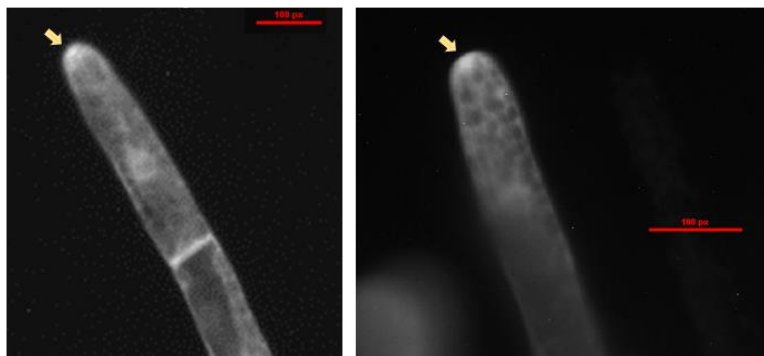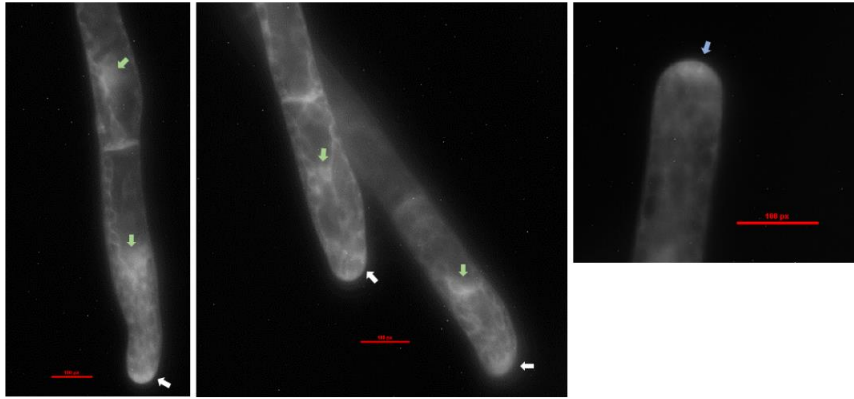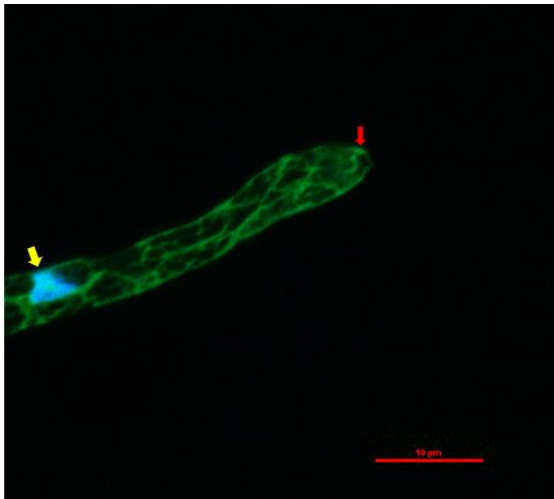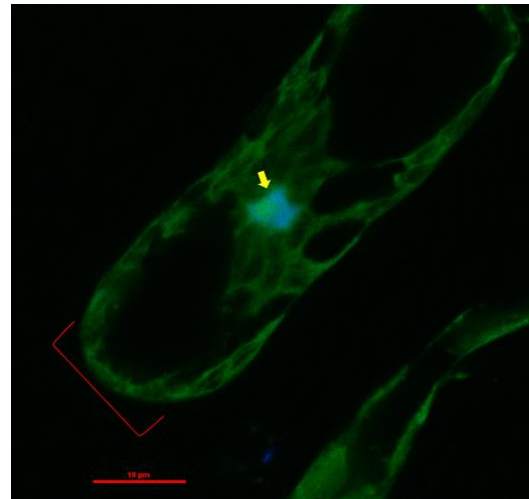
4. DISCUSSION

The present investigation has examined the biological and developmental role of PpPPAL in the moss *Physcomitrium patens*. Developmental fates of *P. patens* chloronema cells are highly regulated by auxin and cytokinin. A chloronema cell can proliferate by apical division to form either a new chloronema cell, a caulonema cell (induced by auxin), or a bud initial (induced by cytokinin) (Ashton et al., 1979; Decker et al., 2006; Prigge et al., 2010; Thelander et al., 2018). The knockdown mutants' phenotype showed inhibition of both the chloronema to caulonema transition and bud development, as well as inhibition of growth as shown by highly reduced colony size (Figures 2 and 3 A and B). Auxin treatment induces chloronema to caulonema transition, an effect that increases with increasing concentration of auxin. Also, auxin has inhibitory effects on chloronemata growth, which increases with higher auxin concentration (Ashton et al., 1979; Decker et al., 2006; Prigge et al., 2010; Thelander et al., 2018). The data showed that mutants responded to auxin inhibition of chloronemata only at the highest concentration tested (100μM NAA), as shown by a decreased in mutants' colony diameter (Figure 6 and 7).

We also observed a reduction in the amount of caulonemal filaments protruding the colony when mutants were grown in 100μM of NAA (Figure 6 and 7). These results suggest that the mutants are insensitive to the stimulatory effects of auxin on chloronema to caulonema transition. However, the mutants do appear to respond to NAA inhibition on chloronemata growth, as shown by reduced colony growth. The stimulatory effect of auxin on the chloronema to caulonema transition and efficient bud formation have been revealed to rely on the TIR1/AFB–Aux/IAA–ARF machinery for auxin perception and signaling

(Hayashi et al., 2012; Plavskin et al., 2016; Prigge et al., 2010), SHI/STY regulators of auxin biosynthesis (Eklund et al., 2011), and PIN auxin exporters (Thelander et al., 2018; Viaene et al., 2014). Enzyme immunoassays suggest that increased protonemal auxin levels are necessary for caulonema emergence and for maintenance of caulonemal characteristics over time (Thelander et al., 2018). It is suggested that auxin is actively transported in moss protonema, and that auxin is also exported out of the filament tip (Thelander et al., 2018; Viaene et al., 2014). Thus, acropetal PpPIN-mediated auxin transport could potentially be responsible for generating the auxin levels needed to initiate caulonemal differentiation in a chloronemal tip cell (Viaene et al., 2014).

It has been shown that caulonema abundance is reduced when auxin biosynthesis is compromised; however, where in protonema auxin biosynthesis takes place is not currently known (Eklund et al., 2011; Lavy & Estelle, 2016; Lavy et al., 2016). As a result, it is unclear whether the assumed acropetal PpPIN-mediated transport serves as the main provider of auxin to the tip cell, by creating a gradient superimposed on a uniform biosynthesis axis, or if it keeps an already apical production site sharp in its maximum. In addition, the sensitivity and response to these auxin levels is regulated by the auxin-responsive regulatory network, TAS3 tasiRNAs and AUXIN RESPONSE FACTORS (ARFs) (Thelander et al., 2018).

The ROOT HAIR DEFECTIVE SIX-LIKE1 (PpRSL1) and PpRSL2 basic helix–loop–helix transcription factors and auxin have been shown to promote the development of caulonema in *P. patens* (Jang & Dolan, 2011). However, the mechanism by which these regulators interact during development is unknown (Jang & Dolan, 2011; Menand, Yi, et al., 2007) . It was demonstrated that auxin positively regulates the gradual

transition from chloronema to caulonema that occurs along protonemal filaments, by positively regulating the activity of PpRSL1 and PpRSL2. Mutants that lack both PpRSL1 and PpRSL2 activity do not develop caulonema even when treated with auxin. PpRSL1 and PpRSL2 expression is sufficient to promote caulonema differentiation in moss protonema even in the absence of auxin (Jang & Dolan, 2011). These data showed how PpRSL1 and PpRSL2 and auxin interact to control the gradual transition of cell fates along a developmental gradient (Jang & Dolan, 2011).

Auxin seems to have a dual role in bud formation. Studies have suggested that auxin is needed together with cytokinin for the actual bud differentiation, and that auxin stimulates caulonemal differentiation thereby providing more targets for cytokinin-induced bud formation (Thelander et al., 2018). Thus, it has been suggested that auxin stimulates bud formation by sensitizing target cells to cytokinin (Ashton et al., 1979; Jang & Dolan, 2011; Prigge et al., 2010; Thelander et al., 2018). Four *P. patens* AP2 transcription factors, PpAPB1–PpAPB4, were found to be required for bud formation (Aoyama et al., 2012). That study showed that auxin positively regulates the expression of APB genes, and that APBs are necessary for the cytokinin signaling-mediated formation of gametophore. However, very little is known about the mechanisms mediating the response (Aoyama et al., 2012; Thelander et al., 2018).

In *P. patens*, cytokinin induces bud formation in a concentration-dependent manner. Bud formation increases with increasing concentration of cytokinin (Figure 8). High concentrations of exogenously applied cytokinin inhibit growth and provoke callus-like growth of buds which do not further differentiate to leafy gametophores (Figure 8) (Brandes & Kende, 1968; Deruere & Kieber, 2002; Reski & Abel, 1985; von

Schwartzenberg et al., 2007).The knockdown mutants responded to BAP inhibition of growth (Figure 7). However, they were less sensitive to BAP induction of bud and callus formation compared to wild type (Figure 8). Cytokinin biosynthesis in *P. patens* relies solely on the tRNA-isopentenylation pathway. Cytokinin signaling is transduced through a simple phosphorylation cascade with components include CHASE-domain receptors, as well as type A and type B RESPONSE REGULATORs (RRs) (Yevdakova and von Schwartzenberg 2007; Frébort et al. 2011).

The fact that mutants respond to auxin inhibition of chloronema growth suggests that the machinery for auxin perception and signaling, biosynthesis and transport may not be affected for that specific response. Mutants also showed normal phototropic and gravitropic responses. Thus, the components needed for processing of light cues, including auxin biosynthesis, transporters, and receptors, to derive proper adaptive phototropic and gravitropic responses appear to be intact in the knockdown mutants (Figure 9), which further suggests that the auxin machinery may not be disrupted in mutants (Bao et al., 2019; Liscum et al., 2014). In addition, even though the mutants were less sensitive to cytokinin compared to wild type, they still responded to BAP inhibition of growth and induction of bud formation. The data suggest that any sensing and signaling required to elicit these responses may still function in the knockdown mutants to some extent, and that PPAL may be needed to sensitize moss to some auxin and cytokinin responses.

The PpPPAL mutants' basal rate of growth, chloronema to caulonema transition, and bud development are highly reduced compared to wild type, irrespective of growth conditions. It therefore appears that these processes are impaired and that the developmental programs that control these processes are disturbed in the mutants.

Therefore, PpPPAL could be a regulator of PpRSL1 and PpRSL2, whose expression is needed to promote caulonema differentiation. Alternatively, PpPPAL maybe needed for proper auxin and PpRSL1 and PpRSL2 interaction to control transition of cell fate. On the other hand, since APB genes are required for bud formation and are necessary for the cytokinin signaling-mediated formation of gametophore, PpPPAL could also be a regulator of the APB-auxin-cytokinin interaction to induce bud formation. Moreover, caulonema cell fate and bud development are favored under high energy conditions such as continuous high light (50 μmol $m^{-2}\, s^{-1}$) and auxin. Therefore, PpPPAL could also be needed to sense the energy status by regulating factors such as kinases that have roles in energy homeostasis.

We also found that the *PPAL* mutants' protonemata exhibited misdirection and reduced expansion of apical cell tip growth, curved apical cell tips, and swelling at or near the apical tip of protonema cells with some cells forming extra tips (Figures 3 and 4). Moss protonemata cells are tip-growing cells containing fine cortical actin filaments along the length of the cell and an enrichment of F-actin at the very apex (Vidali, van Gisbergen, et al., 2009; Wu & Bezanilla, 2018). In moss protonemata there are also two populations of microtubules: cortical and cytoplasmic. In the apical cell, the polarity of cytoplasmic microtubules between the nucleus and the cell apex is tipward, with an apical focus of microtubule plus end. On the other hand, the cortical microtubule array is composed of shorter microtubules that lack polarity (Vidali, van Gisbergen, et al., 2009; Wu & Bezanilla, 2018). Cross talk between microtubules and actin occurs across eukaryotes and is crucial for diverse cellular functions. Secretory cargos that alternate on microtubules and actin tracks require precise coordination between the two cytoskeletons for proper secretion

(Penalva et al., 2017; Wu & Bezanilla, 2018). Numerous studies suggest that long-range microtubule delivery impacts short-range actin-mediated cellular remodeling, thus providing a mechanism to polarize cells (Wu & Bezanilla, 2018).

Polarized cell growth is achieved by the coordination between the actin and microtubule cytoskeletons. Actin is key for most tip growing cells in plants, since depolymerizing actin filaments completely abolishes growth (Baluska et al., 2000; Hepler et al., 2001; Vidali & Hepler, 2001; Vidali et al., 2001; Vidali, van Gisbergen, et al., 2009). Microtubules are normally not essential for tip growth in plants; however, in moss protonemata and root hairs microtubules dictate the directionality of growth (Bibikova et al., 1999; Sieberer, Ketelaar, et al., 2005; Sieberer, Timmers, et al., 2005). It was found that a cluster of actin filaments is continuously generated near the cell tip during growth and the direction of cell expansion is tightly coupled with the location of this cluster (Vidali, Rounds, et al., 2009; Wu & Bezanilla, 2018). Also, a population of cytoplasmic microtubules, whose plus ends converge just below the actin accumulation, is required for maintaining the size and apical position of the actin cluster (Vidali, Rounds, et al., 2009; Wu & Bezanilla, 2018). Disruption of this population of microtubules alters the dynamics of the actin cluster dramatically, resulting in cell expansion defects that lead to uncontrolled growth instead of persistently straight growth and in some cases growth from multiple sites resulting in cell forking (Wu & Bezanilla, 2018). This demonstrates that a tight coupling between the actin and microtubule cytoskeletons is required to guide polarized growth (Hiwatashi et al., 2014; Vidali, Rounds, et al., 2009; Wu & Bezanilla, 2018).

The apical actin cluster formation depends at least partially on class II formins, involved in the polymerization of actin. Microtubules are required for the proper

distribution of these formins in wild type cells (Wu & Bezanilla, 2018). For2A, a class II formin in moss protonenal cells, was found to be unlikely transported on or directly associate with microtubules (Wu & Bezanilla, 2014, 2018). It is not entirely clear how microtubules affect the distribution of class II formins and the formation of the actin cluster (Wu & Bezanilla, 2018). It is possible that there are factors, like PpPPAL, that may promote membrane internalization and thus trafficking of class II formins, or alternatively factors that activate the actin polymerization activity of the formins, creating a local enrichment of active class II formins that would generate the actin cluster (van Gisbergen et al., 2012; Vidali, van Gisbergen, et al., 2009; Wu & Bezanilla, 2014, 2018).

Another element that plays a central role in tip growth is the convergence and focus of microtubule plus ends below the actin cluster in tip cells (Wu & Bezanilla, 2018). This is achieved by kinesins, KINID1a and KINID1b; these microtubule-based motors function to focus apical microtubules in protonemata (Hiwatashi et al., 2014; Wu & Bezanilla, 2018). Double deletion of KINID1a and KINID1b leads to both misdirection and reduced expansion of tip growth, with proportion of tips showing straight and curved shapes (Wu & Bezanilla, 2018). In addition, actin motor protein myosin VIII activity coordinates the actin and microtubule cytoskeletons near the cell apex. Loss of myosin VIII enhances long actin bundles formation (Wu & Bezanilla, 2014, 2018)

Defects in actin-proteins and/or actin-binding proteins exhibit severe phenotypes, many resulting in very stunted cells, loss of directionality of growth, unprecise deposition of new cell wall material to the lateral walls instead of the tip region leading to an enlarged cell, and uncontrolled trafficking and deposition of vesicles during cell growth (Kovar et al., 2000; Ringli et al., 2002; Staiger, 2000; Vidali & Hepler, 2001; Vidali et al., 2001;

Vidali, Rounds, et al., 2009; Vidali, van Gisbergen, et al., 2009). Disturbance in microtubule assembly and organization causes swelling at or near the cell apex, cells bending in random directions, and the formation of multiple tips (Fidel et al., 1988). Microtubule disruption causes perturbance in the actin cytoskeleton (Wu & Bezanilla, 2018).

Since the knockdown mutants' protonemata phenotypes resembles the phenotypic disturbances in both microtubules and actin cytoskeletons, it can be suggested that PpPPAL is a direct or indirect regulator of cytoskeleton assembly, organization, and function. PpPPAL could be a factor that interacts with microtubules and class II formins to help generate the actin cluster. PpPPAL might also regulate kinesin and myosin VIII interaction with the actin and microtubule cytoskeletons. These interactions are important since the convergence of forward-oriented microtubules confine the activity and distribution of class II formin, and thus the formation of an actin cluster to the tip region, which results in the restriction of the site of cell expansion by the actin cluster, ensuring growth in a persistent direction (Wu & Bezanilla, 2018). Since microtubules influence the formation of the actin cluster, this potentially establishes a positive feedback loop to ensure actin polymerization and cell expansion do not deviate from the center of the cell apex too much over time (Wu & Bezanilla, 2014, 2018).

Moreover, the phenotypic changes observed in *Ppppal* mutants resemble those observed in *Ppera1*, the β subunit knockout mutant of PFT prenylation enzyme. It is known that *PPAL* shares weak homology to known prenyltransferase alpha subunits but falls within its own clade (Thole et al., 2014). AtPPAL has also been shown to bind specifically to one of the Rab-GGT β-subunits, RGTB1 (data not shown). In addition, a study described

a novel protein prenyltransferase α subunit, Tempura, that regulates Notch signaling and cell fate determination in *Drosophila*. Loss of Tempura leads to mis-trafficking of signaling components and mislocalization of Rab1 and Rab11, two major coordinators of vesicular trafficking. It was found that Tempura functions as a subunit of a previously uncharacterized lipid modification complex to geranylgeranylate (a type of prenylation) Rab1 and Rab11 (Charng et al., 2014; Thole et al., 2014).

Furthermore, a subfamily of Rab GTPase proteins, RABA4d, was shown to localize at the tips of pollen tubes (Szumlanski & Nielsen, 2009). Disruption in RABA4d resulted in reduced rate of pollen tube growth and swelling at or near the tip region (Szumlanski & Nielsen, 2009). We also found that YFP-RabA4d protein localizes specifically at the tip of the apical cell in *P. patens* protonemata, showing growth points of the apical cells. *Ppppal* mutants showed disruption in RABA4d localization. The expression of RABA4d in *Ppppal* mutants was spread throughout the protonema filament rather than concentrated at the cell tip, and there was swelling at or near the tip cells. RABA4d is responsible for intracellular vesicle trafficking, protein transport, and regulation of tip growth. The association of Rabs with cellular membranes for activity and membrane attachment is mediated by prenyl post-translational modification (Pereira-Leal et al., 2001).

Prenylation is a post-translational modification shown to be required for the proper subcellular localization and function of vital signaling proteins. And the process of prenylation is known to play roles in cell identity determination, cell differentiation, vesicular transport, and polar cell elongation. (Antimisiaris & Running, 2014; Charng et al., 2014; Thole et al., 2014). PpPPAL could potentially participate in the prenylation

process or interact with the prenylation components. PpPPAL1 and 2 may be yet to be identified subunits of the prenylation enzymes or an unidentified regulator of the prenylation components that have acquired various biological and developmental functions . Here we demostrate that both PpPPAL1 and PpPPAL2 have major roles in plant growth and development including cell identity determination, cell differentiation, cell expansion, polar cell elongation, organization of the cytoskeleton, vesicle transport, and response to hormones and external stimuli. Future studies should focus on exploring the biochemical and metabolic role of PpPPAL in the moss *Physcomitrium patens,* as well as its mechanism of action.

Fig S1. microRNA Construction. The artificial microRNA designer WMD delivers 4 oligonucleotide sequences (I to IV), which are used to engineer the artificial microRNA into the endogenous miR319a precursor by site-directed mutagenesis. As a template for the PCRs, the plasmid pRS300 is used, which contains the miR319a precursor in pBSK. (Schwab et al., 2006; Schwab et al., 2005), (PHYSCObase).

amiRNA Forward Primers	amiRNA Reverse Primers	Target Gene
A 339	IV 603	PPAL 1,2
III 602	II 601	PPAL 1,2
I 600	B 389	PPAL 1,2
339	607	PPAL 1,2
606	605	PPAL 1,2
604	389	PPAL 1,2
339	611	PPAL 1
610	609	PPAL 1
608	389	PPAL 1
339	615	PPAL 1
614	613	PPAL 1
612	389	PPAL 1
339	619	PPAL 2
618	617	PPAL 2
616	389	PPAL 2
339	623	PPAL 2
622	621	PPAL 2
620	389	PPAL 2
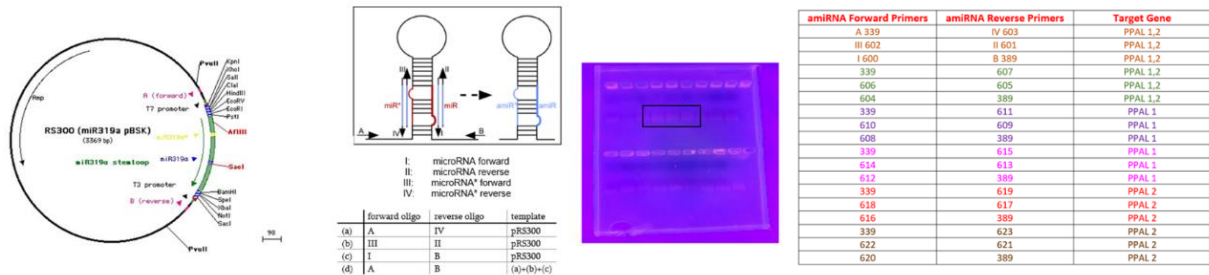
Fig S2. Real Time PCR: Primers, Reaction, and Program.

Sample name	Primer Set	Average C_Q Value
WT	UBQ-10	17.11
WT	PPAL1	24.07
WT	PPAL2	22.51
#4 PPAL1 DMSO	UBQ-10	19.51
#4 PPAL1 DMSO	PPAL1	25.94
#4 PPAL1 B-Est	UBQ-10	17.82
#4 PPAL1 B-Est	PPAL1	26.30
#6 PPAL2 DMSO	UBQ-10	18.24
#6 PPAL2 DMSO	PPAL2	23.81
#6 PPAL2 B-Est	UBQ-10	15.78
#6 PPAL2 B-Est	PPAL2	23.14
#2 PPAL1,2 DMSO	UBQ-10	18.95
#2 PPAL1,2 DMSO	PPAL1	26.41
#2 PPAL1,2 DMSO	PPAL2	24.46
#2 PPAL1,2 B-Est	UBQ-10	17.90
#2 PPAL1,2 B-Est	PPAL1	28.30
#2 PPAL1,2 B-Est	PPAL2	24.48

Reaction

Component	Volume
BlasTaq™ 2X qPCR MasterMix (Cat. G891)	10 µL
Forward primer (10 µM)	0.5 µL
Reverse primer (10 µM)	0.5 µL
Nuclease-free H_2O	8 µL
cDNA Template (10 ng) or Nuclease-free H_2O for NTC	1µL

qPCR Program

Step	Temperature	Duration	Cycle
Enzyme Activation	95°C	05:00	1
Denaturation	95°C	00:30	35
Annealing/Extension	60°C	00:45	
Melting Curve	55°C to 95°C	00:05/0.5°C	1

Fig S3. Entry and Expression Plasmids. (A) Entry vector for topo cloning (Kubo et al., 2013). (B) amiRNA expression vector (PHYSCObase). (C) Probes' expression vectors: pTZ:UBI for expression Lifeact-mEGFP (https://sites.dartmouth.edu/bezanillalab/moss-methods/overexpression/) and pT1OG for expression of RABA4D (PHYSCObase). (D)Expression vector used in complementation assay. (https://www.arabidopsis.org/servlets/TairObject?type=vector&id=501100106).

Fig S4. Complementation Assay. (A) PpPPAL2 and *Atppal-1*. (B) PpPPAL1 and *Atppal-1*. (C) PpPPAL1, PpPPAL2, and *Atppal-1*. (D) PpPPAL1, PpPPAL2, *Atppal-1,* and wild type. (E) PpPPAL2 CDS 1666 bp, PpPPAL1 CDS 1411bp and 2-log DNA ladder gel. Orange arrow is wild type, blue arrow is PpPPAL2, red arrow is PpPPAL1, and green arrow is *Atppal-1*.
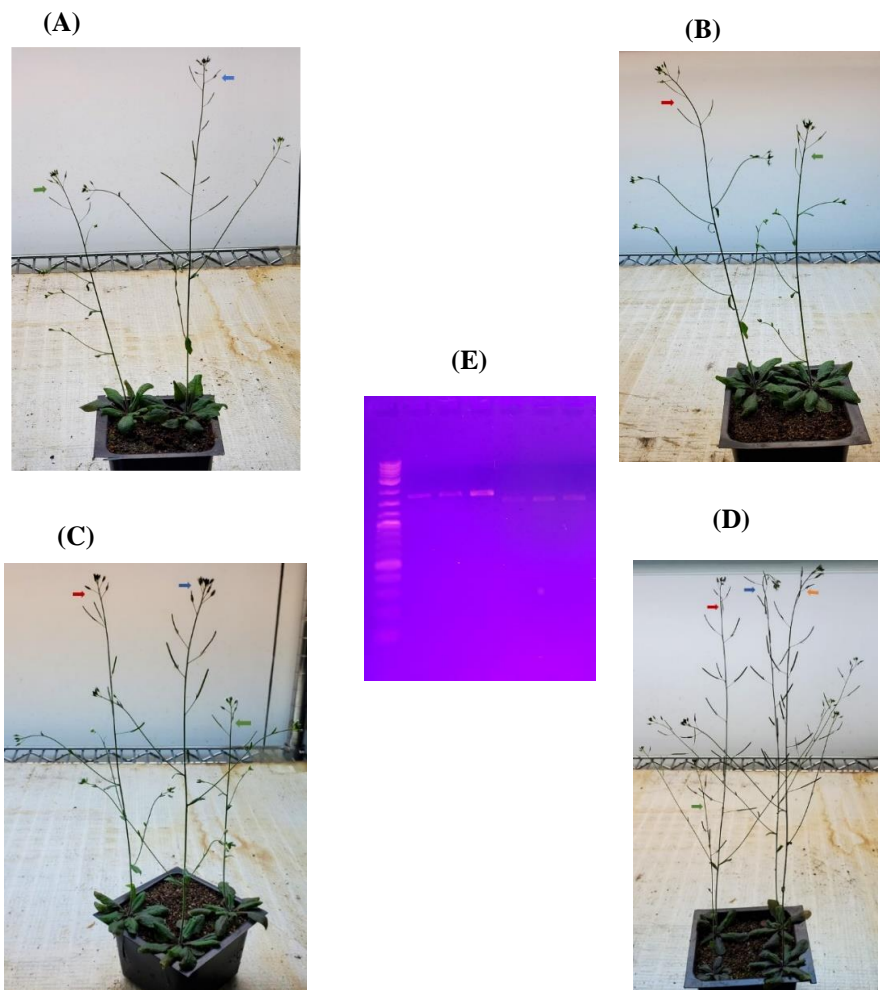
Table 1:

Primers	Sequences	Purpose
600-PPAL1,2 amiRNA-I miR-s	gaTATCCTTGCTAAACGAAGCTAtctctcttttgtattcc	Constructing amiRNA
601-PPAL1,2 amiRNA-II miR-a	gaTAGCTTCGTTTAGCAAGGATAtcaaagagaatcaatga	Constructing amiRNA
602-PPAL1,2 amiRNA-III miR*s	gaTAACTTCGTTTAGGAAGGATTtcacaggtcgtgatatg	Constructing amiRNA
603-PPAL1,2 amiRNA-IV miR*a	gaAATCCTTCCTAAACGAAGTTAtctacatatatattcct	Constructing amiRNA
604-PPAL1,2 amiRNA-I miR-s	gaTAGCTACATGTAGTTGCCCCAtctctcttttgtattcc	Constructing amiRNA
605-PPAL1,2 amiRNA-II miR-a	gaTGGGGCAACTACATGTAGCTAtcaaagagaatcaatga	Constructing amiRNA
606-PPAL1,2 amiRNA-III miR*s	gaTGAGGCAACTACAAGTAGCTTtcacaggtcgtgatatg	Constructing amiRNA
607-PPAL1,2 amiRNA-IV miR*a	gaAAGCTACTTGTAGTTGCCTCAtctacatatatattcct	Constructing amiRNA
608 -PPAL1 amiRNA-I miR-s	gaTGTATACCTAAAAGTAGACACtctctcttttgtattcc	Constructing amiRNA
609-PPAL1 amiRNA-II miR-a	gaGTGTCTACTTTTAGGTATACAtcaaagagaatcaatga	Constructing amiRNA
610-PPAL1 amiRNA-III miR*s	gaGTATCTACTTTTACGTATACTtcacaggtcgtgatatg	Constructing amiRNA
611-PPAL1 amiRNA-IV miR*a	gaAGTATACGTAAAAGTAGATACtctacatatatattcct	Constructing amiRNA
612-PPAL1 amiRNA-I miR-s	gaTCAATACGCGTTTTCTAGCAAtctctcttttgtattcc	Constructing amiRNA
613-PPAL1 amiRNA-II miR-a	gaTTGCTAGAAAACGCGTATTGAtcaaagagaatcaatga	Constructing amiRNA
614-PPAL1 amiRNA-III miR*s	gaTTACTAGAAAACGGGTATTGTtcacaggtcgtgatatg	Constructing amiRNA

615-PPAL1 amiRNA-IV miR*a	gaACAATACCCGTTTT CTAGTAAtctacatatatattc ct	Constructing amiRNA
616 -PPAL2 amiRNA-I miR-s	gaTTAATATACGCTTT CTGGCGTtctctcttttgtattc c	Constructing amiRNA
617-PPAL2 amiRNA-II miR-a	gaACGCCAGAAAGCG TATATTAAtcaaagagaatc aatga	Constructing amiRNA
618-PPAL2 amiRNA-III miR*s	gaACACCAGAAAGCG AATATTATtcacaggtcgtg atatg	Constructing amiRNA
619- PPAL2amiRNA- IV miR*a	gaATAATATTCGCTTT CTGGTGTtctacatatatattcc t	Constructing amiRNA
620-PPAL2 amiRNA-I miR-s	gaTTTCTAAGACTAAG TCTACCGtctctcttttgtattcc	Constructing amiRNA
621-PPAL2 amiRNA-II miR-a	gaCGGTAGACTTAGTC TTAGAAAtcaaagagaatca atga	Constructing amiRNA
622-PPAL2 amiRNA-III miR*s	gaCGATAGACTTAGTG TTAGAATtcacaggtcgtgat atg	Constructing amiRNA
623-PPAL2 amiRNA-IV miR*a	gaATTCTAACACTAAG TCTATCGtctacatatatattcc t	Constructing amiRNA
389-Sequence-B2- in	GCTCTAGAACTAGTG GATCCCCC	Constructing amiRNA
339-Sequence- A2-in	caccAGCTTGATATCGA ATTCCTG	Constructing amiRNA
304-M13-21	TGTAAAACGACGGCC AGT	pENTR/35s-npt2(pTN182)/35s- aph4(pTN186)/35s-zso/35s-BSD sequencing and and cloning PCR
305-RV17	CAGGAAACAGCTATG ACCA	pENTR/35s-npt2(pTN182)/35s- aph4(pTN186)/35s-zso/35s-BSD sequencing and and cloning PCR
LBa1	TGGTTCACGTAGTGG GCCATCG	Sequencing to check for ppal-1 mutant in Arabidopsis
ppal-1 RP	ACTATCGGCTACATG AAGCCC	Sequencing to check for ppal-1 mutant in Arabidopsis
ppal-1 LP	TGTATTCCCGAGAGT GACGTC	Sequencing to check for ppal-1 mutant in Arabidopsis
pTK-UBI-GATE	TCTAGAACTAGTGGA TCC	Sequencing and genotyping expression markers
pTK-UBI-GATE	TCGAGGTCGACGGTA TCGA	Sequencing and genotyping expression markers
pTZ-UBI-GATE	TGATATCGAATTCCT GCAG	Sequencing and genotyping expression markers
pTZ-UBI-GATE	GCCAAGTTAATTCGA GCT	Sequencing and genotyping expression markers

469-eYFP-atRabA4d-F	caccATGGTGAGCAAGGGCGAGG	Sequencing and genotyping expression markers
470-eYFP-atRabA4d-R	TTACGATTTGCCGCAACATCC	Sequencing and genotyping expression markers
PpPPAL1 CDS	CACCATGGCGGAAGAAGAGGACTCGTGGCAG	PpPPAL CDS Sequencing and cloning PCR
PpPPAL1 CDS	TCAGCAATGCGAGCTGCTTTTTGAAAAAATC	PpPPAL CDS Sequencing and cloning PCR
PpPPAL2 CDS	CACCATGGCGGAAGAGGAGGATTCATG	PpPPAL CDS Sequencing and cloning PCR
PpPPAL2 CDS	CTAGACCAGGTTCGGAATCAGACCATTC	PpPPAL CDS Sequencing and cloning PCR
Left Primer PPAL2	TTGTCTCGCGCATGTCACT	Checking expression levels qPCR of PpPPAL2
Right Primer PPAL2	CGCCCATTTCTTTGTGTTCT	Checking expression levels qPCR of PpPPAL2
Left Primer PPAL1	AGTCCAACTCTGGTCGCTTC	Checking expression levels qPCR of PpPPAL1
Right Primer PPAL1	CTGCGGGTTCACAATCAAA	Checking expression levels qPCR of PpPPAL1
473-UbiF2 Endogenous Control	ACTACCCTGAAGTTGTATAGTTCGG	Checking expression levels qPCR of Ubiquitin 10 gene
474-UbiR Endogenous Control	CAAGTCACATTACTTCGCTGTCTAG	Checking expression levels qPCR of Ubiquitin 10 gene
458-PPAL1-RT	AACGTGCAGTTCCAAGGAC	RT PCR Analyzing expression level
459-PPAL1-RT	TGTGGACTCACATCCTTCAG	RT PCR Analyzing expression level
460-PPAL2-RT	CAGAGAACTGATGGACCTG	RT PCR Analyzing expression level
461-PPAL2-RT	GTAGTTCATCGTCGACCTC	RT PCR Analyzing expression level

MANUSCRIPT 2

PPPPAL IS NEEDED TO SENSE AND RESPOND TO THE AVAILABLE

NUTRIENT AND ENERGY STATUS AND TO MEDIATE GLUCOSE AND

HORMONE SIGNALING IN *PHYSCOMITRIUM PATENS*

1. INTRODUCTION

The ability of a cell to sense the availability of nutrients is essential to sustain the growth and development of both microorganisms such as yeast and multicellular organisms such as plants. Sugars have a central role in energy metabolism, and the ability to sense and adapt to the availability of energy in the form of sugars is vital to maintaining energy homeostasis (Rolland et al., 2006; Thelander et al., 2005). The sensing and signaling of sugar have been most extensively studied in the model organism *Saccharomyces cerevisae*: however, the exact mechanism for sugar sensing and signaling in plants is still not fully understood. Plant growth and development are driven by the intricate interaction between energy availability, environmental cues, genetic programs, and hormones (Jaeger & Moody, 2021; Thelander et al., 2005). Largely studied plant signaling mechanisms focus on plant hormones, such as abscisic acid (ABA), cytokinin and auxin (Decker et al., 2006; Frebort et al., 2011; Hutchison & Kieber, 2002; Jang & Dolan, 2011; Viaene et al., 2014; von Schwartzenberg et al., 2007) . Plant hormones are involved in the regulation of a wide variety of processes, and the signaling pathways exhibit a broad cross talk with more than one hormone being involved in the same process. Sugars have been shown to have similar

signaling capabilities to those of plant hormones, and there is an extensive cross talk between plant hormones and sugar signaling (Leon & Sheen, 2003; Rolland et al., 2006; von Schwartzenberg et al., 2007).

The moss *Physcomitrium patens* has become a powerful model system in plant molecular genetics and development due to its simple body plan and limited number of tissue and cell types, its sequenced and annotated genome, and the ability to perform stable and efficient targeted genes knockouts (Nishiyama et al., 2003; Schaefer, 2002; Schaefer & Zryd, 1997; Thole et al., 2014). *Physcomitrium* colonies are formed from regenerating spores or protoplasts, which are initially made up of protonemal filaments that grow by apical cell divisions (Cove et al., 2006; Pressel et al., 2008). *P. patens* has two types of protonemal filaments, chloronemata and caulonemata. The first filaments to arise are chloronemal, which have well-developed chloroplasts and are more photosynthetically active. Caulonema filaments result from a transition from select chloronemal apical cells. Caulonemata help to spread the colony by rapid radial growth, contain fewer chloroplast, and form buds that develop into gametophores (Menand, Calder, et al., 2007; Menand, Yi, et al., 2007; Pressel et al., 2008; Thole et al., 2014). We have recently identified a gene, *PROTEIN PRENYLTRANSFERASE ALPHA SUBUNIT-LIKE (PPAL)*, which encodes a cytosolic protein (Thole et al., 2014). *PPAL* homologs are present in plants, mammals, and other animals where their function is unknown, and they have not been identified in fungi. The moss *P. patens* contains two copies of *PPAL*, *PPAL1* and *PPAL2,* and both are required for viability (Thole et al., 2014). The characterization of the *Physcomitrium ppal* knockdown mutants, *Ppppal1*, *Ppppal2* and *Ppppal1,2*, revealed the importance of PPAL for moss growth and development (Manuscript 1). The phenotypes of the mutants include

inhibition of the chloronema to caulonema transition, bud formation for gametophore development, and colony growth even when grown in high energy conditions such as continuous high light, 50 μmol $m^{-2}\,s^{-1}$ intensity (Manuscript 1).

The energy supply regulates the balance between chloronemal and caulonemal growth. Caulonema formation is favored under high energy conditions, and under low energy conditions the chloronema to caulonema differentiation is suppressed (Thelander et al., 2005). This suggests that *Ppppal* mutants are defective in sensing the energy status, which prompted the present investigation of how chloronemal and caulonemal growth is affected by high and low energy conditions in the mutants compared to wild type. *Ppppal* knockdown mutants were treated with glucose (high energy source), low light (low energy) and the hormone ABA. The most striking finding was the inability of the mutants to respond to glucose treatment: mutants do not respond to the glucose induction of caulonemata and gametophores formation. We also found that *Ppppal* mutants are hypersensitive to ABA treatment, and endogenous ABA content is higher compared to wild type. We explored further by specifically looking at the effects of glucose treatment on protein, fatty acid, terpenoid and ABA content in the mutants compared to wild type.

2. MATERIALS & METHODS

2.1 Plant Materials and Growth Conditions

Normal growth conditions of P. patens

The generation of the PPAL knockdown lines (*ppal1*, *ppal2*, and *ppal1,2*) is described in Manuscript 1. Protonemal tissue of wild type and *Ppppal* inducible knockdown mutant lines were subcultured using a Polytron homogenizer T20B.S1 (IKA) and grown on BCDAT medium (https://moss.nibb.ac.jp/protocol.html) with cellophane for 5 days. Knockdown mutant lines were then grown in both 1μM Beta Estradiol/DMSO/BCDAT inducible medium and DMSO/BCDAT control medium for 7 days. Plants were grown at 25°C under continuous light at 50 μmol m^{-2} s^{-1} intensity.

Low light and dark conditions of P. patens

Samples were subcultured and grown the same way as in normal growth conditions. For low light, plants were grown at 25°C at 6 μmol m^{-2} s^{-1}. For dark conditions, plants were grown at 25°C in complete dark.

2.2 Phenotypic Analysis of Protonemata

For morphological studies, small pieces of fresh protonemal tissue (approximately 2 mm in diameter) were inoculated on BCDAT plates without cellophane. Samples were grown in different conditions and with different additives—100 mM glucose and 100 μM abscisic acid (ABA). For colony growth assays, representative 18 day old colonies were photographed

(using a dissecting microscope with a 20w LED fiber optic dual gooseneck lights microscope illuminator) and the diameters of four independent colonies were measured. In the caulonemal filament induction assay, the numbers of caulonemal filaments clearly protruding from the edge of an 18 day old colony were counted using a dissecting microscope. Moss colonies grown under these standard conditions have a closely connected edge in the wild type, and even more so in the *Ppppal* mutants. This made it possible to define a filament extending beyond the rim of the colony as a protruding filament. Such protruding filaments were counted for four colonies in each case.

2.3 Hormone Treatment in *P. patens*

Knockdown mutants in the wild type background and wild type moss were grown in normal growth conditions for 5 days. Samples were then treated with 1 μM, 10 μM, and 100 μM of abscisic acid (ABA) for 18 days. Mutants were transferred to both 1 µM Beta Estradiol/DMSO/BCDAT inducible medium and DMSO/BCDAT control medium with the different concentration of hormone. Wild type was grown on BCDAT with the different concentration of hormone. Plants were grown at 25°C under continuous light at 50 μmol $m^{-2} s^{-1}$ intensity.

2.4 *P. patens* Glucose Treatment

Wild type and *Ppppal* mutant lines were cultured in normal growth conditions for 5 days. Then, samples were treated with 10 mM, 50 mM and 100 mM of glucose for 18 days. Knockdown mutants were grown in both 1uM Beta-Estradiol/DMSO/BCDAT inducible medium and DMSO/BCDAT control medium with the different concentrations of glucose.

Wild type was grown on BCDAT with the different concentrations of glucose. Plants were grown at 25°C under continuous light.

2.5 Estimation of Total Terpenoids

Estimation of samples' total terpenoid followed a published protocol (Ghorai et al., 2012) with some modifications. Briefly, 100 mg freeze-dried plant material was treated with 1 mL of ice-cold methanol (95% vol/vol) grinded and centrifuged at 4000 g for 15 m at room temperature. The supernatant was extracted, 135 uL of supernatant was then mixed with 1mL chloroform, and the solution was left standing for 3 min. 70 uL concentrated sulfuric acid was then added to the solution followed by incubated for 2 h; a reddish-brown precipitate should form if terpenoids are present. The linalool standard was incubated for only 5min. After incubation, the supernatant was gently decantated without disturbing the precipitant. 1mL of 95% methanol was added to resuspend the precipitant and vortexed until completely dissolved. 240 uL of the solution was transferred into 96 well plate in triplicates. The samples were read at 538 nm with 95% methanol as a blank and a linalool standard curve.

GC/MS

Estimation of samples' total terpenoid followed a published protocol (Heath et al., 2014). Briefly, 100 mg freeze-dried plant material was treated with 2 ml of methanol and incubated for 24 h at room temperature. The solution was then centrifuged for 2 min at 830 g and the supernatant was transferred to glass vials. 1.5 ml of HPLC-graded hexane was added to the vials, and the solution was incubated for another 24 h at room temperature. 1 uL injection volume of the organic layer was run over hexane-preconditioned silica-gel columns (0.20 g) GC/MS maintained at a temperature of 250°C. Tetralin was used as an internal standard.

2.6 Methyl Ester Derivatization of Plant Tissues

100 mg of freeze-dried samples was used. 1 mg of internal standard (TAG 17:00), 300 μL of toluene and 1 mL of BF3 in 14% MeOH was added to all samples. Samples were heated at 90°C for 1hr. 2 ml hexane was added to the solution and centrifuged at 300 g for 1 minute to collect the organic layer; this was done three times. The organic phase was dried to measure the mass of recovered fatty acid methyl esters. Hexane was added to reconstitute the recovered fatty acid methyl esters to 5-10 mg/mL concentration. Samples were analyzed by Gas chromatography using various fatty acid standards (Harmanescu, 2012).

2.7 Protein Extraction

Coomassie (Bradford) Protein Assay Kit protocol from ThermoFisher was used to quantify total protein content in samples. Briefly, 5 ml of PBS 1X pH 7.4 buffer was added to 100 mg of freeze-dried samples, mixed thoroughly and centrifuged. The supernatant was collected and diluted 0.1x and 0.5x. Albumin (BSA) Standard curve was made, and 10 μL of each standard and unknown were added into microplate wells. 250 μL of the Coomassie Plus Reagent was also added to each well. The absorbance was measured at or near 595 nm with a Spectramax 190 Microplate Reader.

2.8 Composition Analysis

The cell wall composition of moss samples was determined by National Renewable Energy Laboratory analytical procedures (Sluiter et al., 2012). Briefly, 0.1 g of sample was mixed with 2 ml of 72% H_2SO_4 and incubated at 30°C for 1 hr. The solution was diluted to 4% H_2SO_4 with 56 g of H_2O and autoclaved at 121°C for 1 hr. The autoclaved sample was then filtered by filter crucible, and the filtrate was used in HPLC for sugar analysis. For lignin

analysis, autoclaved samples were dried at 105°C overnight and calcined at 575°C for 8 hr. All sugars and organic acid concentrations in the acid-digested solutions were analyzed by HPLC equipped with a refractive index detector (RID) and a diode array detector (DAD). The Aminex HPX-87H column (300 x 7.8 mm, Bio-Rad®, Hercules, CA, USA) was used to separate sugars at 60°C with 0.6 ml/min of 4mM H_2SO_4 as a mobile phase. The concentrations of sugars were determined by the RID signals' peak area (HMF and furfural were determined by DAD signals at 280nm). All sugars were calibrated against certified standards (Absolute Standards Inc., Hamden, CT, USA).

2.9 ABA Quantification

Methanolic extraction from samples followed a published protocol (Yi et al., 2011). 100 mg freeze dried samples were homogenized and extracted overnight with 10 ml 80% cold aqueous methanol at 4 °C in the dark. The extract was centrifuged at 5000 r/min for 15 min in 4 °C, supernatant was collected, and more methanol was poured into the remnant, extracted three times. The total methanolic extract was dried and dissolved in 5 ml methanol. ABA levels were measured by the injection of the extract into a reverse-phase HPLC with a methanol gradient in 0.6% acetic acid. ABA levels were also measured by liquid chromatography–mass spectrometry (LC–MS) that is attached to HPLC, equipped with a diode array detector (DAD) use to confirm, and quantify the ABA peak. HPLC conditions used was as follows: Hypersil ODS C18 column, mobile phase was methanol with - 0.6% ethanoic acid, gradient elution, column temperature at 35 °C, sample size was10 µl, flow rate was 1 ml/min, and the ultraviolet detection wavelength was 254 nm.

3. RESULTS

3.1 Knockdown mutants and wild type moss colony morphology under low light and continuous high light conditions

In *P. patens,* high energy conditions induce the chloronema to caulonema transition and promote gametophore development. On the other hand, low energy conditions favor chloronema formation to help restore the energy supply, due to their higher photosynthetic activity of chloronemata (Imaizumi et al., 2002; Jaeger & Moody, 2021; Thelander et al., 2005). We found that continuous high light, a high energy condition, in wild type moss promoted growth and development, by stimulating the chloronema to caulonema transition and gametophore development (Figure 1, A and M). In low light, a low energy condition, wild type moss growth and development was restricted. Under low light, chloronemata formation was favored and caulonema formation was largely absent, although a few short caulonemal filaments were seen (Figure 1, B and M). In addition, wild type colony diameter and gametophore development was reduced when grown in low light compared to constant high light (Figure 1 A, B, and M).

Ppppal knockdown mutants grown in constant high light exhibited inhibition of growth and development. Different from wild type, the transition from chloronema to caulonema was highly inhibited in the mutants, with only a few caulonema filaments formed with reduced elongation (Figure 1, D, G, J and M). Mutant colony diameters were reduced, and gametophore formation was impaired (Figure 1, D, G, J and M). Mutants in low light behaved similarly to how they behave in high constant light, as shown by inhibition of the chloronema to caulonema transition and gametophore formation (Figure

64

1, E, H, K and M). However, low light seems to further inhibit the mutants' growth and development as shown by a reduction in colony diameter and caulonema filaments and no gametophore formation (Figure 1, E, H, K and M). Knockdown mutants' phenotype when grown in constant high light resemblance that of wild type moss grown in low light, in that formation of caulonemata and gametophores are restricted, and colony size is reduced (Figure 1 B, D, G, J and M). Nevertheless, in both constant high light and low light conditions mutants' growth and development is more inhibited compared to wild type (Figure 1, M).

In addition, both wild type and mutants can grow for weeks in the dark (Figure 1, C, F, I, L and M). Dark conditions highly inhibited the growth and development of protonemata in wild type moss, compared to when grown in low light and constant high light (Figure 1, C and M). In the dark, wild type colony size and caulonema formation were much more reduced than in low light, and no gametophores were formed (Figure 1, C and M). The inhibition of growth and development of mutants when grown in the dark is much more severe than when grown in high constant light and low light, as demonstrated by highly reduced colony diameter and complete inhibition of caulonemata and gametophore formation (Figure 1, F, I, L and M). We found that colony growth, caulonema formation, and gametophore development are much reduced in the mutants compared to wild type, regardless of growth condition (Figure 1 M). Significant differences (P <0.01) in caulonema formation, gametophore number, and colony growth were observed between wild type and the mutants in high light (Figure 1 M). In low light significant differences in caulonema formation (P <0.01), gametophore number (P <0.01), and colony growth (P <0.05) were observed between wild type and the mutants as well (Figure 1 M).

Dark condition also showed significant differences ($P <0.01$) in caulonema formation and colony growth between wild type and mutants (Figure 1 M). In addition, in high light significant differences in caulonema formation were observed between *Ppppal1,2* and *Ppppal1* ($P <0.01$), *Ppppal1,2* and *Ppppal2* ($P <0.01$), and *Ppppal1* and *Ppppal2* ($P <0.05$) mutants (Figure 1 M). Significant differences ($P <0.05$) in gametophore number were observed between *Ppppal1,2* and *Ppppal1,* and *Ppppal1,2* and *Ppppal2* mutants in high light (Figure 1 M). Furthermore, *Ppppal1,2* and *Ppppal2* mutants show significant differences ($P <0.05$) in colony diameter during high light and low light conditions. Our data corroborated studies that have shown that in *P. patens* caulonema development requires relatively high light intensities; as expected under low light conditions caulonema formation is largely absent and gametophore formation is reduced (Imaizumi et al., 2002; Schumaker & Dietrich, 1997; Thelander et al., 2005). Therefore, we used colonies grown in high constant light to quantify the effects of glucose and ABA treatment in the mutants and wild type.

Figure 1. Knockdown mutants and wild type moss grown for 18 days in constant high light, low light and in the dark. Wild type moss (A, B, C), *Ppppal1,2* (D, E, F), *Ppppal1*(G, H, I), and *Ppppal2* (J, K, L). Below we can see a comparison between samples grown in constant high light (A, D, G, J), low light (B, E, H, K), and in the dark (C, F, I, L). In wild type, constant high light promotes caulonemata and gametophore development while low light inhibits growth and development. Different from wild type, mutants grown in both constant high light and low light showed inhibition of caulonema formation, gametophore development, and colony growth with difference in degree of inhibition. All samples grown in the dark exhibited the highest inhibition of growth and development but

remained viable. (M) Quantification of samples growth and development. The histograms show the average ±SEM of four colonies, error bars indicate standard errors of the mean. Constant high light (50 μmol m^{-2} s^{-1}) and low light (6 μmol m^{-2} s^{-1}). The significances of the observed differences between samples were tested using a two-tailed two-sample t-test assuming unequal variances. Scale 4 mm.
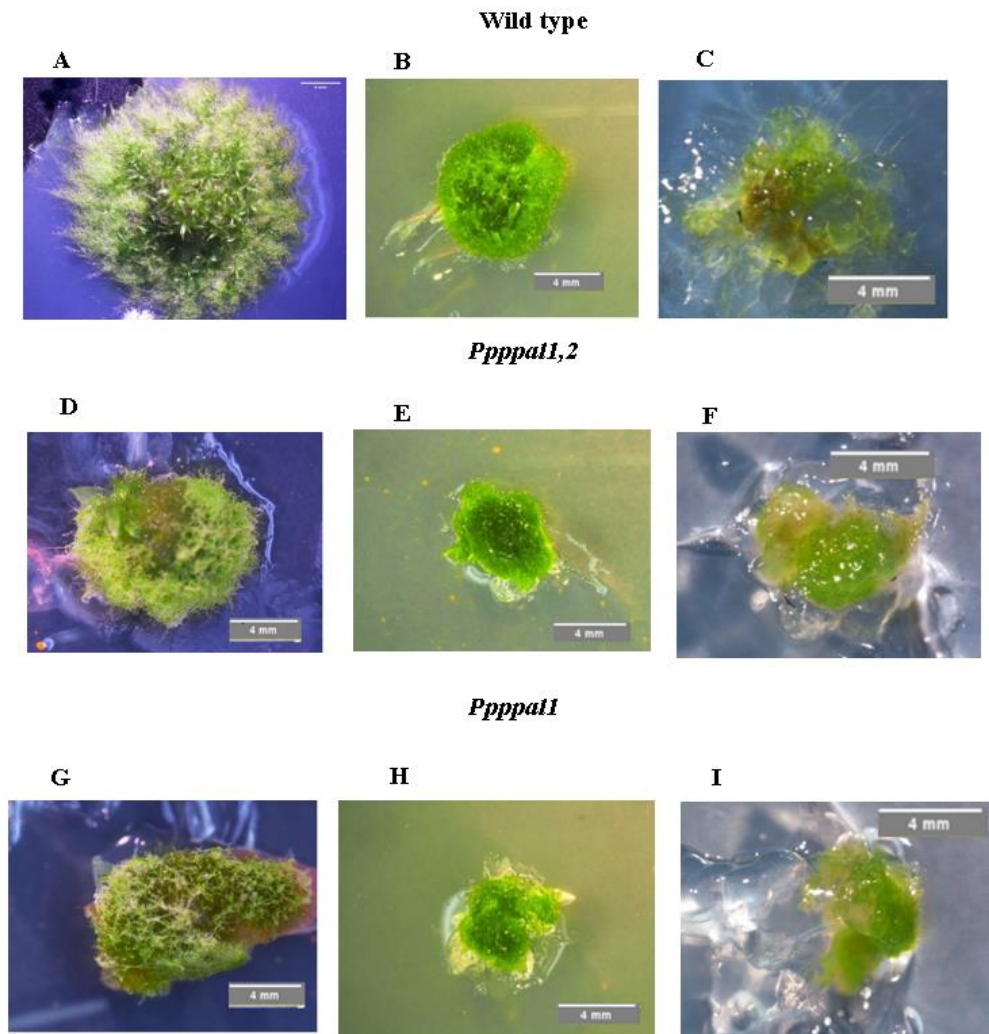
Ppppal2
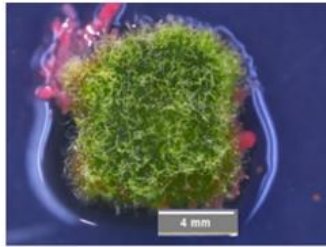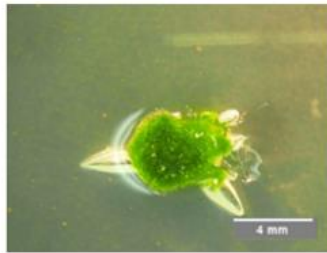
J　　　　　　　　　　K　　　　　　　　　　L
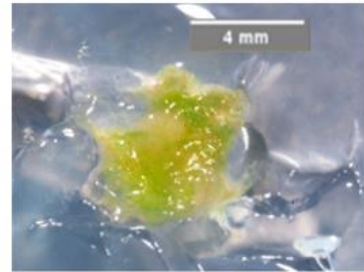
M
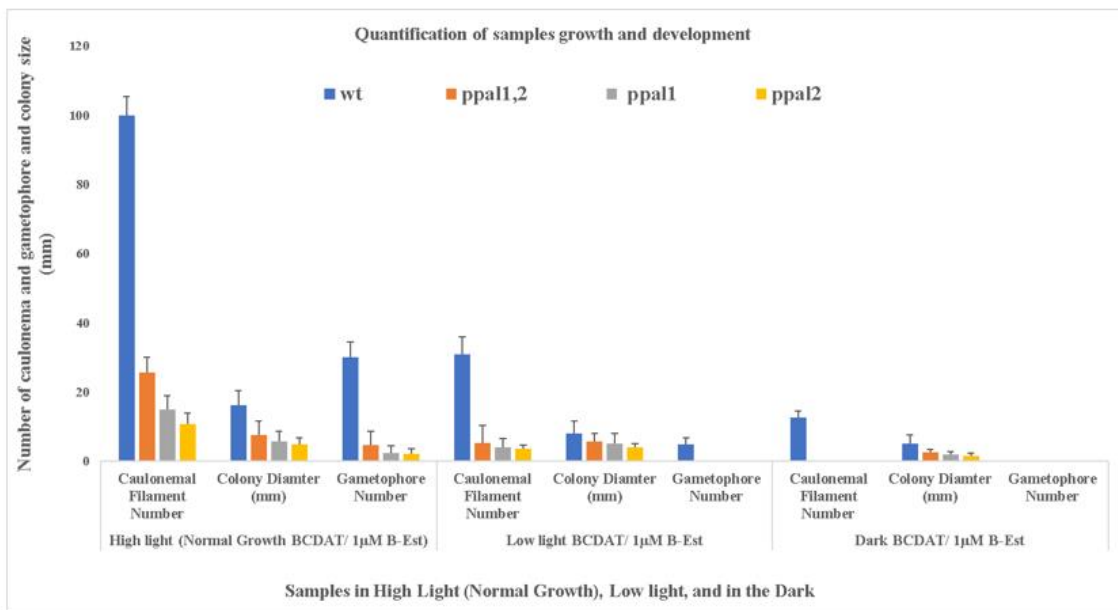
3.2 Abscisic Acid response in wild type and *Ppppal* mutants

ABA application in wild type results in the differentiation of protonemal tissue into vegetative diaspores (brachycytes) that are characterized by thickened cell walls, tiny vacuoles and the storage of lipids and starch, as these structures are meant to withstand drought and regerminate upon more favorable conditions (Arif et al., 2019; Knight et al., 1995). Elevated exogenous ABA levels are sufficient to provoke all transcriptional changes underlying this specific developmental fate. The formation of brachycytes is ABA-dependent, as ABA non-responsive mutants do not produce any brachycytes (Arif et al., 2019). Mutants and wild type were treated with increasing concentration of ABA, 1 µM, 10 µM, and 100 µM. The inhibitory effects of ABA in both wild type and mutants are dose-dependent, ranging from a minor effect at 1 µM to severe growth inhibition at 100 µM. Significant differences (P <0.01) in brachycytes formation and colony size were observed between wild type and mutants (Figure 2 I). *Ppppal1,2* and *Ppppal2* mutants showed significant differences (P <0.01) in colony size and brachycyte formation (Figure 2 I). *Ppppal1,2* and *Ppppal1* mutants showed significant differences (P <0.05) in colony size and brachycyte formation. *Ppppal1* and *Ppppal2* mutants showed significant differences in colony size (P <0.05) and brachycyte formation (P <0.01) (Figure 2 I). Compared to wild type, mutants displayed a hypersensitivity to ABA treatment at all concentrations, as shown by increased brachycyte formation and pronounced growth inhibition at comparable levels of ABA treatment (Figure 2).

Figure 2. Abscisic acid treatment of samples. Samples were grown in induction medium with 100 μM of ABA for 18 days. Wild type moss colony (A) and protonema cell (B) grown on ABA exhibited formation of brachycytes and inhibition of growth but not as pronounced as in mutants. *Ppppal1,2* colony (C) and protonema cell (D). *Ppppal1* colony (E) and protonema cell (F). *Ppppal2* colony (G) and protonema cell (H). Mutants were hypersensitive to ABA treatment as shown by severe inhibition of growth and increased formation of brachycytes. (I) Quantification of samples growth and development. The histograms show the average ±SEM of four colonies, error bars indicate standard errors of the mean. The significances of the observed differences between samples were tested using a two-tailed two-sample *t*-test assuming unequal variances. Scale 4 mm and 100 μm
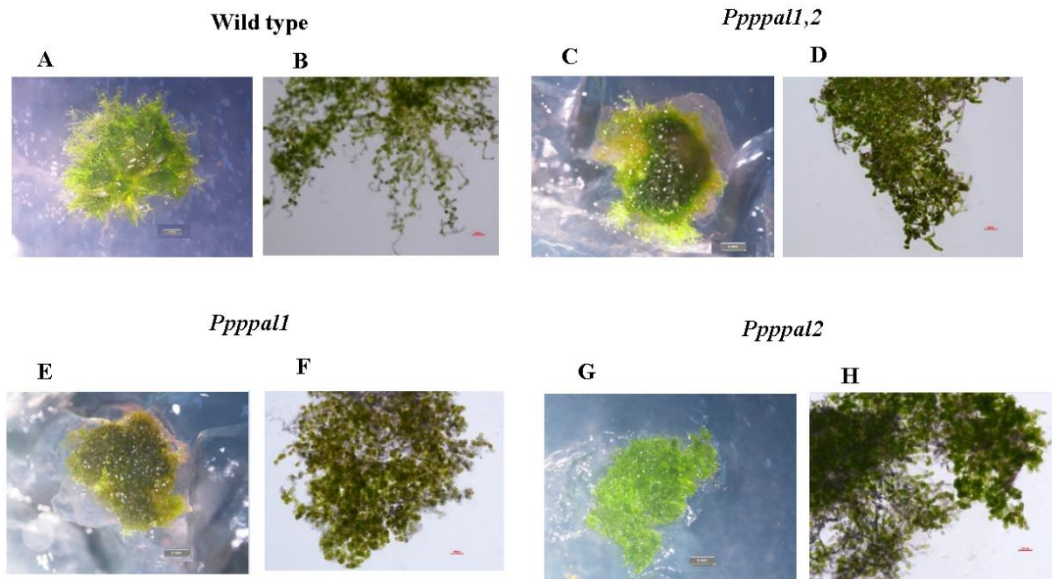
I
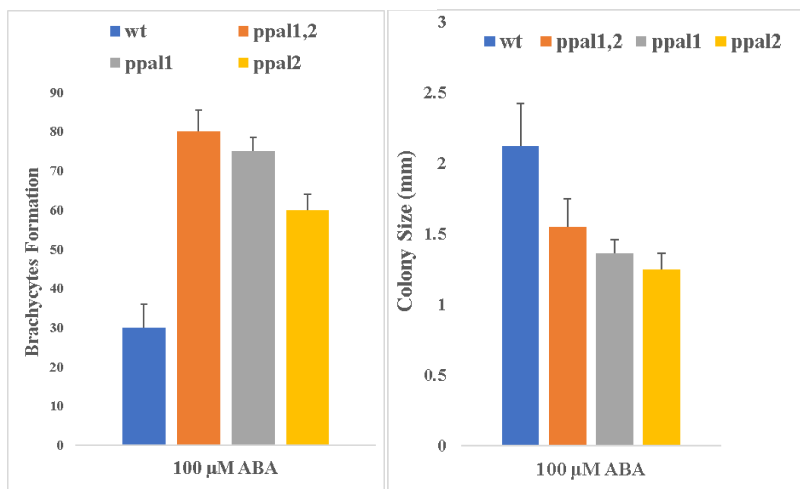
3.3 Glucose response in *Ppppal* mutants and wild type

PpPPAL knockdown mutants and wild type moss were grown in increasing glucose and mannitol (as an osmotic control) concentrations of 10 mM, 50 mM and 100 mM. In wild type moss external glucose, a high energy condition, promotes the transition from chloronema to caulonema cells (Figure 3 B) (Rolland et al., 2006; Thelander et al., 2005). Transitioning from chloronema to caulonema helps in colony expansion and sets the stage for gametophore development, as gametophores develop from buds that form in caulonema cells (Figure 3 B and M) (Thelander et al., 2005). Glucose induced caulonemata are different from those induced by other conditions, in that caulonema filaments are branched, reach far from the colony's edge, and are more heavily pigmented (Figure 3 B) (Thelander et al., 2005). Both the chloronema to caulonema transition and gametophore production requires energy. The glucose response is dose dependent, and it increases with increasing concentration of glucose (Rolland et al., 2006; Thelander et al., 2005).

71

Ppppal mutants are defective in the response to external glucose treatment for all the concentrations. When mutants are grown on glucose, the chloronema to caulonema transition and gametophore formation is not promoted (Figure 3 E, H, K and M). Mutant colony growth was further inhibited when grown on glucose, which was most pronounced at 100mM glucose (Figure 3 E, H, K and M). Mannitol treatment in wild type cannot mimic the enhancement of gametophore development and the induction of caulonema filaments that protrude from the edge of the colony provoked by glucose treatment (Figure 3 C and M). Mutant colonies grown in mannitol look different compared to mutant colonies grown in glucose: in mannitol, mutants form some gametophores and more caulonema cells (Figure 3 F, I, L and M). Also, high (100mM) glucose concentration induces a reduction in mutant and wild type colony growth; this is mimicked by equimolar concentrations of the non-metabolizable sugar mannitol (Figure 3) (Thelander et al., 2005). This suggests that growth inhibition in *Ppppal* mutants could be, at least partially, a result of an osmotic effect created by both mannitol and glucose.

Significant differences (P <0.01) in caulonema formation, colony growth, and gametophore number were observed between wild type and mutants for all treatments (Figure 3 M). In normal growth conditions, significant differences in caulonema formation were found between *Ppppal1,2* and *Ppppal1* (P <0.01), *Ppppal1,2* and *Ppppal2* (P <0.01), and *Ppppal1* and *Ppppal2* (P <0.05) mutants (Figure 3 M). Significant differences in colony growth were found between *Ppppal1,2* and *Ppppal2* (P <0.05) mutants in normal growth conditions (Figure 3 M). In addition, significant differences (P <0.05) in gametophore number were observed between *Ppppal1,2* and *Ppppal1*, and *Ppppal1,2* and *Ppppal2* mutants during normal growth (Figure 3 M). When grown in glucose, significant

differences (*P* <0.01) in caulonema formation were observed between *Ppppal1,2* and *Ppppal2* mutants (Figure 3 M). Significant differences (*P* <0.01) in caulonema formation were observed between *Ppppal1,2* and *Ppppal2* mutants treated with mannitol (Figure 3 M). *Ppppal1,2* and *Ppppal2* mutants showed significant differences (*P* <0.05) in colony growth when treated with mannitol (Figure 3 M). Furthermore, significant differences (*P* <0.05) in gametophore number were observed between *Ppppal1,2* and *Ppppal1*, and *Ppppal1,2* and *Ppppal2* mutants grown in mannitol (Figure 3 M).

Figure 3. Glucose and mannitol response in *Ppppal* mutants and wild type. Samples were grown in normal growth conditions (A, D, G, J), 100 mM of glucose (B, E, H, K) and 100 mM of mannitol (C, F, I, L) for 18 days. Wild type moss (B) responded normally to the glucose induction of branched and heavily pigmented caulonemal filaments that protrude from the colony edge, and gametophore formation. *Ppppal1,2* (E), *Ppppal1* (H) and *Ppppal2* (K) mutants grown in glucose exhibited inhibition of colony growth, caulonema formation and gametophore development. Mutants and wild type were treated with 100mM mannitol as an osmotic control. Wild type (C) grown in mannitol exhibited a few large gametophores and short caulonema filaments. However, glucose treated wild type showed long pigmented caulonema filaments that expand the colony and multiple smaller gametophores (B). *Ppppal1,2* (F), *Ppppal1* (I) and *Ppppal2* (L) mutants grown in mannitol showed some gametophore and more caulonema cells formed, which was not the case when treated with glucose. (M) Quantification of samples' growth and development. The histograms show the average ±SEM of four colonies, error bars indicate standard errors of the mean. The significances of the observed differences between samples were tested using a two-tailed two-sample *t*-test assuming unequal variances. Scale 4 mm.

Wild Type

A
B
C

Pppal1,2

D
E
F

Pppal1

G
H
I

Pppal2

J
K
L
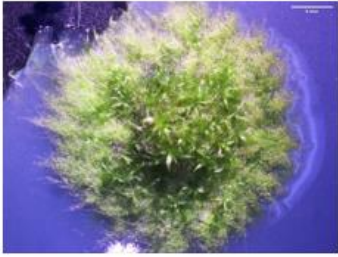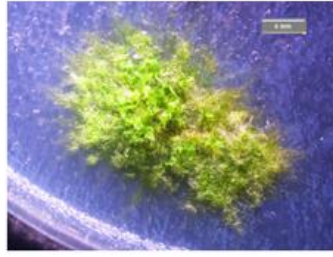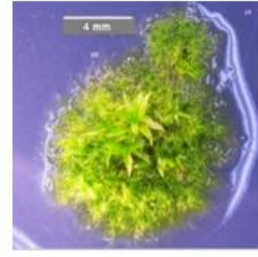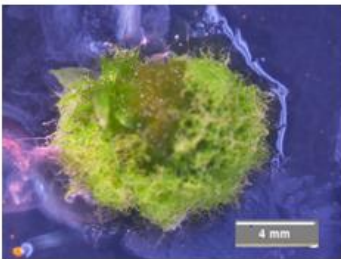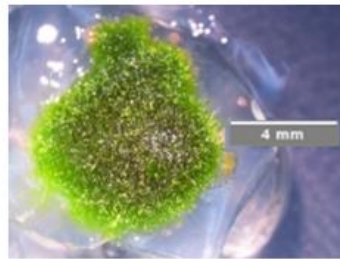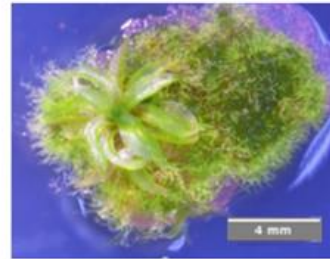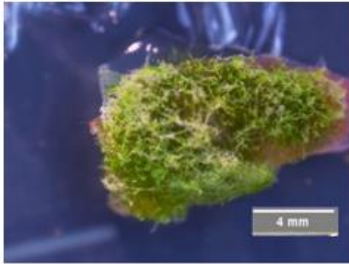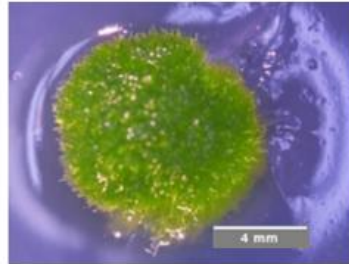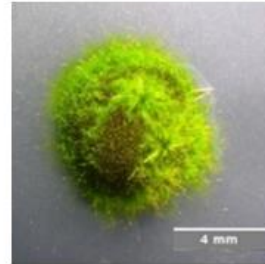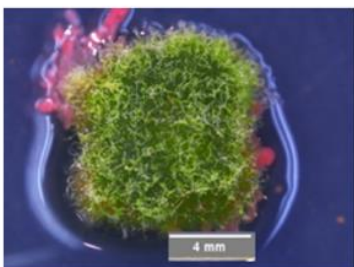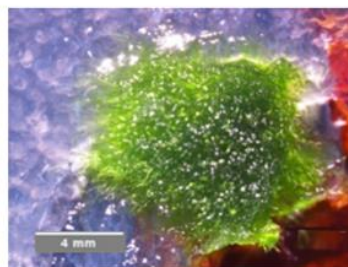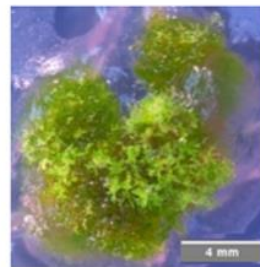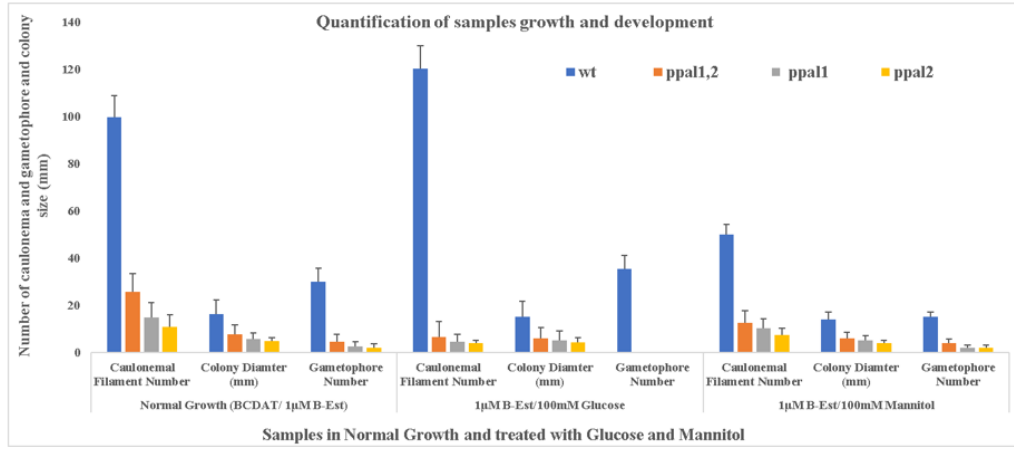
3.4. Analyzing total fatty acid content in wild type and knockdown mutants

Analysis of fatty acid (FA) composition in biological samples is commonly done by gas chromatography (GC) after the transesterification of fatty acids to volatile FA methyl esters (FAMEs). Methyl esters are highly stable and suitable for GC analysis. Esterification is best done in the presence of a catalyst. Studies have analyzed methods for the liberation and conversion of free fatty acids to methyl esters using different catalysts, and boron trifluoride (BF3) in MeOH has been shown to be an effective reagent (Harmanescu, 2012; Ostermann et al., 2014; Salimon et al., 2014). To explore whether PpPPAL has a function in fatty acid composition and/or synthesis in *P. patens*, methyl ester derivatization of tissue was performed in wild type, *Ppppal1*, *Ppppal2*, and *Ppppal1,2* mutants. 100mg of freeze-dried tissue per sample was utilized, and the derivatization was done using BF3 in 14% MeOH. In normal growth conditions, it was found that compared to wild type and the *Ppppal2* mutant, both *Ppppal1,2* and *Ppppal1* mutants had significantly higher (P <0.01) number of the following FAs listed from highest to lowest quantity: C16:0 palmitic acid SFA, C22:1Δ13 erucic acid UFA, C18:3Δ9,12,15 α-linolenic acid UFA, C18:2Δ9,12 linoleic acid UFA, C18:1Δ9 oleic acid UFA, C17:0 heptadecanoic acid SFA, C15:0 pentadecylic acid SFA, C18:0 stearic acid SFA and C13:0 tridecylic acid SFA (Figure 4 A).

In normal growth conditions, the *Ppppal1,2* knockdown mutant has the greatest amount of fatty acid content, followed by the *Ppppal1* mutant, which has more fatty acid content compared to both *Ppppal2* mutant and wild type (Figure 4 A and C). The amount of fatty acid found in both wild type and *Ppppal2* mutant are similar (Figure 4 A and C).

Significant differences ($P < 0.01$) in fatty acid content were observed in *Ppppal1,2* and *Ppppal1* mutants compared to wild type and *Ppppal2* mutant in normal growth conditions (Figure 4 A and C). In addition, we found that there was a significant increase ($P < 0.01$) in FAs in all samples when grown in glucose compared to normal growth conditions, except for the *Ppppal1* mutant (Figure 4 B and C). When grown in glucose, the *Ppppal2* knockdown mutant had the most FA content. The *Ppppal1,2* mutant had slightly more FAs than wild type, and the *Ppppal1* mutant had the least FA content, even less than when grown in normal growth conditions (Figure 4 B and C). Significant differences ($P < 0.01$) in fatty acid content were observed between wild type and *Ppppal1* mutant, and wild type and *Ppppal2* mutant treated with glucose (Figure 4 B and C). In addition, significant differences ($P < 0.01$) in fatty acid content were found between *Ppppal1,2* and *Ppppal1, Ppppal1,2* and *Ppppal2,* and *Ppppal1* and *Ppppal2* mutants when grown in glucose (Figure 4 B and C).

Figure 4. Methyl ester derivatization of samples using GC. Fatty acid methyl esters were quantified in wild type and knockdown mutants grown in normal growth conditions and treated with glucose. (A) and (B) show the amount of each FAMEs present per sample (ug FAMEs per mg of sample dry weight). It was found that during normal growth conditions, both *Ppppal1,2* and *Ppppal1* mutants had overall a greater number of FAMEs compared to *Ppppal2* mutant and wild type (A). However, when treated with glucose it shifted to *Ppppal2* having the largest quantity of FAMEs, *Ppppal1,2* and wild type had similar amount of FAMEs and *Ppppal1* had the lowest amount of all samples (B). Total FAMEs per mg of dry weight (C) shows that there is an increase in total amount of fatty acid methyl esters when samples are grown in glucose versus normal growth conditions,

except for the *Ppppal1* mutant. The histograms show the average ±SEM of four colonies, error bars indicate standard errors of the mean. The significances of the observed differences between samples were tested using a two-tailed two-sample *t*-test assuming unequal variances.
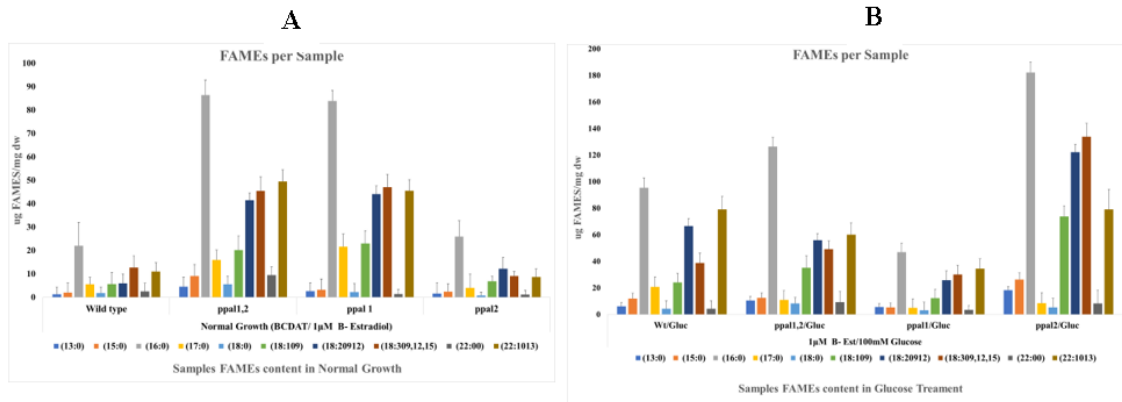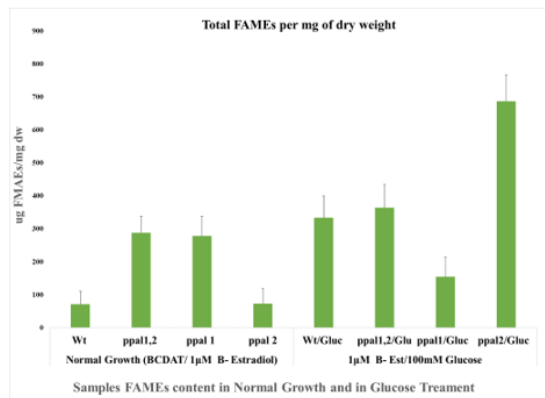
**3.5 Studying total terpenoid content in wild type and knockdown mutants**

Isoprenoids, also known as terpenoids, constitute the most functionally and structurally diverse group of metabolites, and are found predominately in plants. Studies have shown that isoprenoids are capable of functioning as both primary and specialized metabolites. As primary metabolites, they have functions in respiration, photosynthesis, regulation of growth and development and membrane fluidity, among others (Aharoni et al., 2003; Pandreka et al., 2015; Thulasiram et al., 2007). On the other hand, as specialized metabolites they are involved in plant-pathogen and allelopathic interactions and have health-promoting properties. Terpenoids are modified terpenes; both are hydrocarbons formed from the condensation of several 5-carbon isoprene units. The difference between both compounds is that terpenoids are often oxygenated versions of terpenes. However, some authors will use the term terpene to include all terpenoids (Aharoni et al., 2003; Pandreka et al., 2015; Thulasiram et al., 2007). To study changes in terpenoid number and content, two high-throughput assays were used. The first assay used a methanolic extraction and a linalool (monoterpene) standard curve in 95% methanol (Ghorai et al., 2012). All estimations were done spectroscopically at 538 nm. The other assay included a methanolic extraction treated with HPLC-grade hexane, an internal standard (tetralin) and analysis by GS/MS (Heath et al., 2014).

When samples were grown in 100mM of glucose

In normal growth conditions the highest terpenoid level was found in *Ppppal1* and the lowest in *Ppppal2*, with *Ppppal1,2* and wild type having similar amounts of terpenoids (Figure 5). Wild type, *Ppppal1,2* mutant, and *Ppppal1* mutant showed significant differences ($P < 0.05$) in terpenoid content compared to *Ppppal2* mutant during

normal growth (Figure 5). When samples were grown in 100 mM glucose, wild type showed the highest amount of terpenoid followed by *Ppppal2* and *Ppppal1,2* mutant had the lowest amount (Figure 5). The number of terpenoids found in wild type increased significantly (P <0.01) when grown in glucose compared to normal growth conditions, something that did not happen in the mutants (Figure 5). Compared to normal growth conditions mutants grown in glucose showed, in the case of *Ppppal2*, a notable increase in terpenoid, although much less than the response seen in wild type, and both *Ppppal1,2* and *Ppppal1* had a slight decrease in terpenoid level (Figure 5). Significant differences (P <0.01) in terpenoid content between wild type and the mutants were observed when treated with glucose (Figure 5). In addition, significant differences (P <0.05) in terpenoid content between *Ppppal2 and Ppppal1,2* mutants were observed when grown in glucose (Figure 5).

Figure 5. Terpenoid quantification of samples. The terpenoid content in mutants and wild type was estimated by two methods, GC/MS and a plate reader. Both methods gave consistent results for each sample; data comes from the average of the values obtained from both methods. The chart shows the terpenoid content (mg/g) found per sample. It was found that the terpenoid content increased for wild type and *Ppppal2* mutants when grown in glucose, while terpenoid content for *Ppppal1,2* and *Ppppal1* mutants was higher in normal growth conditions. The histograms show the average ±SEM of four colonies, error bars indicate standard errors of the mean. The significances of the observed differences between samples were tested using a two-tailed two-sample *t*-test assuming unequal variances.

Terpenoid Content

Samples Terpenoid content in Normal Growth and in Glucose Treament
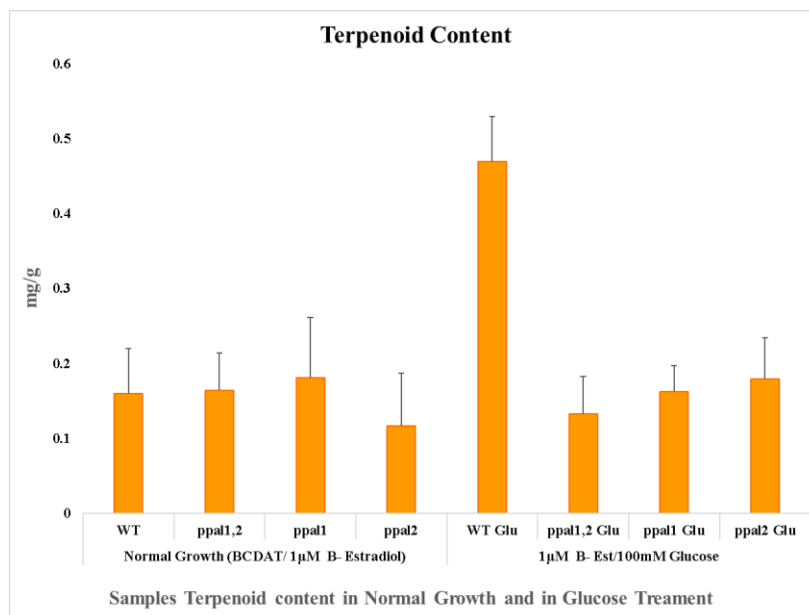
3.6 Estimation of total protein content in wild type and knockdown mutants

The Bradford assay was used to study protein content of wild type and mutants. The assay uses Coomassie reagent for binding proteins in samples, the protein albumin (BSA) standard to create a standard curve, and a light spectrophotometer with maximum transmission in the region of 595 nm. The estimation of protein concentration is achieved by reference to absorbances obtained for a series of standard protein dilutions assayed alongside the unknown samples. It was found that during normal growth conditions, wild type contained significantly ($P < 0.01$) more protein compared to the mutants. Among the mutants, *Ppppal1* had the most protein content followed by *Ppppal1,2*, while *Ppppal2* had the least amount of protein. In addition, we found that the protein content in wild type drastically decreased when grown in 100mM of glucose (Figure 6). However, protein content increased for all mutants when grown in glucose compared to normal growth conditions, with *Ppppal1* having the most and *Ppppal2* the least amount of protein (Figure

6). Significant differences (P <0.01) in protein content between wild type and the mutants were observed during both normal growth conditions and glucose treatment (Figure 6). *Ppppal1,2 and Ppppal1* mutants showed significant differences (P <0.01) in protein content compared to *Ppppal2* in normal growth conditions (Figure 6). Glucose treated mutants exhibited significant differences (P <0.01) in protein content with one another (Figure 6).

Figure 6. Protein quantification of samples. The Bradford assay was used to estimate total protein content in wild type and mutants. The data show that the amount of protein in mutants increased when treated with glucose versus normal growth conditions. However, the amount of protein in wild type decreased when grown in glucose. The histograms show the average ±SEM of four colonies, error bars indicate standard errors of the mean. The significances of the observed differences between samples were tested using a two-tailed two-sample *t*-test assuming unequal variances.
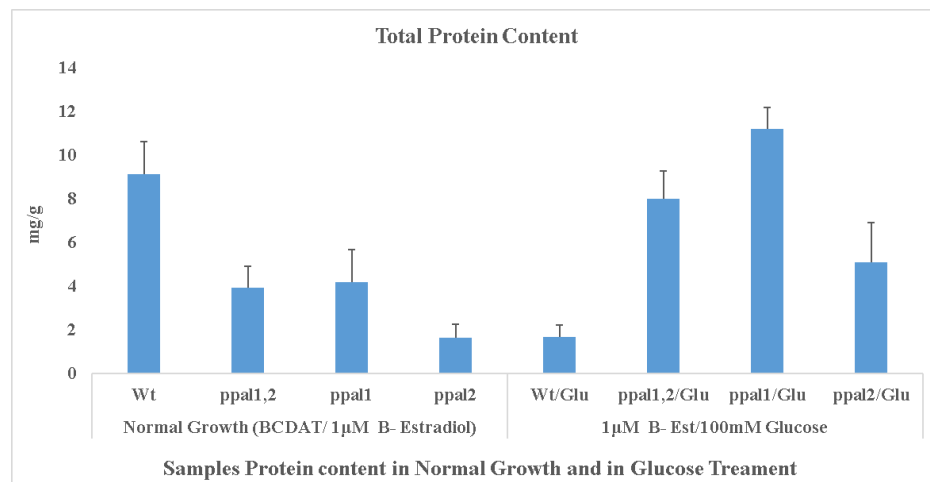
3.7 Assessing cell wall carbohydrate composition in mutants and wild type

Plant biomass is a promising source for carbon neutral, renewable, and sustainable raw material for industry and society. Plant biomass is mostly compromised of cell walls composed of energy rich polymers including cellulose (glucan) and the hemicelluloses xylan and arabinan. To study the cell wall composition of wild type moss and mutants, the National Renewable Energy Laboratory analytical procedure (NREL LAP) was used (Sluiter et al., 2012). All sugars and organic acid concentrations in the acid-digested solutions were analyzed by HPLC equipped with a refractive index detector (RID) and a diode array detector (DAD). For samples grown in normal growth conditions, we found that the *Ppppal2* mutant contains the highest amount of glucan followed by wild type and *Ppppal1,2*. The *Ppppal1* mutant contains the least amount of glucan (Figure 7). For xylan content in samples grown under normal growth conditions, the lowest amount of xylan was found in both wild type and *Ppppal2*, with wild type having the least amount. The greatest xylan content was in *Ppppal1* followed by *Ppppal1,2* mutant (Figure 7). During normal growth conditions, the highest amount of arabinan was observed in *Ppppal1* mutant followed by *Ppppal2* mutant. Both wild type and *Ppppal1,2* contained lower levels of arabinan compared to *Ppppal1* and *Ppppal2*. Of all samples wild type contained the least amount of arabinan (Figure 7). Significant differences (P <0.05) in glucan content were found between *Ppppal1* and *Ppppal2* mutants in normal growth conditions (Figure 7). During normal growth conditions, significant differences in xylan content were observed between wild type and *Ppppal1,2* mutant (P <0.05), wild type and *Ppppal1* mutant (P <0.01), *Ppppal1,2* and *Ppppal2* mutants (P <0.05)*,* and *Ppppal1* and *Ppppal2* mutants (P <0.01) (Figure 7)*.*

Compositional analysis was also performed in mutants grown in 100 mM glucose. We found that there was a significant (P <0.01) increase in the amount of glucan when wild type moss is exposed to glucose, which was not true for mutants (Figure 7). Wild type had the highest amount of glucan, even greater than when grown in normal growth conditions, followed by the *Ppppal1,2* mutant. *Ppppal1* and *Ppppal2* had less glucan content, with *Ppppal1* having the lowest amount. Xylan content decreased for all samples when grown in glucose. The most xylan content was observed in both *Ppppal1* and *Ppppal2* mutants, with the *Ppppal1* mutant having the highest amount. Both *Ppppal1,2* and wild type had low xylan content, with *Ppppal1,2* having the lowest amount (Figure 7). Glucose treatment also decreased the number of arabinan for all samples. The samples with the highest content of arabinan were *Ppppal1* and *Ppppal2*, with *Ppppal1* mutant having the most arabinan. Low amount of arabinan were found in both wild type and *Ppppal1,2* mutant, with the least amount of arabinan found in wild type (Figure 7).

Significant differences (P <0.01) in glucan content were found between wild type and mutants treated with glucose (Figure 7). In addition, significant differences (P <0.05) in glucan content were observed between *Ppppal1,2* and *Ppppal1* mutants, and *Ppppal1,2* and *Ppppal2* mutants in glucose (Figure 7). Significant differences (P <0.05) in xylan content were found between wild type and *Ppppal1,2* mutant, and wild type and *Ppppal1* mutant treated with glucose (Figure 7). In glucose, significant differences in xylan content were observed between *Ppppal1,2* and *Ppppal1* (P <0.01) mutants, *Ppppal1,2* and *Ppppal2* (P <0.05) mutants, and *Ppppal1* and *Ppppal2* (P <0.05) (Figure 7).

Figure 7. Wild type and mutant solid assay. Samples cell wall carbohydrate composition was determined by (NREL LAP) protocol and analyzed with HPLC. Below we see the amount of glucan, xylan, and arabinan found in each sample (wt. %). The histograms show the average ±SEM of four colonies, error bars indicate standard errors of the mean. The significances of the observed differences between samples were tested using a two-tailed two-sample *t*-test assuming unequal variances.

Composition	Wild type	#2 PPAL1,2	#4 PPAL1	#6 PPAL2	Wild type/Glu	#2 PPAL1,2/Glu	#4 PPAL1/Glu	#6 PPAL2/Glu
Glucan (wt.%) g/g	32.24	32.21	30.56	35.84	47.52	31.91	24.96	26.59
Xylan (wt.%) g/g	4.08	5.77	7.65	4.62	2.93	1.80	4.42	3.30
Arabinan (wt.%) g/g	1.06	1.10	1.53	1.40	0.59	0.91	1.39	0.96

Samples Glucan, Xylan, and Arabinan content in Normal Growth and Glucose Treatment
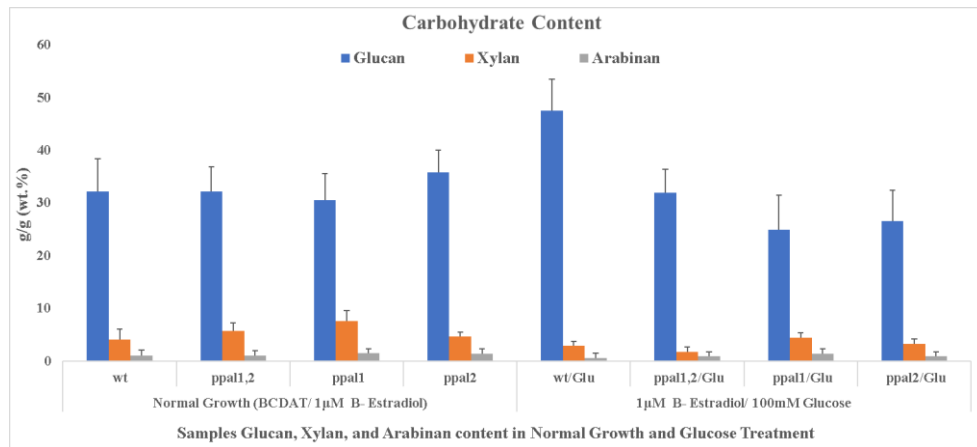
3.8 Studying endogenous abscisic acid levels in wild type and mutants

Abscisic Acid (ABA) has multiple roles in plant growth, development, and adaptive responses to environmental constraints. ABA is of major importance in its interaction with the sugar signaling pathway, as various mutations affecting sugar signaling and sensing are allelic to genes encoding components of the ABA synthesis and signal transduction pathways (Finkelstein et al., 2002; Rohde et al., 2000; Sakr et al., 2018; Vishwakarma et al., 2017). Wild type and knockdown mutants were grown in medium containing increasing concentrations of 1 μM, 10 μM, and100 μM of ABA. We found that, compared to wild type, mutants were hypersensitive to ABA as shown by severe growth inhibition and increased brachycyte formation. The inhibitory effects of ABA in both wild type and mutants are dose-dependent, ranging from a minor effect at 1 μM to almost complete growth inhibition at 100 μM ABA (see Figure 2).

The hypersensitivity of mutants to ABA treatment may be explained by an elevated level of endogenous ABA in the mutants versus wild type. To study endogenous ABA levels in mutants and wild type, two approaches were used. The samples were extracted with 80% methanol and the methanolic extract was used to study ABA levels using both approaches. We first studied ABA levels by using reversed-phase high performance liquid chromatography (HPLC). The HPLC system consisted of a hypersensitive ODS C18 reverse phase column (150 mm × 4.6 mm, 5 μm) with a methanol gradient in 0.6% acetic acid and UV detector set at 254 nm (Yi et al., 2011). The other approach used liquid chromatography–mass spectrometry (LC–MS) that is attracted to HPLC, equipped with a diode array detector (DAD) used to confirm and quantify the ABA peak. The data showed that the knockdown mutants had a higher content of ABA compared

to wild type when grown in normal growth conditions (Figure 8). *Ppppal2* and *Ppppal1,2* had the most ABA content with *Ppppal2* having the highest, and among the mutants *Ppppal1* had the lowest amount (Figure 8).

Samples were grown in 100mM of glucose. We found that glucose treatment increased the ABA content in wild type, agreeing with other studies that have shown that glucose treatment increases endogenous ABA levels in plants (Figure 8) (Arenas-Huertero et al., 2000; Cheng et al., 2002; Leon & Sheen, 2003; Price et al., 2003). However, the ABA content in the mutants decreased when treated with glucose compared to when grown in normal growth conditions (Figure 8). This indicates that the knockdown mutants are defective in the response to glucose. In any case, the mutants still contained more ABA than wild type when grown in glucose. Wild type had the least ABA content followed by *Ppppal1* mutants. Both *Ppppal1,2* and *Ppppal2* had the most ABA content, with *Ppppal2* having the highest amount of all samples (Figure 8). Significant differences (P <0.01) in ABA content were observed between wild type and mutants in normal growth conditions (Figure 8). Wild type and *Ppppal1,2* mutant (P <0.05), and wild type and *Ppppal2* mutant (P <0.01) showed significant differences in ABA content when grown in glucose (Figure 8). In addition, significant differences were found between *Ppppal1,2* and *Ppppal1* (P <0.05)*, Ppppal1,2* and *Ppppal2* (P <0.05), and *Ppppal1* and *Ppppal2* (P <0.01) mutants treated with glucose (Figure 8).

Figure 8. Endogenous ABA levels in knockdown mutants and wild type. The samples' abscisic acid levels were determined using both HPLC and LC-MS. The data show that during normal growth conditions mutants contain higher ABA levels than wild type. When samples are treated with glucose, ABA levels increases in wild type but not in the mutants. Mutants contain more ABA than wild type in both growth conditions. The histograms show the average ±SEM of four colonies, error bars indicate standard errors of the mean. The significances of the observed differences between samples were tested using a two-tailed two-sample *t*-test assuming unequal variances.
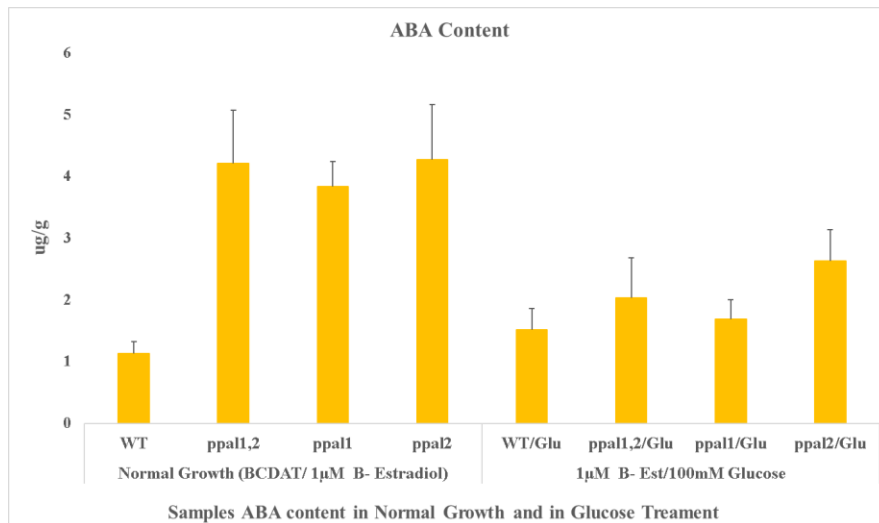
4. DISCUSSION

Central carbon metabolism is vital in all organisms to provide energy and building blocks for biosynthesis of macromolecules. This makes the sensing and allocation of available carbohydrates an important function both for individual cells and for the entire organism (Rolland et al., 2006). Compared to caulonemal cells, chloronemal cells have larger and more well-developed chloroplasts, and sugar transport from chloronemal to caulonemal cells might then help to support the latter cell type. This has important implications for both colony expansion, since caulonemal filaments grow faster, and development, since gametophores usually develop from buds formed on caulonemal filaments. Studies have suggested that a regulated balance exists between chloronemata and caulonemata, and that conditions that inhibit the formation of one of them generally enhance the other (Cove et al., 2006; Jaeger & Moody, 2021; Menand, Calder, et al., 2007; Thelander et al., 2005).

Therefore, the available energy supply may control the balance between chloronemal and caulonemal filament formation. Caulonemal filaments are formed to help to spread the colony in the presence of excess energy, such as during growth in constant high light and glucose medium. When less energy is available, as in low light, there is instead increased formation of the photosynthetically more active chloronemal filaments, which helps to restore the energy supply (Thelander et al., 2005). We confirmed this to be true, when we grew wild type moss in high energy conditions, the transition from chloronema to caulonema was promoted and formation of gametophores from buds in caulonemal cells was induced (Figure 1, A and M). As expected, the opposite happened

when wild type was grown in low energy conditions: caulonema cell transition was restricted and chloronema formation was favored, resulting in inhibition of growth (Figure 1, B and M).

Knockdown *Ppppal* mutants grown in high energy conditions exhibited inhibition of growth and development, as shown by a decrease in caulonema cell formation and a depletion in gametophore number resulting in a small colony (Figure 1, D, G, J and M). The phenotype of mutants grown in high energy conditions resembles that of wild type moss grown in low energy conditions in that colony growth is inhibited and the chloronema to caulonema transition and gametophore development are restricted (Figure 1, B, D, G, J and M). Mutants in low energy conditions behaved similarly to how they behave in high energy conditions, but with a difference in degree of inhibition (Figure 1). Low energy condition further increased inhibition of growth and development, as shown by reduced colony diameter and caulonema formation and no gametophore development (Figure 1, E, H, K and M). The mutants act as starvation mutants when exposed to either high or low energy, thus it seems that the mutants are impaired in sensing and responding to the energy status (Figure 1).

An interesting question is how and what is sensing the availability of energy supply. Glucose occupies a central role in plant metabolism by acting as a metabolic substrate, a signaling molecule, and inducing biological changes at all levels of cellular activity (Jang & Sheen, 1994; Li & Sheen, 2016; Rolland et al., 2006; Sakr et al., 2018). Metabolic sensors are crucial for maintaining energy homeostasis and for serving as cellular energy gauges. Two metabolic sensors that respond to changes in nutrient and energy status in plants are the TOR complex kinase and the plant Snf1-related kinase

(SnRK1). SnRK1 is activated by a decrease in energy level, and TOR kinase is activated by favorable and nutrient-replete conditions (Sheen, 2014; Thelander et al., 2004; Tsai & Gazzarrini, 2014; Wurzinger et al., 2018; Xiong et al., 2013). Another important metabolic sensor is hexokinase (HXK), which has been shown to act as a glucose sensor (Jang et al., 1997; Moore et al., 2003; Nilsson et al., 2011; Olsson et al., 2003; Xiao et al., 2000).

The glucose signaling network modulates the regulatory mechanisms and functions of the three master regulators, hexokinase, SnRK1, and TOR kinase. Hexokinase acts as the direct glucose sensor mediating multiple functions in the glucose response. Glucose inhibits SnRK1 and activates TOR to promote plant growth and development. TOR and SnRK1 act downstream of sugar sensing, and their activities are modulated by the sugar status of plants, mostly uncoupled from hexokinase actions as a glucose sensor. However, hexokinase also contributes to the generation of energy and metabolite signals derived from glucose (Baena-Gonzalez et al., 2007; Jang et al., 1997; Jang & Sheen, 1994; Karve et al., 2010; Kim et al., 2013; Lastdrager et al., 2014; Moore et al., 2003; Nilsson et al., 2011; Olsson et al., 2003; Price et al., 2003; Rolland et al., 2006; Sheen, 2014; Thelander et al., 2004; Tsai & Gazzarrini, 2014; Wurzinger et al., 2018; Xiong et al., 2013).

Plants use hexokinase as a glucose sensor to interrelate light, nutrient, and hormone signaling networks for controlling growth and development in response to the changing environment (Granot et al., 2013; Jang et al., 1997; Moore et al., 2003; Nilsson et al., 2011; Olsson et al., 2003; Xiao et al., 2000). The *Arabidopsis* Type B hexokinase, AtHXK1, has been shown to be involved in hexose sensing and signaling (Jang et al., 1997; Jang & Sheen, 1994; Moore et al., 2003; Xiao et al., 2000). It was found that the glucose induced repression of photosynthetic genes expression, including plastocyanin (PC), the

genes encoding the ribulose-1,5-bisphosphate carboxylase small subunit (RBCS), and the chlorophyll a/b-binding protein (CAB), is mediated through an AtHXK1-dependent pathway (Jang et al., 1997; Jang & Sheen, 1994; Moore et al., 2003; Xiao et al., 2000). In addition, the *Athxk1* loss-of-function mutant is insensitive to the inhibitory effect of high glucose concentrations as well as being cytokinin hypersensitive and auxin insensitive. AtHXK1-signaling positively and negatively interacts with auxin and cytokinin signaling, respectively (Granot et al., 2013; Hutchison & Kieber, 2002; Kushwah & Laxmi, 2014; Sakr et al., 2018). Moreover, glucose signaling mediated by AtHXK1 causes an increase in endogenous ABA levels by inducing both ABA-synthesis and signaling to control seedling development (Arenas-Huertero et al., 2000; Cheng et al., 2002; Leon & Sheen, 2003; Price et al., 2003).

The moss *Physcomitrium* has 11 putative hexokinase genes (Aguilera-Alvarado & Sanchez-Nieto, 2017; Nilsson et al., 2011; Olsson et al., 2003). In *P. patens*, *PpHXK1* gene encodes the major glucose-phosphorylating hexokinase, which accounts for 80% of total activity in protonemal tissue (Aguilera-Alvarado & Sanchez-Nieto, 2017; Nilsson et al., 2011; Olsson et al., 2003; Thelander et al., 2005). It was found that the *Pphxk1* loss-of-function mutant in moss is hypersensitive to both cytokinin (BAP) and abscisic acid (ABA). Caulonema formation is impaired in the *Pphxk1* mutant in the presence of glucose, auxin (NAA), high light and low light. However, there was an increase in caulonema filaments formation when *Pphxk1* mutant was grown in glucose and auxin, but much less compared to wild type (Olsson et al., 2003; Thelander et al., 2005). *Ppppa1* mutant phenotypes share similarities with both *Athxk1* and *Pphxk1* mutant phenotypes. However, PpHXK1 differs from AtHXK1 in that it is a Type A hexokinase that resides inside the

chloroplast stroma, making it less likely to be involved in signal transduction (Nilsson et al., 2011; Olsson et al., 2003; Xiao et al., 2000).

The hexokinase that is more likely to function as a glucose sensor in *P. patens* is type C hexokinase, PpHXK4, which has neither a membrane anchor nor a transit peptide and localizes to the cytosol and to some extent to the nucleus (Aguilera-Alvarado & Sanchez-Nieto, 2017; Claeyssen & Rivoal, 2007; Nilsson et al., 2011; Olsson et al., 2003). In *P. patens*, the double knockout of the genes encoding Snf1-related kinases belonging to the SnRK1 subfamily, PpSNF1a and PpSNF1b, exhibited an opposite phenotype to that of the *Pphxk1* mutant. This further suggests that hexokinase may function upstream of SnRk1(Nilsson et al., 2011; Thelander et al., 2004). *Ppppal* mutants are unable to properly sense the energy status, are insensitive to glucose, and are hypersensitive to ABA treatment. The mutants seem to be in a state of artificial starvation regardless of whether they are exposed to high or low energy conditions. The higher the level of energy to which they are exposed, the more they act as starvation mutants, resulting in increased growth and developmental inhibition (Figure 1).

 Our hypothesis is that to ensure *Ppppal* mutants have the energy to survive, mutants keep metabolic processes that require energy like anabolic pathways at a level lower than wild type. This is shown in part by reduced protein content in mutants compared to wild type when grown in normal growth conditions (Figure 6). In normal growth conditions, we also observed an increased in FAs in mutants *Ppppal1,2* and *Ppppal1* compared to wild type, which could be due to lipid catabolism to release fatty acids to serve as substrates for energy producing pathways (Figure 4). Plants possess the ability to switch between carbohydrates and FAs as respiratory substrates during normal growth (Roth,

Westcott, et al., 2019; Yu et al., 2018). A wide range of biological changes are induced by sugars at all levels of cellular activity from transcription and translation to protein stability and activity. Sugar signaling networks impact thousands of genes, including those involved in DNA and protein synthesis, cell cycle, nucleotide synthesis, amino acid metabolism, glycolysis, TCA cycle, electron transport chain, cell wall synthesis, carotenoid biosynthesis, fatty acid biosynthesis, protein degradation, lipid degradation, amino acid degradation, gluconeogenesis, carbohydrate metabolism, and photosynthesis (Baena-Gonzalez et al., 2007; Li & Sheen, 2016; Li et al., 2006; Osuna et al., 2007; Roth, Gallaher, et al., 2019; Xiong et al., 2013).

Various photosynthetic organisms repress photosynthesis, reduce Calvin cycle enzymes, decrease chlorophyll, and/or accumulate lipids and/or starch in response to glucose treatment (Ahuatzi et al., 2004; MATSUKA et al., 1969; Rolland et al., 2006; Roth, Gallaher, et al., 2019; Sheen, 2014; SHIHIRA-ISHIKAWA & HASE, 1964). Judging by to *Ppppal* mutants' insensitivity to glucose treatment, they seem to not be able to respond to the glucose mediated inhibition of photosynthesis seen in other organisms. Glucose treatment induces first an accumulation of glucose that then creates a feedback inhibition on photosynthesis, which leads to a decrease in overall protein production, especially protein related to the photosynthetic apparatus (Aguilera-Alvarado & Sanchez-Nieto, 2017; Rolland et al., 2006; Roth, Gallaher, et al., 2019; Roth, Westcott, et al., 2019; Xiao et al., 2000). This is likely the reason we see a drastic decrease in protein content in wild type grown in glucose, compared to normal growth conditions (Figure 6). However, the data show that mutants do not respond to the glucose mediated inhibition of photosynthesis, as we observed an increase in protein content for all three knockdown mutants instead of a

decrease when grown in glucose, which is true in the *hxk1* mutant (Figure 6) (Moore et al., 2003; Roth, Westcott, et al., 2019; Xiao et al., 2000).

In addition, solid assay data show that there is an increase in glucan content when wild type is treated with glucose, which did not happen in the mutants (Figure 7). Moreover, glucose treatment also increased FAs content in wild type and mutants *Ppppal1,2* and *Ppppal2* compared to normal growth conditions (Figure 4). For wild type, this can be explained by glucose treatment serving as a carbon source, thus there is no need to produce more glucose. As a result, glucose signaling inhibits photosynthesis, and, since there is less glucose for respiration, fatty acids can serve as candidates for respiration instead (Aguilera-Alvarado & Sanchez-Nieto, 2017; Jang et al., 1997; Kim et al., 2013; Moore et al., 2003; Nilsson et al., 2011; Rolland et al., 2006; Roth, Westcott, et al., 2019; Xiao et al., 2000). For *Ppppal* mutants, however, it seems that since they cannot properly sense the energy status, when grown in increasing high energy conditions like in glucose medium, the more they sense that there is less energy available, so they keep photosynthesis going to make sure they have substrates for respiration. But they also make sure to have fatty acids available to ensure that there are other substrates that can be used for energy production during respiration. When grown in glucose, *Ppppal* mutants seem to exhibit an overall increase in protein and fatty acid content while growth and development are highly inhibited (Figures 4 and 6). Glucose treatment also increased terpenoid content in wild type (Figure 5). Glucose treatment did not increase terpenoid levels in *Ppppal* mutants, which was also true in the *hxk1* mutant (Figure 5) (Roth, Westcott, et al., 2019).

Furthermore, glucose signaling mediated by hexokinase increases ABA content (Arenas-Huertero et al., 2000; Cheng et al., 2002; Leon & Sheen, 2003; Price et al., 2003), which was observed in wild type but not in the mutants when grown in glucose (Figure 8). However, mutants contain higher ABA content than wild type when grown in either normal growth conditions or in glucose (Figure 8). This explains the hypersensitivity of mutants to ABA treatment: mutants seem to respond to the vegetative stress response caused by ABA independent of hexokinase. The data serve as evidence that demonstrates that mutants are defective in their response to glucose. The fact that we see differences between *Ppppal* knockdown mutants as we are performing these assays serve as indication of both differences and similarity of function. Hexokinase is essential for mediating glucose response and signaling, to increase glucose accumulation leading to the shutdown of photosynthesis, proper response to auxin, cytokinin, and ABA to guide growth and development, and upregulation of ABA signaling and synthesis, among other things. The hexokinase in *P. patens* that acts as a glucose sensor, possibly PpHXK4, may be affected in *Ppppal* mutants. This could help explain at least partially the *Ppppal* mutants' phenotype, suggesting that any glucose induced signaling mediated by hexokinase would be affected as observed in the mutants.

In addition, *PpPPAL* could mediate the response to changes in nutrient and energy status by regulating the energy and metabolic sensors SnRK1 and TOR, as we observe that mutants behave as starvation mutants in both high and low energy conditions. Since the glucose signals that control SnRK1 and TOR mechanisms and functions are suggested to be mostly uncoupled from hexokinase function as a glucose sensor, PpPPAL

could not only be a regulator of the hexokinase dependent glucose signaling pathway, but PpPPAL could also mediate the glucose signals that modulate SnRK1 and TOR function. Thus, it seems that PpPPAL is important for sensing and responding to the nutrient and energy status and for regulating factors that control growth, propagation, development, glucose response, and hormone responses in *P. patens.* It makes sense for PpPPAL to have various vital functions in *P. patens*, has both homologs are required for viability.

One question that arose upon the discovery of two *PPAL* homologs in *P. patens* was whether they have the same or diverged function. Both are required for viability (Thole et al., 2014), but either *PpPPAL1* or *PpPPAL2* can rescue the *ppal* mutant of *Arabidopsis* (see Manuscript 1). The differing responses of *Ppppal1*, *Ppppal2*, and the double *Ppppal1,2* knockdowns suggest that there are both overlapping and separate functions for the PPAL homologs, warranting further investigation. Future studies focusing on the integration of sensitive proteomic analysis, and powerful functional genomic and chemical screens, will enable the identification and characterization of factors like PpPPAL, that participate in sugar, energy, and hormone signaling pathways to learn more about how these pathways are connected, and how they work together to drive growth and developmental programs (de Jong et al., 2014; Sheen, 2014; Urano et al., 2012).

MANUSCRIPT 3

CHARACTERIZATION OF NOVEL MOSS BIOMASS, *PHYSCOMITRIUM PATENS*, AS A CANDIDATE BIOMASS FEEDSTOCK FOR BIOFUEL PRODUCTION

INTRODUCTION

Modern society has immense energy demands that accelerate the rate of increase in global greenhouse gas (GHG) emissions. The overuse of fossil fuels such as coal, petroleum oil, natural gas, and its derivatives such as diesel and gasoline have environmental impacts in water, soil, and air pollution and the mobilization of tons of carbon from subsoil to the atmosphere leading to global warming. The search for renewable, more carbon-neutral sources, has encouraged global bioresearch to find new biomass to alleviate and/or replace the dependency on fossil fuels. Biomass includes all the organic materials that conduct photosynthesis such as moss, softwood, hardwood, algae, herbs, and all organic-biodegradable waste. Most biofuels are being produced by fermentation of plant-derived free or polymerized sugars, or by transesterification of plant oils. Specially, ethanol, as the final fermentation product of carbohydrate consuming organisms like *Saccharomyces cerevisiae*, is essential for bioethanol production (Groves et al., 2018; Hill et al., 2006; Jeswani et al., 2020; Charles E. Wyman, 1999).

First-generation biofuels produced from biomass that is also used for food, such as sugarcane and sugar beet, often offers at best minor benefits compared to fossil fuels, given the high agricultural inputs to the crop feedstock. This, alongside the increasing global food demand and the limitation of agricultural expansion, has hindered the expansion of such first-generation biofuels, resulting in a shift to a more sustainable biofuel production based on nonfood plant biomasses like softwoods (pine) and moss (*Physcomitrium patens*) (Groves et al., 2018; Hill et al., 2006; Jeswani et al., 2020; Charles E. Wyman, 1999). Various lignocellulosic biomasses, like rice straw and softwood, have been used as a renewable feedstock to produce biofuels and bioproducts. However, various challenges have arisen, including the highly cross-linked nature of these lignocellulosic biomasses, which restricts enzyme access to its sugars. Thus, to access the sugars, harsh pretreatment (180−280 °C) conditions and/or high enzyme loading are often implemented. These severe conditions are not desirable, as it contributes to sugar degradation, increased costs, and lignin condensation which makes difficult lignin utilization (Hossain et al., 2020; Hossain et al., 2021).

Less disruptive pretreatments include cellulose solvents, like deep eutectic solvents (DESs) and H_3PO_4, which allow for the dissolution of lignocellulose and separation the lignocellulose components. Pretreatment with H_3PO_4 decrystallizes the highly ordered cellulose structure and disrupts the lignin-carbohydrate complex (LCC) linkages. DESs solvents interact with lignin groups to enable lignin fractionation for better cellulose accessibility. However, both solvent pretreatments present challenges, such as the fractioning of lignin without affecting glucan, preservation of lignin, enzyme loading, and reaction conditions. Although plant lignocellulosic biomasses like pine and rice straw are

of great potential as a feedstock to produce bioproducts and biofuels, because of their complex cross-linked structure, pretreatment is required to maximize glucan yield for fermentation (Chen & Mu, 2019; Herbaut et al., 2018; Hossain et al., 2020; Hossain et al., 2021; Md Khairul Islam et al., 2020; Peter R. Seidl & Adriana K. Goulart, 2016; Xu et al., 2016; Zhu et al., 2010).

As a result, this research is intended to investigate the potential of the moss *Physcomitrium patens* (*P. patens*), previously known as *Physcometrilla Patens,* in the production of biofuels. As one of the earliest plants to colonize land, *P. patens* leads a haploid-dominant life cycle. The haploid gametophyte is characterized by two important developmental stages: protonema and gametophore (or leafy shoot). Protonema is a filamentous tissue composed of chloronema and caulonema cells. The gametophore differentiates from protonemal buds that initiate reproductive organs and anchoring root-like structures called rhizoids. Chloronema cells are rich in chloroplasts and are the first cell type present following spore germination or from regeneration from protoplasts. Caulonema cells are the result of a transition from select chloronemal apical cells. They divide and grow quickly, facilitating colonization and spreading, and contain fewer chloroplasts (Antimisiaris & Running, 2014; Cove et al., 2006; Decker et al., 2006; Menand, Calder, et al., 2007).

In addition, *P. patens* is unique among plants in that it allows for stable and efficient gene targeting and replacement, because of its specifically high rate of homologous recombination (Kamisugi et al., 2006; Khraiwesh et al., 2008; Schaefer, 2002; Schaefer & Zryd, 1997). The moss *P. patens* grows naturally in moist open soil along paths or in fields, and in wet areas such as flood plains of lakes and edges of rice fields (Rensing

et al., 2020). This moss tolerates dehydration and does not demand any special care, fertilizer, and nutrient except optimal environments (Roberts et al., 2012). In addition, *P. patens* is also grown for research in controlled lab conditions (temperature bellow 28°C) using growth chambers and bioreactors for large scale production. In this paper we would like to propose moss, especially *Physcomitrium patens,* as a renewable biomass feedstock for biofuel production. Here we describe a biological and chemical technology for the conversion of lignocellulose-derived glucose from moss into biofuel (**Scheme 1**). First the moss was hydrolyzed with commercial enzymes at 15 g glucan/L and 10 mg proteins/g glucan. We obtained a 96% glucose yield and a 13.32 g/L glucose solution from enzymatic hydrolysis. Finally, we presented the moss lignocellulose-derived glucose to *Saccharomyces cerevisiae BY4743* strain and obtained 7.8 g ethanol/L.
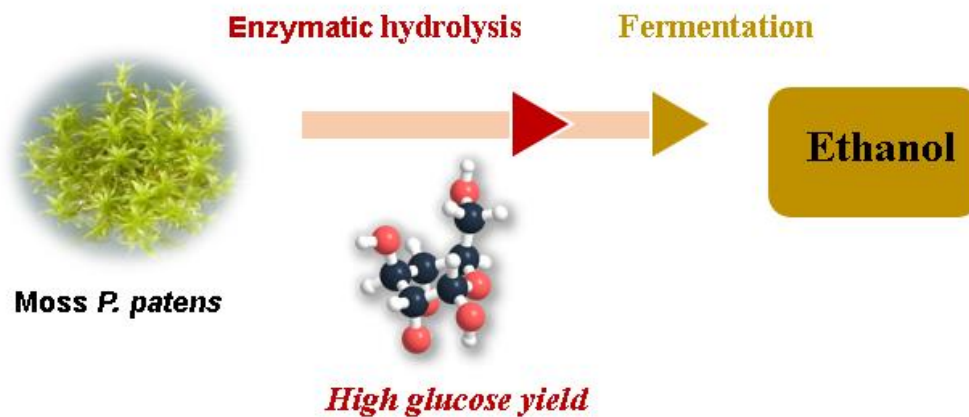
Scheme 1. Biofuels production from moss *Physcomitrium Patens*.

2. MATERIALS AND METHODS

2.1 Plant materials and growth conditions

For small-scale production, moss wild type protonemal tissue was subcultured using a Polytron homogenizer T20B.S1 (IKA) and grown on BCDAT media (https://moss.nibb.ac.jp/protocol.html) with cellophane for 7 days. Moss was grown at 25°C under continuous light at 50 µmol m^{-2} s^{-1} intensity.

2.2 Composition Analysis of biomass

The composition of moss biomass was determined by National Renewable Energy Laboratory analytical procedures (Sluiter et al., 2012). An Agilent 1100 HPLC equipped with a refractive index detector (RID) and a diode array detector (DAD) was used to analyze all sugar concentrations in the acid-digested solutions. Sugars were separated at 60 ^{o}C using the Aminex HPX-87H column (300 x 7.8 mm, Bio-Rad®, Hercules, CA, USA) with 0.6 ml/min of 4 mM H_2SO_4 as a mobile phase. The RID signals' peak area (HMF and furfural were determined by DAD signals at 280 nm) was used to determine the concentrations of sugars. All sugars were calibrated against certified standards (Absolute Standards Inc., Hamden, CT, USA).

2.3 Enzymatic Hydrolysis

Enzymatic hydrolysis of moss was conducted in 50 mM phosphate buffer, pH 4.5 (6.80 g of potassium dihydrogen phosphate in 1 L water (European Directorate for the Quality of Medicines & HealthCare, 2011)) with a solid loading of 30 g glucan/L (23.2 g biomass/L) in 50 mL centrifuge tubes. A rotary oven was used to control the hydrolysis temperature.

Hydrolysis was performed in a rotary shaker at 50°C at 250 rpm. Stir bars were custom-made using a quartz coated steel rod (5 mm inner diameter x 50 mm length) to ensure uniform mixing of the solid slurry and enzymes. The enzyme loading was 30 mg protein/g glucan, unless otherwise noted. The Novozyme® cellulase (Ctec 2, protein concentration: 188 mg protein/mL) to hemicellulose (Htec 2, protein concentration: 190 mg protein/mL) ratio of 9/1 (v/v) was used or otherwise described. Enzymatic glucose yield was calculated by Eq. 1:

$$\text{Enzymatic glucose yield (\%)} = \frac{\text{glucose released by enzymes (g)}}{\text{glucose equivalent in the treated solid (g)}} \times 100 \qquad (1)$$

2.4 Yeast strain, media, and cultivation

The diploid *Saccharomyces cerevisiae* BY4743 wild type strain, generated from a cross between BY4741 and BY4742, which themselves are derived from S288C, was used. The strain was stored in potato agar slants at 4°C. For the inoculum preparation of *S. cerevisiae*, a loopful of cells were added to 250 mL E-flask containing 100 mL of sterile culture medium in which the concentrations of nutrients in g/L were: yeast extract, 0.5; Na_2HPO_4, 0.5; glucose, 20; urea, 1; $(NH_4)2SO_4$, 1; $FeSO_4$, 0.001; KH_2PO_4, 2.5; $MgSO_4$, 1. The E-flask was incubated in a rotary shaker at 30°C and 150 rpm for 48 hours, following a published protocol (Ge et al., 2011).

2.5 Fermentation of moss hydrolysate into bioethanol

The moss enzymatic hydrolysate was concentrated by rotary evaporation and was sterilized at 121 °C for 15 min. Fermentation was performed in a flask at 30 °C and pH 6.5 consisting of supplementary nutrients, concentrated hydrolysate, and inoculum of yeast (1.3 x 108 /mL). The final concentration of nutrients was 0.9 g/L $(NH_4)2SO_4$ and 0.375 g/L yeast extract (Staniszewski et al., 2009). The flask was sealed with rubber stopper through which

hypodermic needles had been inserted for the removal of the CO_2 produced. The flask was incubated for 36 hours and stirred at times. Samples were withdrawn after fermentation for 0, 12, 24 and 36 h, respectively and analyzed with regard to the content of ethanol and residual glucose. Fermentation experiments were performed in triplicate following a published protocol from (Ge et al., 2011).

2.6 Characterization of moss *P. patens* biomass

To determine the physiochemical characteristics of moss biomass, X-ray diffraction (XRD) and Fourier-transform infrared spectroscopy (FTIR) were used.

2.6.1. X-ray Diffraction (XRD)

To determine the degree of crystallinity, X-ray diffraction was performed on *P. patens* using the Bruker D8 (Billerica, MA, USA) with CuKα radiation ($\lambda = 0.15418$ Å). The scanning rate was 0.5 seconds/step (0.02 step increment), ranging from 10° to 45° unless otherwise noted.

2.6.2. Fourier-transform infrared (FTIR) spectroscopy

The JASCO 4700 FT-IR Spectrometer (Akron, OH, USA) equipped with Attenuated Total Reflection (ATR, Pike Technologies, Madison, WI, USA) was utilized to characterize the changes in the chemical structures of moss (bond strength between sugar monomers and lignin-carbohydrates). Moss biomass was scanned in the spectral range between 400 and 4000 cm^{-1} for 256 scans at 4 cm^{-1} resolution.

2.7 Transmission electron microscopy (TEM)

Moss was grown on BCDAT medium supplemented with 0.5% glucose and 0.4% 354 gellan gum and cultured for 6 days under white light. For transmission electron microscopy (TEM) they were processed following published protocols (Pressel et al., 2008). Briefly, the moss tissues were fixed in a fixative containing 3 % (v/v) glutaraldehyde, 1 % (v/v) formaldehyde (freshly prepared from paraformaldehyde) and 0.5 % (w/v) tannic acid in 0.05 M Na-phosphate buffer (pH 7.0) for 3 h at room temperature. After rinsing in 0.1 M Na-phosphate buffer, the material was post-fixed with 1 % (w/v) osmium tetroxide in 0.1 M Na-phosphate buffer (pH 6.8) overnight at 4°C, dehydrated through an ethanol series as above and embedded in Embed resin via propylene oxide (Electron Microscopy Sciences). Ultrathin sections (60 nm) were cut using a diamond knife and were sequentially stained with 8 % (v/v) methanolic uranyl acetate for 30 min and lead citrate for 2 min, and the sections were examined with an HT7700 electron microscope (Hitachi).

2.8 Calcofluor white microscopy

Calcofluor white (Sigma, 18909-100ML-F) was filter sterilized with a 0.22 μm filter and stored at 4°C before use. About 3 mm diameter of moss protonemal tissue was mixed with 10 μl of the sterilized calcofluor white for 2 min. A Nikon TE200 microscope equipped with a DS-U3 camera was used for visualization of samples in the light field and treated with calcofluor with the 418 nm laser.

3. RESULTS

3.1. Cell wall chemical composition of moss *P. patens*

To study the cell wall composition of wild type moss, the National Renewable Energy Laboratory analytical (NREL LAP) procedure was used. All sugars and organic acid concentrations in the acid-digested solution was analyzed by HPLC equipped with a refractive index detector (RID) and a diode array detector (DAD). Table 1 shows the sugar content found in moss. We observed that the amount of cellulose (15-50 wt.%) found in *P. patens* is comparable to other lignocelluloses such as rice straw, agricultural wastes like wheat straw and cotton gin, and softwoods like yellow pine and Douglas fir, among others (Abdeshahian et al., 2020; Espiñeira et al., 2011; Hossain et al., 2020; Hossain et al., 2021; Mishima et al., 2008; Weng & Chapple, 2010; Xu et al., 2009). The hemicelluloses xylan and arabinan content are also comparable to other lignocelluloses (0.1-25 wt.%) (Abdeshahian et al., 2020; Espiñeira et al., 2011; Hossain et al., 2020; Hossain et al., 2021; Mishima et al., 2008; Weng & Chapple, 2010; Xu et al., 2009). In addition, lignin was not found in *Physcomitrium* (Espiñeira et al., 2011; Weng & Chapple, 2010; Xu et al., 2009).

Composition	Glucan (wt. %)	Xylan (wt. %)	Arabinan (wt. %)	*Other (wt. %)
Wild type	32.2	4.08	1.06	62.7

Table 1. Solid composition of moss *Physcomitrium Patens* (wt. % (g)). *Others (proteins and extractives). Each data point is the average of three independent biological replicates.

No significant differences were found among the replicates. Differences were tested using a two-tailed two-sample *t*-test assuming unequal variances.

3.1. Mass balance of *P. patens* biomass for enzymatic hydrolysis

Lignocellulosic biomass often requires pretreatment to maximize sugar yield for fermentation, due to its complex cross-linked structure and the presence of lignin and crystalline cellulose (Espiñeira et al., 2011; Hossain et al., 2020; Hossain et al., 2021; Md Khairul Islam et al., 2020; Peter R. Seidl & Adriana K. Goulart, 2016; Weng & Chapple, 2010; Xu et al., 2016; Xu et al., 2009; Zhu et al., 2010). To assess whether *P. patens* requires any pretreatment, the enzymatic hydrolysis of moss biomass was conducted with a solid loading of 10 g glucan/L along with 10 mg protein/g glucan as a control. We obtained 94% glucose yield after 72 h (Figure 2). The high enzymatic hydrolysis yield of glucose suggested that *P. patens* biomass does not require mild or harsh pretreatment conditions to access its sugars.

To corroborate the results, we then proceeded to hydrolyze the moss using 15g glucan/L, higher solid loading than that of the control (Figure 2). At this solid loading the moss lignocellulose first acted like a sponge and formed a viscous slurry, then it became thinner after 24h. As shown in the mass balance (Figure 1), the enzymatic hydrolysis of 100g moss lignocellulose resulted in 96% glucose yield and a 13.32 g/L glucose solution after 72h (Figure 2). The high enzymatic hydrolysis yield of glucose at a high glucan loading further suggests that moss lignocellulose can be used as is, without the need for

pretreatment to access cellulose. The resulting moss hydrolysate was then presented to *Saccharomyces cerevisiae* BY4743 strain for the fermentation assay.

Hydrolysis (50C°, Ph= 4.8, 72h)
15 g glucan/L, 10 mg proteins/g glucan

Moss Biomass

Enzymatic Hydrolysis

Fermentation

(1)

(2) Solid

(3) Liquid

100 g dry weight
32.2 g glucan
4.08 g xylan
1.06 g arabinan
62.66 g others

Solids: 47.24 g
5.8 g glucan
0.2 g xylan
0.04 g arabinan
41.2 g others

96% Glucose Yield
Enzymatic Hydrolysate
13.32 g/L Glucose
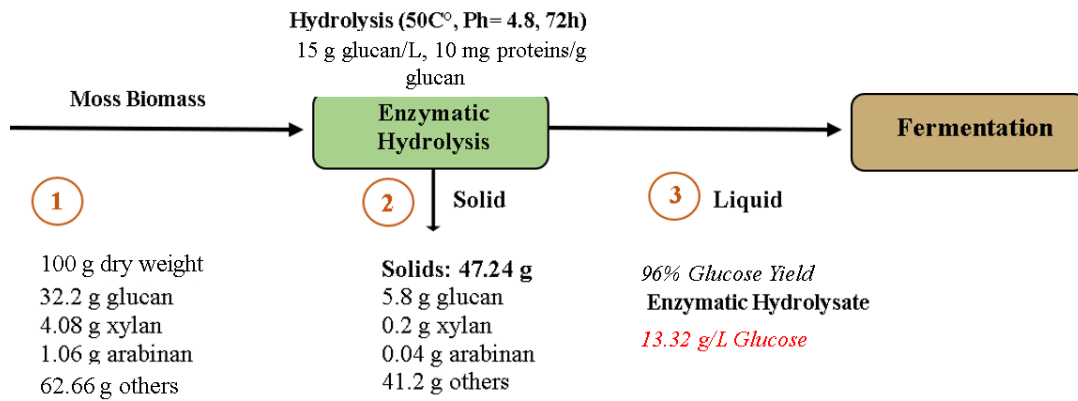
Figure 1. Mass balance of sugar release from moss biomass. Each data point is the average of three independent biological replicates. No significant differences were found among the replicates. Differences were tested using a two-tailed two-sample *t*-test assuming unequal variances.
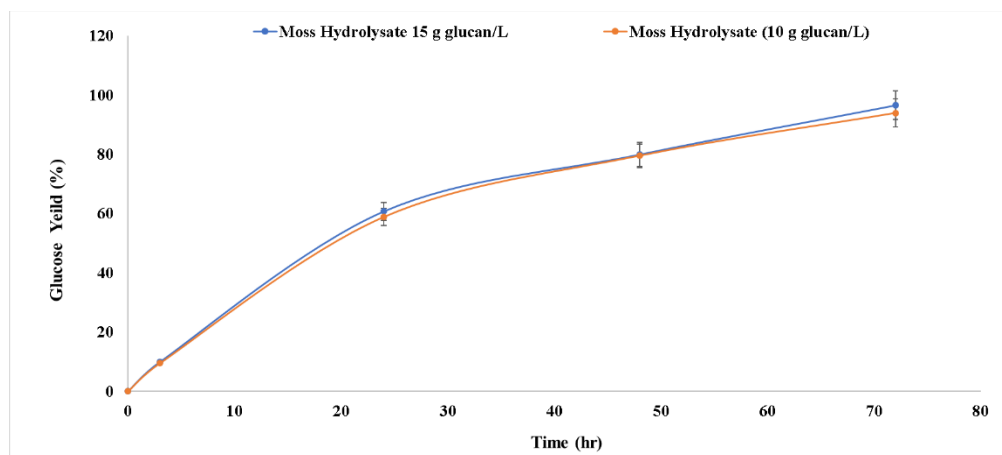
Figure 2. Glucose yield during enzymatic hydrolysis of *P. patens* at 10g glucan/ L, ,10mg proteins/g glucan (94% glucose yield) and 15g glucan/L,10mg proteins/g glucan (96% glucose yield) solid loading. The data show that high glucose yield can be obtained at both low (10g glucan/ L) and high (15g glucan/ L) solid loading. Each data point is the average of three independent biological replicates, SEM error bar. No significant differences were found among the replicates. Differences were tested using a two-tailed two-sample *t*-test assuming unequal variances.

3.2. Characterization of moss biomass

To identify the functional groups and chemical bonds responsible for the high enzymatic glucose yield at a high glucan loading, moss biomass was characterized using FTIR (Figure 3) and XRD (Figure 4). FTIR spectra give the comprehensive information of protein, carbohydrate, nucleic acid, lipid, cellulose, and hemicellulose in moss biomass. Absorption bands from Figure 3 in the range 895 to 4000 cm−1 are due to functional groups. Absorption bands located around 3292 cm−1 correspond to O–H and N–H

stretching vibrations that mainly occur from proteins and carbohydrates. The bands around 2859 and 2920 cm−1 represent C–H stretching vibrations that are caused by the presence of polysaccharides, lipids, and carbohydrates. Absorption bands around 1745 cm−1 correspond to an isolated carbonyl group (COOR), indicating ester-containing compounds commonly found in membrane lipid and cell wall pectin (Cao et al., 2014; Hossain et al., 2020; Hossain et al., 2021; Hu et al., 2011).

Three protein absorption bands located around 1640 (C=O), 1548 (N–H) and 1250 (C–N) cm−1 are assigned as amide I, II and III bands, respectively. The peaks from 1200 cm−1 to 400 cm−1can be attributed to the transmittance of low-molecular weight carbohydrates and celluloses; this region is characterized as the fingerprint. The peaks at 1152, 1110, and 1023 cm−1 are associated with the amorphous cellulose region. The 1152 cm−1 band is mostly due to the antisymmetric C–O–C stretching mode of the glycosidic linkage. The 1110 cm−1 band corresponds to the C–O stretching mode of secondary alcohols. The peak at 1023 cm−1 can be attributed to oligosaccharides, glycoprotein, and C–O stretching mode of primary alcohols in amorphous celluloses (Figure 3) (Cao et al., 2014; Hossain et al., 2020; Hossain et al., 2021; Hu et al., 2011).

The 956 to 850 cm−1 region corresponds to crystalline celluloses. The 956 cm−1 band comes from the C–O stretching mode of primary alcohols in crystalline celluloses. The band at 895 cm−1, from the 956 to 850 cm−1 region, is associated with anomeric vibration at β-glycosidic linkage in cellulose. The absorbance regions related to the presence of lignin includes ketone/aldehyde C=O stretching at 1730 cm−1, C= O stretch and aromatic skeletal vibrations at 1595 cm−1, aromatic ring stretch in lignin at 1507 cm−1, in-plane C−H deformations of lignin at 1451 cm−1, CH₂ bending vibration from

cellulose and lignin at 1430 cm−1, and C−O stretching in guaiacyl ring at 1263 cm−1 (Figure 3) (Cao et al., 2014; Hossain et al., 2020; Hossain et al., 2021; Hu et al., 2011).

The FTIR spectra revealed that the vibrations mode from the absorbance region associated with the presence of lignin are not present (Figure 3). We also observed high band intensity associated with the amorphous cellulose region but not in the crystalline cellulose region (Figure 3). The XRD patterns of moss biomass further confirmed these results (Figure 4). Standard cellulose shows diffraction peaks at 14.9°, 16.5°, and 22.5°, which are characteristic of the crystalline form of cellulose (Lim et al., 2015; Oubani et al., 2011). However, *P. patens* XRD spectra showed no sharp peaks, indicating a lack of crystallinity and thus a transition of the structure of cellulose from crystalline to amorphous region (Figure 4) (Lim et al., 2015; Oubani et al., 2011). Imaging of *P. patens* protonemal cell (Figure 5) shows the simplicity of moss tissue and its characteristic thin cell wall. Overall, these characterization results suggested that the lack of lignin, predominance of amorphous cellulose, and thin cell walls and the simple cell plan in moss biomass contributed to the cellulose accessibility to enzymes and facilitated the high sugar release.
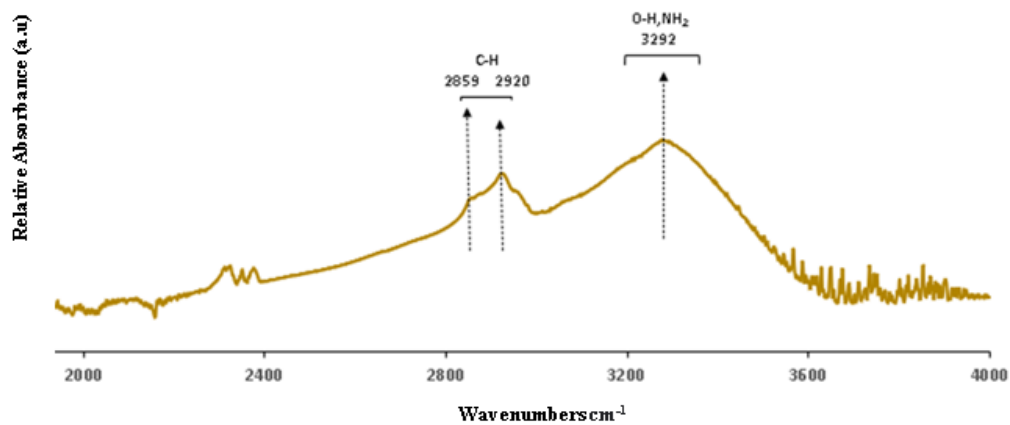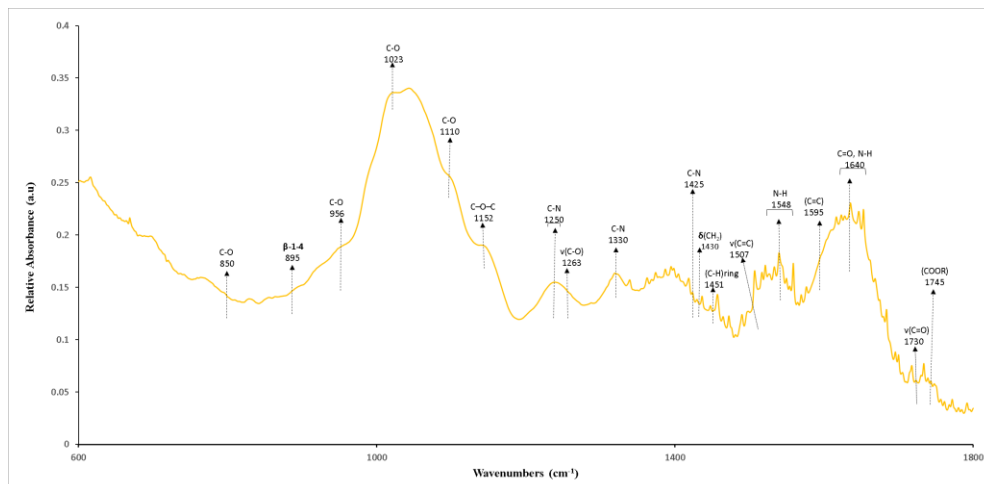
Figure 3. FTIR spectra of moss *P. patens* biomass. Absorbance range from 600 to 4000 cm^{-1} shows functional groups and chemical bonds present in moss.
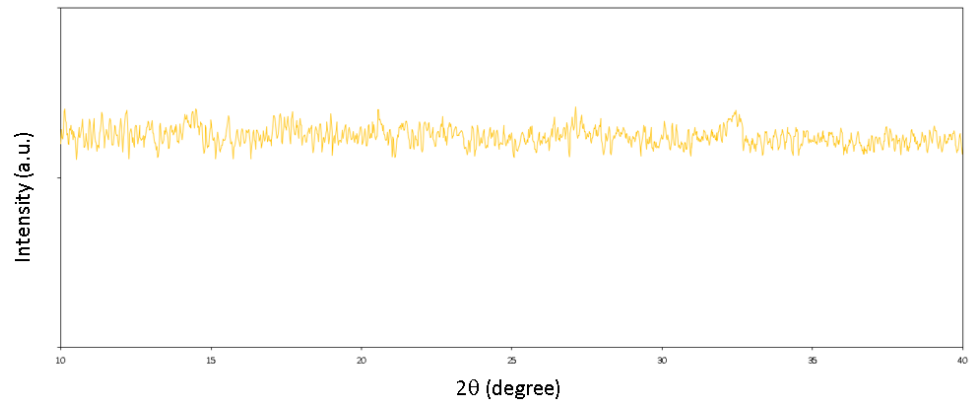
Figure 4. XRD spectra of moss *P. patens* biomass. Shows the amorphous nature of moss biomass.

A

B

C
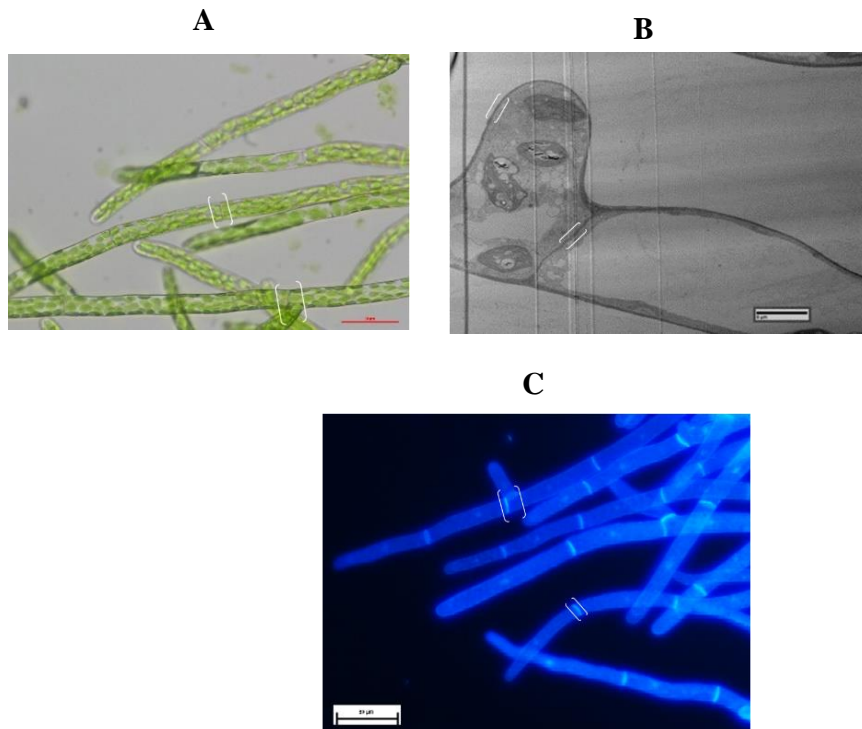
Figure 5. Imaging of moss *P. patens* protonemata. (A) Image of filamentous protonemata with a light microscope, scale 50μm. (B) TEM image of a protonemal cell, scale 8μm. (C) Calcofluor white fluorescent dye specific for fibrillar β (1→4) glucans of plant cell walls such as cellulose, scale 50μm. (A) and (C) were imaged using a Nikon TE200 microscope equipped with a DS-U3 camera and (B) was imaged with a HT7700 electron microscope (Hitachi). White 〔〕 shows the thin cell wall of moss simple tissue.

3.3. Fermentation of enzymatically derived moss sugars into ethanol

Moss sugar hydrolysate was presented to *S. cerevisiae* BY4743. The hydrolysate was concentrated by rotary evaporation. The ethanol production by *S. cerevisiae* from concentrated moss hydrolysate is shown in Figure 6. After cultivation for 36 hours, an ethanol yield of 7.8 g/L was reached in fermentation medium containing (glucose 13.32 g/L) moss hydrolysate as the fermentation substrate. The ethanol conversion rate of concentrated hydrolysate was 58.6%, which corresponded to 16.74 weight % ethanol with respect to biomass. The result demonstrated that 7.8 g/L ethanol could be produced from 100 g moss dry weight, which is a 0.1674 g g dry -1 ethanol yield per unit of biomass.
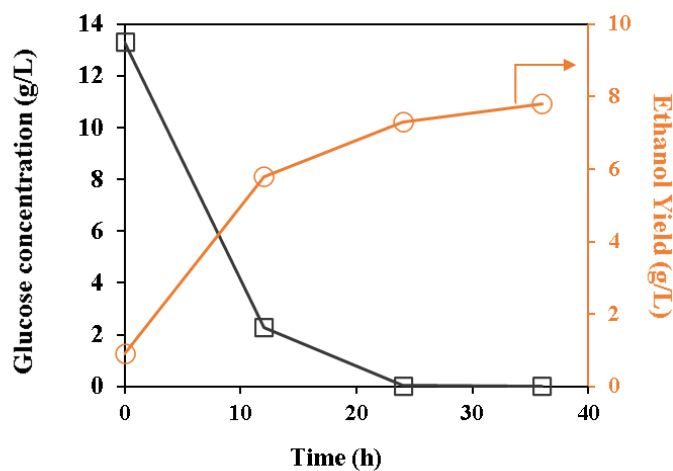
Figure 6. Fermentation of ethanol by *S. cerevisiae* BY4743 at 30 °C using moss hydrolysate (glucose content, 13.32 g/L) as the substrate. The moss hydrolysate was prepared by enzymatic hydrolysis using 15g glucan /L, 10mg proteins/g glucan at 50 °C, pH 4.5 for 72 h. Glucose consumption and ethanol yield in fermentation medium was monitored by SBA-40C biology analyzer. The conversion rate of ethanol was calculated according to the ratio of ethanol yield and initial glucose content in the fermentation medium.

DISCUSSION

The main challenge of using lignocellulosic materials for the generation of bioethanol is the low conversion of cellulose and hemicellulose because of the presence of lignin and crystalline cellulose. Therefore, various technologies for ethanol production from lignocellulosic material conversion processes are being developed, primarily focused on lignocellulose pretreatment. Pretreatment methods are either chemical or physical, while some incorporate both effects. A variety of pretreatments, such as dilute acid, liquid hot water, cellulose dissolution reagents, alkaline wet oxidation, microbial pretreatment, and lime pretreatment, have been used to improve the saccharification of the feedstocks. The purpose of pretreatments is to hydrolyze much of the hemicellulose, solubilize or disrupt the lignin, and break down the crystalline structure of cellulose (Den et al., 2018b; Ge et al., 2011; Herbaut et al., 2018; Hossain et al., 2020; Hossain et al., 2021; Mishima et al., 2008; Oubani et al., 2011).

The use of these pretreatment conditions, however, presents a major challenge in creating profitable biorefineries and facilitating the bioeconomy (Chen & Mu, 2019; Den et al., 2018a; M. K. Islam et al., 2020; Lynd et al., 1999; Mishima et al., 2008; P. R. Seidl & A. K. Goulart, 2016; C. E. Wyman, 1999; Yang et al., 2018; Zheng et al., 2009). We demonstrated the efficiency and potential of the moss *P. patens* for the biological-chemical conversion of moss biomass into biofuels. The contents of cellulose, hemicellulose, and lignin in common lignocelluloses like corn straw, rice straw, and wheat straw ranges from 0.1-50% (Abdeshahian et al., 2020; Chen & Mu, 2019; Ge et al., 2011; Groves et al., 2018; Herbaut et al., 2018; Hossain et al., 2020; Hossain et al., 2021). In this study, we showed that cellulose comprises 32.2% of the dry weight of *P. patens* and the hemicellulose content

is only around 5.0% (Table1). The HPLC analysis of the hydrolysate confirmed that glucose was the main component of moss (Table 1 and Figure 2). The chemical composition of *P. patens* makes it a very promising substrate for ethanol production (Table 1 and Figure 1).

A significant finding is that *P. patens* biomass does not require any pretreatment for overcoming biomass recalcitrance prior to enzymatic hydrolysis and yeast fermentation for bioethanol production. This is important, as either mild or harsh pretreatments promote formation of degradation products like furans, which are common inhibitors of fermentation. Consequently, a detoxification step before fermentation is required; unfortunately, this increases the cost of the process. The high sugar yield obtained from hydrolysis of moss biomass minimized cost by eliminating the necessity of pretreatment, detoxifying, and concentrating the sugars for downstream conversion (Figure 1 and 2) (Chen & Mu, 2019; Den et al., 2018b; Ge et al., 2011; Herbaut et al., 2018; Hill et al., 2006; Hossain et al., 2020; Hossain et al., 2021; Mishima et al., 2008; Oubani et al., 2011). The resulting moss glucose was a direct precursor for bioethanol production (Figure 1).

Another significant finding was revealed by XRD spectra showing that *P. patens* has an amorphous biomass, which means there is no crystallinity (Figure 4) (Hossain et al., 2020; Hossain et al., 2021; Oubani et al., 2011). Cellulose crystallinity has a critical effect on enzymatic hydrolysis. High amounts of crystalline material in cellulose causes low cellulose accessibility by cellulase. Cellulase readily hydrolyzes the more accessible amorphous portion of cellulose, but the enzyme is not as effective in degrading the less

accessible crystalline portion (Hossain et al., 2020; Hossain et al., 2021; Mishima et al., 2008). Other factors hinder enzymatic hydrolysis and fermentation, include the presence of lignin and hemicelluloses in lignocellulosic biomass. In the plant cell wall, lignin acts as a glue to bind cellulose and hemicellulose together. Hence, various treatment processes have been developed to remove lignin for enhanced cellulose accessibility to enzymes and sugar release (Chen & Mu, 2019; Den et al., 2018b; Espiñeira et al., 2011; Ge et al., 2011; Herbaut et al., 2018; Hossain et al., 2020; Hossain et al., 2021; Weng & Chapple, 2010; Charles E. Wyman, 1999; Xu et al., 2009).

Other moss species have lignin monomers and are capable of lignification. However, FTIR spectra and compositional analysis demonstrated that *P. patens* does not have lignin monomers (Table 1 and Figure 3). This finding agrees with other studies suggesting that *P. patens* is not capable of lignification (Espiñeira et al., 2011; Ligrone et al., 2000). The presence of lignin in the *P. patens* cell wall has not been reported; however, a study reported the presence of lignans, which are lignin-like compounds, related to the plant defense system against pathogens (Espiñeira et al., 2011; Ligrone et al., 2000; Martínez-Cortés et al., 2021; Otero-Blanca et al., 2021). Furthermore, as other studies suggested, we found that the protonema of *P. patens* has a very low content of the hemicelluloses xylan and arabinan compared to other plant biomasses (Table 1) (Dehors et al., 2019; Roberts et al., 2012). Low lignin, xylan, and arabinan content allows for greater enzyme adsorption and enhanced cellulose digestibility (Kumar et al., 2018; Siqueira et al., 2017; Zoghlami & Paes, 2019).

P. patens protonemal tissue is a two-dimensional polarized network of filaments, comprising single cells arranged in linear branching arrays. The gametophore emerges from a protonemal filament as a single cell that undergoes a series of stereotypic cell divisions, switching from polarized expansion to three-dimensional diffuse expansion (Harrison et al., 2009; Rensing et al., 2020). Gametophore leaflets are only a single cell layer thick, except for their midribs. Given *P. patens* small stature and the anatomical simplicity of its tissues, microscopic observation readily occurs without the need for dissection or sectioning (Harrison et al., 2009; Rensing et al., 2020). The images in Figure 5 show moss protonemal tissue and some of its components including a thin cell wall. *P. patens* characteristic simple body plan is more evidence that points at this moss as a great biomass feedstock for biofuel production (Cove et al., 2006; Decker et al., 2006; Harrison et al., 2009; Rensing et al., 2020; Rensing et al., 2008).

Moreover, various biotechnological strategies to increase plant biomass saccharification and, in consequence, bioethanol yield have been tested. An important strategy to decrease saccharification recalcitrance of the cell wall molecular components is the manipulation of transcription factors (TFs) and enzymes. The study of plant genetic diversity is also an important strategy that allows the discovery of new genetic factors with positive impact on these applications (Ge et al., 2011; Herbaut et al., 2018; Jeswani et al., 2020; Pena-Castro et al., 2017; Charles E. Wyman, 1999). The moss *P. patens* serves as an excellent model system for the implementation of these strategies, because of its sequenced and annotated genome and the ability to perform stable and efficient targeted genes knockouts (Rensing et al., 2020; Rensing et al., 2008; Schaefer, 2002; Schaefer & Zryd, 1997).

Previous studies have shown the effectiveness of using the glucose derived from lignocellulose hydrolysates to produce biofuels (Abdeshahian et al., 2020; Chen & Mu, 2019; Ge et al., 2011; Hill et al., 2006; Hossain et al., 2020; Hossain et al., 2021; Jeswani et al., 2020; Mishima et al., 2008; Charles E. Wyman, 1999; Zhu et al., 2010). Compared to others lignocellulose-derived hydrolysates, *P. patens* hydrolysate proved to be effective and efficient as evidenced by a high glucose yield (96%, 13.32 g/L) during hydrolysis, and high ethanol yield (7.8 g/L, 0.1674 g g dry -1) and glucose consumption during fermentation. Moreover, *P. patens* chemical composition, amorphous biomass, simple body plan and limited number of tissue and cell types, sequenced and annotated genome, and targeted gene recombination makes it an ideal bioenergy resource. Our findings propose the moss *Physcomitrium patens* as a candidate biomass feedstock on lignocellulose upcycling for biofuels production.

CONCLUSION

In this investigation we found that PpPPAL is not only essential for survival of *P. patens*, but it also participates in various important biological, developmental, and metabolic processes. *Ppppal* mutants are defective in their response to the phytohormones auxin, cytokinin, and ABA. Knockdown mutants also act as starvation mutants regardless of growth conditions. Mutants showed various growth and development defects including formation of extra apical and subapical protonemal filament tips, inhibition of the developmental transition from chloronema to caulonema cells, restricted bud formation for gametophore development, protonemal apical and subapical cell tip swelling and curving, misdirection of protonemata growth, inhibition of protonemal cell expansion and colony growth, and defects in the cytoskeleton function and vesicle transport.

In addition, *Ppppal* mutants are insensitive to the signaling and responses induced by glucose treatment, including the inhibition of photosynthesis, upregulation of ABA synthesis and signaling, and formation of caulonemata and gametophores. Furthermore, mutants are unresponsive to the function modulation of phytohormones and the master regulators hexokinase, SnRK1, and TOR provoked by glucose to control cellular activities from signaling, transcription, translation, catabolism, anabolism, transport, to growth, development and stress adaptation in response to altered glucose signals.

(Aguilera-Alvarado & Sanchez-Nieto, 2017; Ahuatzi et al., 2004; Arenas-Huertero et al., 2000; Claeyssen & Rivoal, 2007; de Jong et al., 2014; Granot et al., 2013; Kushwah & Laxmi, 2014; Li et al., 2006; MATSUKA et al., 1969; Moore et al., 2003; Olsson et al., 2003; Price et al., 2003; Rolland et al., 2006; Roth, Westcott, et al., 2019; Sheen, 2014; Thelander et al., 2005; Tsai & Gazzarrini, 2014; Xiao et al., 2000; Xiong et al., 2013).

Here we demostrate that both PpPPAL1 and PpPPAL2 have major roles in *P. patens* growth and development including cell identity determination, cell differentiation, cell expansion, polar cell elongation, organization of the cytoskeleton, vesicle transport, and response to hormones and environmental cues. Furthermore, it seems that PpPPAL is important for sensing and responding to the nutrient and energy status and for regulating factors like hexokinase, SnRK1, and TOR that control growth, propagation, development, glucose response, hormone responses and responses to external stimuli in *P. patens*. Future studies should explore further the biochemical and metabolic role of PpPPAL in moss *Physcomitrium* and its mechanism of action. Integrated genetic, cellular, chemical, proteomic and genomic approaches can contribute to dissect the broad range of functions and actions of regulators like PPAL (de Jong et al., 2014; Sheen, 2014; Urano et al., 2012). Based on the role of PpPPAL in energy sensing, we also characterized and proposed moss *Physcomitrium* biomass as a potential feedstock, substituting for fossil fuels, for biofuel production.

REFERENCES

Abdeshahian, P., Ascencio, J. J., Philippini, R. R., Antunes, F. A. F., Dos Santos, J. C., & da Silva, S. S. (2020). Utilization of sugarcane straw for production of beta-glucan biopolymer by Lasiodiplodia theobromae CCT 3966 in batch fermentation process. *Bioresour Technol*, *314*, 123716. https://doi.org/10.1016/j.biortech.2020.123716

Aguilera-Alvarado, G. P., & Sanchez-Nieto, S. (2017). Plant Hexokinases are Multifaceted Proteins. *Plant Cell Physiol*, *58*(7), 1151-1160. https://doi.org/10.1093/pcp/pcx062

Aharoni, A., Giri, A. P., Deuerlein, S., Griepink, F., de Kogel, W. J., Verstappen, F. W., Verhoeven, H. A., Jongsma, M. A., Schwab, W., & Bouwmeester, H. J. (2003). Terpenoid metabolism in wild-type and transgenic Arabidopsis plants. *Plant Cell*, *15*(12), 2866-2884. https://doi.org/10.1105/tpc.016253

Ahuatzi, D., Herrero, P., de la Cera, T., & Moreno, F. (2004). The glucose-regulated nuclear localization of hexokinase 2 in Saccharomyces cerevisiae is Mig1-dependent. *J Biol Chem*, *279*(14), 14440-14446. https://doi.org/10.1074/jbc.M313431200

Antimisiaris, M. F., & Running, M. P. (2014). Turning moss into algae: prenylation targets in Physcomitrella patens. *Plant Signal Behav*, *9*(7), e29314. https://doi.org/10.4161/psb.29314

Aoyama, T., Hiwatashi, Y., Shigyo, M., Kofuji, R., Kubo, M., Ito, M., & Hasebe, M. (2012). AP2-type transcription factors determine stem cell identity in the moss Physcomitrella patens. *Development*, *139*(17), 3120-3129. https://doi.org/10.1242/dev.076091

Arenas-Huertero, F., Arroyo, A., Zhou, L., Sheen, J., & Leon, P. (2000). Analysis of Arabidopsis glucose insensitive mutants, gin5 and gin6, reveals a central role of the plant hormone ABA in the regulation of plant vegetative development by sugar. *Genes Dev*, *14*(16), 2085-2096. https://www.ncbi.nlm.nih.gov/pubmed/10950871

Arif, M. A., Hiss, M., Tomek, M., Busch, H., Meyberg, R., Tintelnot, S., Reski, R., Rensing, S. A., & Frank, W. (2019). ABA-Induced Vegetative Diaspore Formation in Physcomitrella patens. *Front Plant Sci*, *10*, 315. https://doi.org/10.3389/fpls.2019.00315

Ashton, N. W., Grimsley, N. H., & Cove, D. J. (1979). Analysis of gametophytic development in the moss, Physcomitrella patens, using auxin and cytokinin resistant mutants. *Planta*, *144*(5), 427-435. https://doi.org/10.1007/BF00380118

Baena-Gonzalez, E., Rolland, F., Thevelein, J. M., & Sheen, J. (2007). A central integrator of transcription networks in plant stress and energy signalling. *Nature*, *448*(7156), 938-942. https://doi.org/10.1038/nature06069

Baluska, F., Salaj, J., Mathur, J., Braun, M., Jasper, F., Samaj, J., Chua, N. H., Barlow, P. W., & Volkmann, D. (2000). Root hair formation: F-actin-dependent tip growth is initiated by local assembly of profilin-supported F-actin meshworks accumulated

within expansin-enriched bulges. *Dev Biol*, *227*(2), 618-632. https://doi.org/10.1006/dbio.2000.9908

Bao, L., Yamamoto, K. T., & Fujita, T. (2015). Phototropism in gametophytic shoots of the moss Physcomitrella patens. *Plant Signal Behav*, *10*(3), e1010900. https://doi.org/10.1080/15592324.2015.1010900

Bao, L., Yamamoto, K. T., & Fujita, T. (2019). An Experimental System for Examining Phototropic Response of Gametophytic Shoots in the Moss Physcomitrella patens. *Methods Mol Biol*, *1924*, 45-51. https://doi.org/10.1007/978-1-4939-9015-3_5

Bibikova, T. N., Blancaflor, E. B., & Gilroy, S. (1999). Microtubules regulate tip growth and orientation in root hairs of Arabidopsis thaliana. *Plant J*, *17*(6), 657-665. https://doi.org/10.1046/j.1365-313x.1999.00415.x

Brandes, H., & Kende, H. (1968). Studies on cytokinin-controlled bud formation in moss protonemata. *Plant Physiol*, *43*(5), 827-837. https://doi.org/10.1104/pp.43.5.827

Cao, Z., Liu, Y., & Zhao, J. (2014). Efficient Discrimination of Some Moss Species by Fourier Transform Infrared Spectroscopy and Chemometrics. *Journal of Spectroscopy*, *2014*, 191796. https://doi.org/10.1155/2014/191796

Charng, W. L., Yamamoto, S., Jaiswal, M., Bayat, V., Xiong, B., Zhang, K., Sandoval, H., David, G., Gibbs, S., Lu, H. C., Chen, K., Giagtzoglou, N., & Bellen, H. J. (2014). Drosophila Tempura, a novel protein prenyltransferase alpha subunit, regulates notch signaling via Rab1 and Rab11. *PLoS Biol*, *12*(1), e1001777. https://doi.org/10.1371/journal.pbio.1001777

Chen, Y., & Mu, T. (2019). Application of deep eutectic solvents in biomass pretreatment and conversion. *Green Energy & Environment*, *4*(2), 95-115. https://doi.org/10.1016/j.gee.2019.01.012

Cheng, W. H., Endo, A., Zhou, L., Penney, J., Chen, H. C., Arroyo, A., Leon, P., Nambara, E., Asami, T., Seo, M., Koshiba, T., & Sheen, J. (2002). A unique short-chain dehydrogenase/reductase in Arabidopsis glucose signaling and abscisic acid biosynthesis and functions. *Plant Cell*, *14*(11), 2723-2743. https://doi.org/10.1105/tpc.006494

Claeyssen, E., & Rivoal, J. (2007). Isozymes of plant hexokinase: occurrence, properties and functions. *Phytochemistry*, *68*(6), 709-731. https://doi.org/10.1016/j.phytochem.2006.12.001

Cove, D. (2005). The moss Physcomitrella patens. *Annu Rev Genet*, *39*, 339-358. https://doi.org/10.1146/annurev.genet.39.073003.110214

Cove, D., Bezanilla, M., Harries, P., & Quatrano, R. (2006). Mosses as model systems for the study of metabolism and development. *Annu Rev Plant Biol*, *57*, 497-520. https://doi.org/10.1146/annurev.arplant.57.032905.105338

Curtis, M. D., & Grossniklaus, U. (2003). A gateway cloning vector set for high-throughput functional analysis of genes in planta. *Plant Physiol*, *133*(2), 462-469. https://doi.org/10.1104/pp.103.027979

de Jong, F., Thodey, K., Lejay, L. V., & Bevan, M. W. (2014). Glucose elevates NITRATE TRANSPORTER2.1 protein levels and nitrate transport activity independently of its HEXOKINASE1-mediated stimulation of NITRATE TRANSPORTER2.1 expression. *Plant Physiol*, *164*(1), 308-320. https://doi.org/10.1104/pp.113.230599

Decker, E. L., Frank, W., Sarnighausen, E., & Reski, R. (2006). Moss systems biology en route: phytohormones in Physcomitrella development. *Plant Biol (Stuttg)*, *8*(3), 397-405. https://doi.org/10.1055/s-2006-923952

Dehors, J., Mareck, A., Kiefer-Meyer, M. C., Menu-Bouaouiche, L., Lehner, A., & Mollet, J. C. (2019). Evolution of Cell Wall Polymers in Tip-Growing Land Plant Gametophytes: Composition, Distribution, Functional Aspects and Their Remodeling. *Front Plant Sci*, *10*, 441. https://doi.org/10.3389/fpls.2019.00441

Den, W., Sharma, V. K., Lee, M., Nadadur, G., & Varma, R. S. (2018a). Lignocellulosic biomass transformations via greener oxidative pretreatment processes: access to energy and value-added chemicals. *Front. Chem.*, *6*, 141.

Den, W., Sharma, V. K., Lee, M., Nadadur, G., & Varma, R. S. (2018b). Lignocellulosic Biomass Transformations via Greener Oxidative Pretreatment Processes: Access to Energy and Value-Added Chemicals. *Front Chem*, *6*, 141. https://doi.org/10.3389/fchem.2018.00141

Deruere, J., & Kieber, J. J. (2002). Molecular Mechanisms of Cytokinin Signaling. *J Plant Growth Regul*, *21*(1), 32-39. https://doi.org/10.1007/s003440010045

Eklund, D. M., Cierlik, I., Staldal, V., Claes, A. R., Vestman, D., Chandler, J., & Sundberg, E. (2011). Expression of Arabidopsis SHORT INTERNODES/STYLISH family genes in auxin biosynthesis zones of aerial organs is dependent on a GCC box-like regulatory element. *Plant Physiol*, *157*(4), 2069-2080. https://doi.org/10.1104/pp.111.182253

Espiñeira, J. M., Novo Uzal, E., Gómez Ros, L. V., Carrión, J. S., Merino, F., Ros Barceló, A., & Pomar, F. (2011). Distribution of lignin monomers and the evolution of lignification among lower plants. *Plant Biology*, *13*(1), 59-68. https://doi.org/10.1111/j.1438-8677.2010.00345.x

European Directorate for the Quality of Medicines & HealthCare. (2011). European Pharmacopoeia 7.0. In (7th Edition ed.).

Fidel, S., Doonan, J. H., & Morris, N. R. (1988). Aspergillus nidulans contains a single actin gene which has unique intron locations and encodes a gamma-actin. *Gene*, *70*(2), 283-293. https://doi.org/10.1016/0378-1119(88)90200-4

Finkelstein, R. R., Gampala, S. S., & Rock, C. D. (2002). Abscisic acid signaling in seeds and seedlings. *Plant Cell*, *14 Suppl*, S15-45. https://doi.org/10.1105/tpc.010441

Frebort, I., Kowalska, M., Hluska, T., Frebortova, J., & Galuszka, P. (2011). Evolution of cytokinin biosynthesis and degradation. *J Exp Bot*, *62*(8), 2431-2452. https://doi.org/10.1093/jxb/err004

Galichet, A., & Gruissem, W. (2003). Protein farnesylation in plants--conserved mechanisms but different targets. *Curr Opin Plant Biol*, *6*(6), 530-535. https://doi.org/10.1016/j.pbi.2003.09.005

Ge, L., Wang, P., & Mou, H. (2011). Study on saccharification techniques of seaweed wastes for the transformation of ethanol. *Renewable Energy*, *36*(1), 84-89. https://doi.org/10.1016/j.renene.2010.06.001

Ghorai, N., Ghorai, N., Chakraborty, S., Gucchait, S., Saha, S. K., & Biswas, S. (2012). Estimation of total Terpenoids concentration in plant tissues using a monoterpene, Linalool as standard reagent. *Protocol Exchange*. https://doi.org/10.1038/protex.2012.055

Granot, D., David-Schwartz, R., & Kelly, G. (2013). Hexose kinases and their role in sugar-sensing and plant development. *Front Plant Sci*, *4*, 44. https://doi.org/10.3389/fpls.2013.00044

Groves, C., Sankar, M., & Thomas, P. J. (2018). Second-generation biofuels: exploring imaginaries via deliberative workshops with farmers. *Journal of Responsible Innovation*, *5*(2), 149-169. https://doi.org/10.1080/23299460.2017.1422926

Harmanescu, M. (2012). Comparative researches on two direct transmethylation without prior extraction methods for fatty acids analysis in vegetal matrix with low fat content. *Chem Cent J*, *6*, 8. https://doi.org/10.1186/1752-153X-6-8

Harrison, C. J., Roeder, A. H. K., Meyerowitz, E. M., & Langdale, J. A. (2009). Local Cues and Asymmetric Cell Divisions Underpin Body Plan Transitions in the Moss Physcomitrella patens. *Current Biology*, *19*(6), 461-471. https://doi.org/10.1016/j.cub.2009.02.050

Hayashi, K., Neve, J., Hirose, M., Kuboki, A., Shimada, Y., Kepinski, S., & Nozaki, H. (2012). Rational design of an auxin antagonist of the SCF(TIR1) auxin receptor complex. *ACS Chem Biol*, *7*(3), 590-598. https://doi.org/10.1021/cb200404c

Heath, J. J., Kessler, A., Woebbe, E., Cipollini, D., & Stireman, J. O., 3rd. (2014). Exploring plant defense theory in tall goldenrod, Solidago altissima. *New Phytol*, *202*(4), 1357-1370. https://doi.org/10.1111/nph.12755

Hepler, P. K., Vidali, L., & Cheung, A. Y. (2001). Polarized cell growth in higher plants. *Annu Rev Cell Dev Biol*, *17*, 159-187. https://doi.org/10.1146/annurev.cellbio.17.1.159

Herbaut, M., Zoghlami, A., Habrant, A., Falourd, X., Foucat, L., Chabbert, B., & Paës, G. (2018). Multimodal analysis of pretreated biomass species highlights generic markers of lignocellulose recalcitrance. *Biotechnology for Biofuels*, *11*(1). https://doi.org/10.1186/s13068-018-1053-8

Hill, J., Nelson, E., Tilman, D., Polasky, S., & Tiffany, D. (2006). Environmental, economic, and energetic costs and benefits of biodiesel and ethanol biofuels. *Proceedings of the National Academy of Sciences*, *103*(30), 11206-11210. https://doi.org/10.1073/pnas.0604600103

Hiwatashi, Y., Sato, Y., & Doonan, J. H. (2014). Kinesins have a dual function in organizing microtubules during both tip growth and cytokinesis in Physcomitrella patens. *Plant Cell*, *26*(3), 1256-1266. https://doi.org/10.1105/tpc.113.121723

Hossain, A., Rahaman, M. S., Lee, D., Phung, T. K., Canlas, C. G., Simmons, B. A., Renneckar, S., Reynolds, W., George, A., Tulaphol, S., & Sathitsuksanoh, N. (2020). Enhanced Softwood Cellulose Accessibility by H3PO4 Pretreatment: High Sugar Yield without Compromising Lignin Integrity. *Industrial & Engineering Chemistry Research*, *59*(2), 1010-1024. https://doi.org/10.1021/acs.iecr.9b05873

Hossain, M. A., Rahaman, M. S., Yelle, D., Shang, H., Sun, Z., Renneckar, S., Dong, J., Tulaphol, S., & Sathitsuksanoh, N. (2021). Effects of polyol-based deep eutectic solvents on the efficiency of rice straw enzymatic hydrolysis. *Industrial Crops and Products*, *167*, 113480. https://doi.org/10.1016/j.indcrop.2021.113480

Hu, T., Jin, W.-Y., & Cheng, C.-G. (2011). Classification of Five Kinds of Moss Plants with the Use of Fourier Transform Infrared Spectroscopy and Chemometrics. *Spectroscopy*, *25*, 908150. https://doi.org/10.3233/SPE-2011-0518

Hutchison, C. E., & Kieber, J. J. (2002). Cytokinin signaling in Arabidopsis. *Plant Cell*, *14 Suppl*, S47-59. https://doi.org/10.1105/tpc.010444

Imaizumi, T., Kadota, A., Hasebe, M., & Wada, M. (2002). Cryptochrome light signals control development to suppress auxin sensitivity in the moss Physcomitrella patens. *Plant Cell*, *14*(2), 373-386. https://doi.org/10.1105/tpc.010388

Islam, M. K., Wang, H., Rehman, S., Dong, C., Hsu, H.-Y., Lin, C. S. K., & Leu, S.-Y. (2020). Sustainability metrics of pretreatment processes in a waste derived lignocellulosic biomass biorefinery. *Bioresour. Technol.*, *298*, 122558.

Islam, M. K., Wang, H., Rehman, S., Dong, C., Hsu, H.-Y., Lin, C. S. K., & Leu, S.-Y. (2020). Sustainability metrics of pretreatment processes in a waste derived lignocellulosic biomass biorefinery. *Bioresource Technology*, *298*, 122558. https://doi.org/10.1016/j.biortech.2019.122558

Jaeger, R., & Moody, L. A. (2021). A fundamental developmental transition in Physcomitrium patens is regulated by evolutionarily conserved mechanisms. *Evol Dev*, *23*(3), 123-136. https://doi.org/10.1111/ede.12376

Jang, G., & Dolan, L. (2011). Auxin promotes the transition from chloronema to caulonema in moss protonema by positively regulating PpRSL1and PpRSL2 in Physcomitrella patens. *New Phytol*, *192*(2), 319-327. https://doi.org/10.1111/j.1469-8137.2011.03805.x

Jang, J. C., Leon, P., Zhou, L., & Sheen, J. (1997). Hexokinase as a sugar sensor in higher plants. *Plant Cell*, *9*(1), 5-19. https://doi.org/10.1105/tpc.9.1.5

Jang, J. C., & Sheen, J. (1994). Sugar sensing in higher plants. *Plant Cell*, *6*(11), 1665-1679. https://doi.org/10.1105/tpc.6.11.1665

Jenkins, G. I., Courtice, G. R., & Cove, D. J. (1986). Gravitropic responses of wild-type and mutant strains of the moss Physcomitrella patens. *Plant Cell Environ*, *9*(8), 637-644. https://doi.org/10.1111/j.1365-3040.1986.tb01621.x

Jeswani, H. K., Chilvers, A., & Azapagic, A. (2020). Environmental sustainability of biofuels: a review. *Proceedings of the Royal Society A: Mathematical, Physical and Engineering Sciences*, *476*(2243), 20200351. https://doi.org/10.1098/rspa.2020.0351

Kamisugi, Y., Schlink, K., Rensing, S. A., Schween, G., von Stackelberg, M., Cuming, A. C., Reski, R., & Cove, D. J. (2006). The mechanism of gene targeting in Physcomitrella patens: homologous recombination, concatenation and multiple integration. *Nucleic Acids Res*, *34*(21), 6205-6214. https://doi.org/10.1093/nar/gkl832

Karve, R., Lauria, M., Virnig, A., Xia, X., Rauh, B. L., & Moore, B. (2010). Evolutionary lineages and functional diversification of plant hexokinases. *Mol Plant*, *3*(2), 334-346. https://doi.org/10.1093/mp/ssq003

Khraiwesh, B., Arif, M. A., Seumel, G. I., Ossowski, S., Weigel, D., Reski, R., & Frank, W. (2010). Transcriptional control of gene expression by microRNAs. *Cell*, *140*(1), 111-122. https://doi.org/10.1016/j.cell.2009.12.023

Khraiwesh, B., Ossowski, S., Weigel, D., Reski, R., & Frank, W. (2008). Specific gene silencing by artificial MicroRNAs in Physcomitrella patens: an alternative to targeted gene knockouts. *Plant Physiol*, *148*(2), 684-693. https://doi.org/10.1104/pp.108.128025

Kieber, J. J. (2002). Tribute to Folke Skoog: Recent Advances in our Understanding of Cytokinin Biology. *J Plant Growth Regul*, *21*(1), 1-2. https://doi.org/10.1007/s003440010059

Kim, Y. M., Heinzel, N., Giese, J. O., Koeber, J., Melzer, M., Rutten, T., Von Wiren, N., Sonnewald, U., & Hajirezaei, M. R. (2013). A dual role of tobacco hexokinase 1 in primary metabolism and sugar sensing. *Plant Cell Environ*, *36*(7), 1311-1327. https://doi.org/10.1111/pce.12060

Knight, C. D., Sehgal, A., Atwal, K., Wallace, J. C., Cove, D. J., Coates, D., Quatrano, R. S., Bahadur, S., Stockley, P. G., & Cuming, A. C. (1995). Molecular Responses to Abscisic Acid and Stress Are Conserved between Moss and Cereals. *Plant Cell*, *7*(5), 499-506. https://doi.org/10.1105/tpc.7.5.499

Kovar, D. R., Staiger, C. J., Weaver, E. A., & McCurdy, D. W. (2000). AtFim1 is an actin filament crosslinking protein from Arabidopsis thaliana. *Plant J*, *24*(5), 625-636. https://doi.org/10.1046/j.1365-313x.2000.00907.x

Kramer, E. M. (2009). Chapter 4. New model systems for the study of developmental evolution in plants. *Curr Top Dev Biol*, *86*, 67-105. https://doi.org/10.1016/S0070-2153(09)01004-7

Kubo, M., Imai, A., Nishiyama, T., Ishikawa, M., Sato, Y., Kurata, T., Hiwatashi, Y., Reski, R., & Hasebe, M. (2013). System for Stable β-Estradiol-Inducible Gene Expression in the Moss Physcomitrella patens. *PLOS ONE*, *8*(9), e77356. https://doi.org/10.1371/journal.pone.0077356

Kumar, R., Bhagia, S., Smith, M. D., Petridis, L., Ong, R. G., Cai, C. M., Mittal, A., Himmel, M. H., Balan, V., Dale, B. E., Ragauskas, A. J., Smith, J. C., & Wyman, C. E. (2018). Cellulose–hemicellulose interactions at elevated temperatures increase cellulose recalcitrance to biological conversion. *Green Chemistry*, *20*(4), 921-934. https://doi.org/10.1039/c7gc03518g

Kushwah, S., & Laxmi, A. (2014). The interaction between glucose and cytokinin signal transduction pathway in Arabidopsis thaliana. *Plant Cell Environ*, *37*(1), 235-253. https://doi.org/10.1111/pce.12149

Lastdrager, J., Hanson, J., & Smeekens, S. (2014). Sugar signals and the control of plant growth and development. *J Exp Bot*, *65*(3), 799-807. https://doi.org/10.1093/jxb/ert474

Lavy, M., & Estelle, M. (2016). Mechanisms of auxin signaling. *Development*, *143*(18), 3226-3229. https://doi.org/10.1242/dev.131870

Lavy, M., Prigge, M. J., Tao, S., Shain, S., Kuo, A., Kirchsteiger, K., & Estelle, M. (2016). Constitutive auxin response in Physcomitrella reveals complex interactions between Aux/IAA and ARF proteins. *Elife*, *5*. https://doi.org/10.7554/eLife.13325

Leon, P., & Sheen, J. (2003). Sugar and hormone connections. *Trends Plant Sci*, *8*(3), 110-116. https://doi.org/10.1016/S1360-1385(03)00011-6

Leung, K. F., Baron, R., & Seabra, M. C. (2006). Thematic review series: lipid posttranslational modifications. geranylgeranylation of Rab GTPases. *J Lipid Res*, *47*(3), 467-475. https://doi.org/10.1194/jlr.R500017-JLR200

Li, L., & Sheen, J. (2016). Dynamic and diverse sugar signaling. *Curr Opin Plant Biol*, *33*, 116-125. https://doi.org/10.1016/j.pbi.2016.06.018

Li, Y., Lee, K. K., Walsh, S., Smith, C., Hadingham, S., Sorefan, K., Cawley, G., & Bevan, M. W. (2006). Establishing glucose- and ABA-regulated transcription networks in

Arabidopsis by microarray analysis and promoter classification using a Relevance Vector Machine. *Genome Res*, *16*(3), 414-427. https://doi.org/10.1101/gr.4237406

Ligrone, R., Ducket, J. G., & Renzaglia, K. S. (2000). Conducting tissues and phyletic relationships of bryophytes. *Philos Trans R Soc Lond B Biol Sci*, *355*(1398), 795-813. https://doi.org/10.1098/rstb.2000.0616

Lim, H. K., Song, H. Y., Kim, D. R., Ko, J. H., Lee, S. A., Lee, K.-I., & Hwang, I. T. (2015). An Alternative Path for the Preparation of Triacetylcellulose from Unrefined Biomass. *Advances in Chemical Engineering and Science*, *05*(01), 33-42. https://doi.org/10.4236/aces.2015.51004

Liscum, E., Askinosie, S. K., Leuchtman, D. L., Morrow, J., Willenburg, K. T., & Coats, D. R. (2014). Phototropism: growing towards an understanding of plant movement. *Plant Cell*, *26*(1), 38-55. https://doi.org/10.1105/tpc.113.119727

Lynd, L. R., Wyman, C. E., & Gerngross, T. U. (1999). Biocommodity engineering. *Biotechnol. Prog.*, *15*, 777-793. https://doi.org/http://pubs.acs.org/cgi-bin/article.cgi/bipret/1999/15/i05/pdf/bp990109e.pdf

Martínez-Cortés, T., Pomar, F., & Novo-Uzal, E. (2021). Evolutionary Implications of a Peroxidase with High Affinity for Cinnamyl Alcohols from Physcomitrium patens, a Non-Vascular Plant. *Plants*, *10*(7), 1476. https://doi.org/10.3390/plants10071476

MATSUKA, M., MIYACHI, S., & HASE, E. (1969). Further studies on the metabolism of glucose in the process of "glucose-bleaching" of Chlorella protothecoides. *Plant and Cell Physiology*, *10*(3), 513-526. https://doi.org/10.1093/oxfordjournals.pcp.a074434

Maurer-Stroh, S., Washietl, S., & Eisenhaber, F. (2003). Protein prenyltransferases. *Genome Biol*, *4*(4), 212. https://doi.org/10.1186/gb-2003-4-4-212

McTaggart, S. J. (2006). Isoprenylated proteins. *Cell Mol Life Sci*, *63*(3), 255-267. https://doi.org/10.1007/s00018-005-5298-6

Menand, B., Calder, G., & Dolan, L. (2007). Both chloronemal and caulonemal cells expand by tip growth in the moss Physcomitrella patens. *J Exp Bot*, *58*(7), 1843-1849. https://doi.org/10.1093/jxb/erm047

Menand, B., Yi, K., Jouannic, S., Hoffmann, L., Ryan, E., Linstead, P., Schaefer, D. G., & Dolan, L. (2007). An ancient mechanism controls the development of cells with a rooting function in land plants. *Science*, *316*(5830), 1477-1480. https://doi.org/10.1126/science.1142618

Mishima, D., Kuniki, M., Sei, K., Soda, S., Ike, M., & Fujita, M. (2008). Ethanol production from candidate energy crops: water hyacinth (Eichhornia crassipes) and water lettuce (Pistia stratiotes L.). *Bioresour Technol*, *99*(7), 2495-2500. https://doi.org/10.1016/j.biortech.2007.04.056

Moore, B., Zhou, L., Rolland, F., Hall, Q., Cheng, W. H., Liu, Y. X., Hwang, I., Jones, T., & Sheen, J. (2003). Role of the Arabidopsis glucose sensor HXK1 in nutrient, light, and hormonal signaling. *Science*, *300*(5617), 332-336. https://doi.org/10.1126/science.1080585

Nguyen, U. T., Goody, R. S., & Alexandrov, K. (2010). Understanding and exploiting protein prenyltransferases. *Chembiochem*, *11*(9), 1194-1201. https://doi.org/10.1002/cbic.200900727

Nilsson, A., Olsson, T., Ulfstedt, M., Thelander, M., & Ronne, H. (2011). Two novel types of hexokinases in the moss Physcomitrella patens. *BMC Plant Biol*, *11*, 32. https://doi.org/10.1186/1471-2229-11-32

Nishiyama, T., Fujita, T., Shin, I. T., Seki, M., Nishide, H., Uchiyama, I., Kamiya, A., Carninci, P., Hayashizaki, Y., Shinozaki, K., Kohara, Y., & Hasebe, M. (2003). Comparative genomics of Physcomitrella patens gametophytic transcriptome and Arabidopsis thaliana: implication for land plant evolution. *Proc Natl Acad Sci U S A*, *100*(13), 8007-8012. https://doi.org/10.1073/pnas.0932694100

Olsson, T., Thelander, M., & Ronne, H. (2003). A novel type of chloroplast stromal hexokinase is the major glucose-phosphorylating enzyme in the moss Physcomitrella patens. *J Biol Chem*, *278*(45), 44439-44447. https://doi.org/10.1074/jbc.M306265200

Ostermann, A. I., Muller, M., Willenberg, I., & Schebb, N. H. (2014). Determining the fatty acid composition in plasma and tissues as fatty acid methyl esters using gas chromatography - a comparison of different derivatization and extraction procedures. *Prostaglandins Leukot Essent Fatty Acids*, *91*(6), 235-241. https://doi.org/10.1016/j.plefa.2014.10.002

Osuna, D., Usadel, B., Morcuende, R., Gibon, Y., Blasing, O. E., Hohne, M., Gunter, M., Kamlage, B., Trethewey, R., Scheible, W. R., & Stitt, M. (2007). Temporal responses of transcripts, enzyme activities and metabolites after adding sucrose to carbon-deprived Arabidopsis seedlings. *Plant J*, *49*(3), 463-491. https://doi.org/10.1111/j.1365-313X.2006.02979.x

Otero-Blanca, A., Pérez-Llano, Y., Reboledo-Blanco, G., Lira-Ruan, V., Padilla-Chacon, D., Folch-Mallol, J. L., Sánchez-Carbente, M. D. R., Ponce De León, I., & Batista-García, R. A. (2021). Physcomitrium patens Infection by Colletotrichum gloeosporioides: Understanding the Fungal–Bryophyte Interaction by Microscopy, Phenomics and RNA Sequencing. *Journal of Fungi*, *7*(8), 677. https://doi.org/10.3390/jof7080677

Oubani, H., Abbas, A., & Harris, A. (2011). Investigation on the mechanical pretreatment of cellulose by high intensity ultrasound and ball milling. In *In: Chemeca 2011: Engineering a Better World: Sydney Hilton Hotel, NSW, Australia, 18-21 September 2011. Barton, A.C.T.: Engineers Australia, 2011: [1765]-[1775].* Engineers Australia. https://doi.org/10.3316/informit.176071187623742

Palsuledesai, C. C., & Distefano, M. D. (2015). Protein prenylation: enzymes, therapeutics, and biotechnology applications. *ACS Chem Biol*, *10*(1), 51-62. https://doi.org/10.1021/cb500791f

Pandreka, A., Dandekar, D. S., Haldar, S., Uttara, V., Vijayshree, S. G., Mulani, F. A., Aarthy, T., & Thulasiram, H. V. (2015). Triterpenoid profiling and functional characterization of the initial genes involved in isoprenoid biosynthesis in neem (Azadirachta indica). *BMC Plant Biol*, *15*, 214. https://doi.org/10.1186/s12870-015-0593-3

Pena-Castro, J. M., Del Moral, S., Nunez-Lopez, L., Barrera-Figueroa, B. E., & Amaya-Delgado, L. (2017). Biotechnological Strategies to Improve Plant Biomass Quality for Bioethanol Production. *Biomed Res Int*, *2017*, 7824076. https://doi.org/10.1155/2017/7824076

Penalva, M. A., Zhang, J., Xiang, X., & Pantazopoulou, A. (2017). Transport of fungal RAB11 secretory vesicles involves myosin-5, dynein/dynactin/p25, and kinesin-1 and is independent of kinesin-3. *Mol Biol Cell*, *28*(7), 947-961. https://doi.org/10.1091/mbc.E16-08-0566

Pereira-Leal, J. B., Hume, A. N., & Seabra, M. C. (2001). Prenylation of Rab GTPases: molecular mechanisms and involvement in genetic disease. *FEBS Lett*, *498*(2-3), 197-200. https://doi.org/10.1016/s0014-5793(01)02483-8

PHYSCObase. http://moss.nibb.ac.jp/

Plavskin, Y., Nagashima, A., Perroud, P. F., Hasebe, M., Quatrano, R. S., Atwal, G. S., & Timmermans, M. C. (2016). Ancient trans-Acting siRNAs Confer Robustness and Sensitivity onto the Auxin Response. *Dev Cell*, *36*(3), 276-289. https://doi.org/10.1016/j.devcel.2016.01.010

Pressel, S., Ligrone, R., & Duckett, J. G. (2008). Cellular differentiation in moss protonemata: a morphological and experimental study. *Ann Bot*, *102*(2), 227-245. https://doi.org/10.1093/aob/mcn080

Price, J., Li, T. C., Kang, S. G., Na, J. K., & Jang, J. C. (2003). Mechanisms of glucose signaling during germination of Arabidopsis. *Plant Physiol*, *132*(3), 1424-1438. https://doi.org/10.1104/pp.103.020347

Prigge, M. J., Lavy, M., Ashton, N. W., & Estelle, M. (2010). Physcomitrella patens auxin-resistant mutants affect conserved elements of an auxin-signaling pathway. *Curr Biol*, *20*(21), 1907-1912. https://doi.org/10.1016/j.cub.2010.08.050

Ramazi, S., & Zahiri, J. (2021). Posttranslational modifications in proteins: resources, tools and prediction methods. *Database (Oxford)*, *2021*. https://doi.org/10.1093/database/baab012

Rensing, S. A., Goffinet, B., Meyberg, R., Wu, S.-Z., & Bezanilla, M. (2020). The Moss Physcomitrium (Physcomitrella) patens: A Model Organism for Non-Seed Plants. *The Plant Cell*, *32*(5), 1361-1376. https://doi.org/10.1105/tpc.19.00828

Rensing, S. A., Lang, D., Zimmer, A. D., Terry, A., Salamov, A., Shapiro, H., Nishiyama, T., Perroud, P. F., Lindquist, E. A., Kamisugi, Y., Tanahashi, T., Sakakibara, K., Fujita, T., Oishi, K., Shin, I. T., Kuroki, Y., Toyoda, A., Suzuki, Y., Hashimoto, S., . . . Boore, J. L. (2008). The Physcomitrella genome reveals evolutionary insights into the conquest of land by plants. *Science*, *319*(5859), 64-69. https://doi.org/10.1126/science.1150646

Reski, R., & Abel, W. O. (1985). Induction of budding on chloronemata and caulonemata of the moss, Physcomitrella patens, using isopentenyladenine. *Planta*, *165*(3), 354-358. https://doi.org/10.1007/BF00392232

Ringli, C., Baumberger, N., Diet, A., Frey, B., & Keller, B. (2002). ACTIN2 is essential for bulge site selection and tip growth during root hair development of Arabidopsis. *Plant Physiol*, *129*(4), 1464-1472. https://doi.org/10.1104/pp.005777

Roberts, A. W., Roberts, E. M., & Haigler, C. H. (2012). Moss cell walls: structure and biosynthesis. *Front Plant Sci*, *3*, 166. https://doi.org/10.3389/fpls.2012.00166

Rohde, A., Kurup, S., & Holdsworth, M. (2000). ABI3 emerges from the seed. *Trends Plant Sci*, *5*(10), 418-419. https://doi.org/10.1016/s1360-1385(00)01736-2

Rolland, F., Baena-Gonzalez, E., & Sheen, J. (2006). Sugar sensing and signaling in plants: conserved and novel mechanisms. *Annu Rev Plant Biol*, *57*, 675-709. https://doi.org/10.1146/annurev.arplant.57.032905.105441

Roth, M. S., Gallaher, S. D., Westcott, D. J., Iwai, M., Louie, K. B., Mueller, M., Walter, A., Foflonker, F., Bowen, B. P., Ataii, N. N., Song, J., Chen, J. H., Blaby-Haas, C. E., Larabell, C., Auer, M., Northen, T. R., Merchant, S. S., & Niyogi, K. K. (2019). Regulation of Oxygenic Photosynthesis during Trophic Transitions in the Green Alga Chromochloris zofingiensis. *Plant Cell*, *31*(3), 579-601. https://doi.org/10.1105/tpc.18.00742

Roth, M. S., Westcott, D. J., Iwai, M., & Niyogi, K. K. (2019). Hexokinase is necessary for glucose-mediated photosynthesis repression and lipid accumulation in a green alga. *Commun Biol*, *2*, 347. https://doi.org/10.1038/s42003-019-0577-1

Running, M. P. (2014). The role of lipid post-translational modification in plant developmental processes. *Front Plant Sci*, *5*, 50. https://doi.org/10.3389/fpls.2014.00050

Sakr, S., Wang, M., Dedaldechamp, F., Perez-Garcia, M. D., Oge, L., Hamama, L., & Atanassova, R. (2018). The Sugar-Signaling Hub: Overview of Regulators and Interaction with the Hormonal and Metabolic Network. *Int J Mol Sci*, *19*(9). https://doi.org/10.3390/ijms19092506

Salimon, J., Omar, T. A., & Salih, N. (2014). Comparison of two derivatization methods for the analysis of fatty acids and trans fatty acids in bakery products using gas chromatography. *ScientificWorldJournal*, *2014*, 906407. https://doi.org/10.1155/2014/906407

Sato, M., Fujisaki, S., Sato, K., Nishimura, Y., & Nakano, A. (2001). Yeast Saccharomyces cerevisiae has two cis-prenyltransferases with different properties and localizations. Implication for their distinct physiological roles in dolichol synthesis. *Genes Cells*, *6*(6), 495-506. https://doi.org/10.1046/j.1365-2443.2001.00438.x

Schaefer, D. G. (2002). A new moss genetics: targeted mutagenesis in Physcomitrella patens. *Annu Rev Plant Biol*, *53*, 477-501. https://doi.org/10.1146/annurev.arplant.53.100301.135202

Schaefer, D. G., & Zryd, J. P. (1997). Efficient gene targeting in the moss Physcomitrella patens. *Plant J*, *11*(6), 1195-1206. https://doi.org/10.1046/j.1365-313x.1997.11061195.x

Schumaker, K. S., & Dietrich, M. A. (1997). Programmed Changes in Form during Moss Development. *Plant Cell*, *9*(7), 1099-1107. https://doi.org/10.1105/tpc.9.7.1099

Schwab, R., Ossowski, S., Riester, M., Warthmann, N., & Weigel, D. (2006). Highly Specific Gene Silencing by Artificial MicroRNAs inArabidopsis. *The Plant Cell*, *18*(5), 1121-1133. https://doi.org/10.1105/tpc.105.039834

Schwab, R., Palatnik, J. F., Riester, M., Schommer, C., Schmid, M., & Weigel, D. (2005). Specific effects of microRNAs on the plant transcriptome. *Dev Cell*, *8*(4), 517-527. https://doi.org/10.1016/j.devcel.2005.01.018

Seidl, P. R., & Goulart, A. K. (2016). Pretreatment processes for lignocellulosic biomass conversion to biofuels and bioproducts. *Curr. Opin. Green Sustain. Chem.*, *2*, 48-53.

Seidl, P. R., & Goulart, A. K. (2016). Pretreatment processes for lignocellulosic biomass conversion to biofuels and bioproducts. *Current Opinion in Green and Sustainable Chemistry*, *2*, 48-53. https://doi.org/10.1016/j.cogsc.2016.09.003

Sheen, J. (2014). Master Regulators in Plant Glucose Signaling Networks. *J Plant Biol*, *57*(2), 67-79. https://doi.org/10.1007/s12374-014-0902-7

SHIHIRA-ISHIKAWA, I., & HASE, E. (1964). NUTRITIONAL CONTROL OF CELL PIGMENTATION IN CHLORELLA PROTOTHECOIDES WITH SPECIAL REFERENCE TO THE DEGENERATION OF CHLOROPLAST INDUCED BY GLUCOSE1. *Plant and Cell Physiology*, *5*(2), 227-240. https://doi.org/10.1093/oxfordjournals.pcp.a079037

Sieberer, B. J., Ketelaar, T., Esseling, J. J., & Emons, A. M. (2005). Microtubules guide root hair tip growth. *New Phytol*, *167*(3), 711-719. https://doi.org/10.1111/j.1469-8137.2005.01506.x

Sieberer, B. J., Timmers, A. C., & Emons, A. M. (2005). Nod factors alter the microtubule cytoskeleton in Medicago truncatula root hairs to allow root hair reorientation. *Mol Plant Microbe Interact*, *18*(11), 1195-1204. https://doi.org/10.1094/MPMI-18-1195

Siqueira, G., Arantes, V., Saddler, J. N., Ferraz, A., & Milagres, A. M. F. (2017). Limitation of cellulose accessibility and unproductive binding of cellulases by pretreated sugarcane bagasse lignin. *Biotechnology for Biofuels*, *10*(1). https://doi.org/10.1186/s13068-017-0860-7

Sluiter, A., Hames, B., Ruiz, R., Scarlata, C., Sluiter, J., Templeton, D., & Crocker, D. (2012). *Determination of structural carbohydrates and lignin in biomass. Laboratory Analytical Procedure (LAP). Avalable: http://www.nrel.gov/biomass/pdfs/42618.pdf. Accessed 2019 November 2.*

Staiger, C. J. (2000). Signaling to the Actin Cytoskeleton in Plants. *Annu Rev Plant Physiol Plant Mol Biol*, *51*, 257-288. https://doi.org/10.1146/annurev.arplant.51.1.257

Staniszewski, M., Kujawski, W., & Lewandowska, M. (2009). Semi-continuous ethanol production in bioreactor from whey with co-immobilized enzyme and yeast cells followed by pervaporative recovery of product – Kinetic model predictions considering glucose repression. *Journal of Food Engineering*, *91*(2), 240-249. https://doi.org/https://doi.org/10.1016/j.jfoodeng.2008.08.026

Szumlanski, A. L., & Nielsen, E. (2009). The Rab GTPase RabA4d regulates pollen tube tip growth in Arabidopsis thaliana. *Plant Cell*, *21*(2), 526-544. https://doi.org/10.1105/tpc.108.060277

Thelander, M., Landberg, K., & Sundberg, E. (2018). Auxin-mediated developmental control in the moss Physcomitrella patens. *J Exp Bot*, *69*(2), 277-290. https://doi.org/10.1093/jxb/erx255

Thelander, M., Olsson, T., & Ronne, H. (2004). Snf1-related protein kinase 1 is needed for growth in a normal day-night light cycle. *EMBO J*, *23*(8), 1900-1910. https://doi.org/10.1038/sj.emboj.7600182

Thelander, M., Olsson, T., & Ronne, H. (2005). Effect of the energy supply on filamentous growth and development in Physcomitrella patens. *J Exp Bot*, *56*(412), 653-662. https://doi.org/10.1093/jxb/eri040

Thole, J. M., Perroud, P. F., Quatrano, R. S., & Running, M. P. (2014). Prenylation is required for polar cell elongation, cell adhesion, and differentiation in Physcomitrella patens. *Plant J*, *78*(3), 441-451. https://doi.org/10.1111/tpj.12484

Thulasiram, H. V., Erickson, H. K., & Poulter, C. D. (2007). Chimeras of two isoprenoid synthases catalyze all four coupling reactions in isoprenoid biosynthesis. *Science*, *316*(5821), 73-76. https://doi.org/10.1126/science.1137786

Tsai, A. Y., & Gazzarrini, S. (2014). Trehalose-6-phosphate and SnRK1 kinases in plant development and signaling: the emerging picture. *Front Plant Sci*, *5*, 119. https://doi.org/10.3389/fpls.2014.00119

Urano, D., Phan, N., Jones, J. C., Yang, J., Huang, J., Grigston, J., Taylor, J. P., & Jones, A. M. (2012). Endocytosis of the seven-transmembrane RGS1 protein activates G-protein-coupled signalling in Arabidopsis. *Nat Cell Biol*, *14*(10), 1079-1088. https://doi.org/10.1038/ncb2568

van Gisbergen, P. A., Li, M., Wu, S. Z., & Bezanilla, M. (2012). Class II formin targeting to the cell cortex by binding PI(3,5)P(2) is essential for polarized growth. *J Cell Biol*, *198*(2), 235-250. https://doi.org/10.1083/jcb.201112085

Viaene, T., Landberg, K., Thelander, M., Medvecka, E., Pederson, E., Feraru, E., Cooper, E. D., Karimi, M., Delwiche, C. F., Ljung, K., Geisler, M., Sundberg, E., & Friml, J. (2014). Directional auxin transport mechanisms in early diverging land plants. *Curr Biol*, *24*(23), 2786-2791. https://doi.org/10.1016/j.cub.2014.09.056

Vidali, L., & Hepler, P. K. (2001). Actin and pollen tube growth. *Protoplasma*, *215*(1-4), 64-76. https://doi.org/10.1007/BF01280304

Vidali, L., McKenna, S. T., & Hepler, P. K. (2001). Actin polymerization is essential for pollen tube growth. *Mol Biol Cell*, *12*(8), 2534-2545. https://doi.org/10.1091/mbc.12.8.2534

Vidali, L., Rounds, C. M., Hepler, P. K., & Bezanilla, M. (2009). Lifeact-mEGFP reveals a dynamic apical F-actin network in tip growing plant cells. *PLoS One*, *4*(5), e5744. https://doi.org/10.1371/journal.pone.0005744

Vidali, L., van Gisbergen, P. A., Guerin, C., Franco, P., Li, M., Burkart, G. M., Augustine, R. C., Blanchoin, L., & Bezanilla, M. (2009). Rapid formin-mediated actin-filament elongation is essential for polarized plant cell growth. *Proc Natl Acad Sci U S A*, *106*(32), 13341-13346. https://doi.org/10.1073/pnas.0901170106

Vishwakarma, K., Upadhyay, N., Kumar, N., Yadav, G., Singh, J., Mishra, R. K., Kumar, V., Verma, R., Upadhyay, R. G., Pandey, M., & Sharma, S. (2017). Abscisic Acid Signaling and Abiotic Stress Tolerance in Plants: A Review on Current Knowledge and Future Prospects. *Front Plant Sci*, *8*, 161. https://doi.org/10.3389/fpls.2017.00161

von Schwartzenberg, K., Nunez, M. F., Blaschke, H., Dobrev, P. I., Novak, O., Motyka, V., & Strnad, M. (2007). Cytokinins in the bryophyte Physcomitrella patens: analyses of activity, distribution, and cytokinin oxidase/dehydrogenase overexpression reveal the role of extracellular cytokinins. *Plant Physiol*, *145*(3), 786-800. https://doi.org/10.1104/pp.107.103176

Weng, J. K., & Chapple, C. (2010). The origin and evolution of lignin biosynthesis. *New Phytologist*, *187*(2), 273-285. https://doi.org/10.1111/j.1469-8137.2010.03327.x

Wu, S. Z., & Bezanilla, M. (2014). Myosin VIII associates with microtubule ends and together with actin plays a role in guiding plant cell division. *Elife*, *3*. https://doi.org/10.7554/eLife.03498

Wu, S. Z., & Bezanilla, M. (2018). Actin and microtubule cross talk mediates persistent polarized growth. *J Cell Biol*, *217*(10), 3531-3544. https://doi.org/10.1083/jcb.201802039

Wurzinger, B., Nukarinen, E., Nagele, T., Weckwerth, W., & Teige, M. (2018). The SnRK1 Kinase as Central Mediator of Energy Signaling between Different Organelles. *Plant Physiol*, *176*(2), 1085-1094. https://doi.org/10.1104/pp.17.01404

Wyman, C. E. (1999). Biomass ethanol: technical progress, opportunities, and commercial challenges. *Annu. Rev. Energy Environ.*, *24*, 189-226.

Wyman, C. E. (1999). BIOMASSETHANOL: Technical Progress, Opportunities, and Commercial Challenges. *Annual Review of Energy and the Environment*, *24*(1), 189-226. https://doi.org/10.1146/annurev.energy.24.1.189

Xiao, W., Sheen, J., & Jang, J. C. (2000). The role of hexokinase in plant sugar signal transduction and growth and development. *Plant Mol Biol*, *44*(4), 451-461. https://doi.org/10.1023/a:1026501430422

Xiong, Y., McCormack, M., Li, L., Hall, Q., Xiang, C., & Sheen, J. (2013). Glucose-TOR signalling reprograms the transcriptome and activates meristems. *Nature*, *496*(7444), 181-186. https://doi.org/10.1038/nature12030

Xu, G.-C., Ding, J.-C., Han, R.-Z., Dong, J.-J., & Ni, Y. (2016). Enhancing cellulose accessibility of corn stover by deep eutectic solvent pretreatment for butanol fermentation. *Bioresource Technology*, *203*, 364-369. https://doi.org/10.1016/j.biortech.2015.11.002

Xu, Z., Zhang, D., Hu, J., Zhou, X., Ye, X., Reichel, K. L., Stewart, N. R., Syrenne, R. D., Yang, X., Gao, P., Shi, W., Doeppke, C., Sykes, R. W., Burris, J. N., Bozell, J. J., Cheng, M. Z.-M., Hayes, D. G., Labbe, N., Davis, M., . . . Yuan, J. S. (2009). Comparative genome analysis of lignin biosynthesis gene families across the plant kingdom. *BMC Bioinformatics*, *10*(S11), S3. https://doi.org/10.1186/1471-2105-10-s11-s3

Yang, B., Tao, L., & Wyman, C. E. (2018). Strengths, challenges, and opportunities for hydrothermal pretreatment in lignocellulosic biorefineries. *Biofuels, Bioprod. Bioref.*, *12*(1), 125-138.

Yi, Tang, Li, Wang, Chao, Ma, Ji, Liu, & Huanxiu. (2011). The Use of HPLC in Determination of Endogenous Hormones in Anthers of Bitter Melon.

Yu, L., Fan, J., Yan, C., & Xu, C. (2018). Starch Deficiency Enhances Lipid Biosynthesis and Turnover in Leaves. *Plant Physiol*, *178*(1), 118-129. https://doi.org/10.1104/pp.18.00539

Zhang, X., Henriques, R., Lin, S. S., Niu, Q. W., & Chua, N. H. (2006). Agrobacterium-mediated transformation of Arabidopsis thaliana using the floral dip method. *Nat Protoc*, *1*(2), 641-646. https://doi.org/10.1038/nprot.2006.97

Zheng, Y., Pan, Z., & Zhang, R. (2009). Overview of biomass pretreatment for cellulosic ethanol production. *Int. J. Agric. Biol. Eng.*, *2*(3), 51-68.

Zhu, J. Y., Pan, X., & Zalesny, R. S., Jr. (2010). Pretreatment of woody biomass for biofuel production: energy efficiency, technologies, and recalcitrance. *Appl Microbiol Biotechnol*, *87*(3), 847-857. https://doi.org/10.1007/s00253-010-2654-8

Zoghlami, A., & Paes, G. (2019). Lignocellulosic Biomass: Understanding Recalcitrance and Predicting Hydrolysis. *Front Chem*, *7*, 874. https://doi.org/10.3389/fchem.2019.00874

Zuo, J., Niu, Q. W., & Chua, N. H. (2000). Technical advance: An estrogen receptor-based transactivator XVE mediates highly inducible gene expression in transgenic plants. *Plant J*, *24*(2), 265-273. https://doi.org/10.1046/j.1365-313x.2000.00868.x

Susana Perez Martinez
Department of Biology, University of Louisville
139 Life Sciences Building, Louisville KY 40292
Tel: 502-819-8444 (Cell phone)
Email: susanaperezmartinez@protonmail.ch

EDUCATION

PhD (Cellular, Molecular & Developmental Biology)   **2017-2022**
Dept. of Biology, University of Louisville, Louisville, KY, USA
Title: Functional role of PPAL and potential for moss in industrial applications

M.Sc. (Cellular, Molecular & Developmental Biology)   **2017-2019**
Dept. of Biology, University of Louisville, Louisville, KY, USA

B.A., Biology   **2013-2017**
Dept. of Biology, University of Louisville, Louisville, KY, USA

PROFESSIONAL EXPERIENCES

Research Mentor, University of Louisville   **2017-Present**
Trained and supervised undergraduate mentees in research projects
- Co-mentored undergraduate student Noela on the project "Prenylation in the moss Physcomitrella patens," Fall 2018.

- Mentored Amanda and Adam in "Arabidopsis fertilization study," Summer 2019

- Mentored Mikayla and Ephraim on the project "Analyzing Physcomitrella patens knockdown lines," Fall 2019.

- Mentored Matthew and Ahn on the project "Transformation of markers in Physcomitrella patens," Fall 2019.

- Mentored Christine on the project "Studying hormone responses in Physcomitrella patens," Fall 2020.

o Mentored Angelica and Riley on the project "Studying the cytoskeleton in Physcomitrella patens," Spring 2021

o Mentored Melissa on the project "Studying glucose response in Physcomitrella patens," Summer 2021

o Mentored Calvin on the project "Utilizing microscopy to characterize mutants," Fall 2021

o Mentoring Calvin and Melissa on the project "P. patens potential in the bioindustry," Spring 2022.

American Society of Plant Biologist (ASPB) Scholar   **October 2018-Present**
Access to many plants science resources
Networking with plant biologists
Write and publish articles in the ASPB Network
Access to career seminars and workshops

Faculty Search Committee Member   **2021-2022**

o Cross-functional Collaboration/Team
  - Collaborating with faculty, staff and graduate students from different departments and background to create, organize, and implement the action plan and strategies for hiring faculty

o Communication
  - Maintaining written and online communication with faculty and applicants
  - Serve as a committee liaison with faculty and graduate students to select an applicant that fits with the departmental culture

o Hiring Training
  - Reviewing and evaluating over 90 applicants
  - Identifying, recruiting, and selecting outstanding and diverse faculty to become part of the department community.
  - Ensure that applicants are treated with equity, fairness, and consistency
  - Creating a consistent interview-reviewing plan throughout the search process.

Research Grant Recipient, University of Louisville   **2019-2021**
Four Mentored Undergraduate Research and Creative Activities Grant
Each $1000 to me, $500 to undergraduate student

STEM Graduate Teaching Assistant Academy Participation   July 23-July 27, 2018
Learned about classroom teaching
Developed skills to create an active environment
Designed interactive classroom and lab activities that meet the student's needs
Micro-teaching activity

GMS Mentor and Advocate, many states in the US and Cuba   **2013-Present**

ESL teacher assistant   **2013-Present**
ESL Summer Programs at Newcomers Academy
Supported data collection and analysis for the program
Helped newcomer English Learners with reading and science classes

Dental assistant   **2016-2017**
ImmediaDent - Urgent Dental Care and Clear Choice Orthodontist
Responsible for seating patients, preparation, and sterilization of instruments, taking
impressions of teeth and handling requested instruments to the dentist

LAHSO Officer   **August 2013-2017**
The Latin American and Hispanic Student Organization, University of Louisville, KY
Planned officer's meetings as well as general body meetings
Elaborated cultural fairs, activities, and events

TEACHING EXPERIENCE

Guest Lecturer   **2018-Present**
Developmental Biology 443
Genetics 330
Intro to Biology 102

PROFESSIONAL PRESENTATION

Perez S and Running M.P.   **August 2019**
Functional role of PPAL in *Physcomitrium patens*. Plant Biology Conference San Jose,
California

Perez S and Running M.P.   **2018-2020**
Functional role of PPAL in *Physcomitrium patens*
Graduate Student Regional Research Conference, University of Louisville

Prenylation is Required for Establishment of Multicellularity and Cell Differentiation in *Physcomitrium patens*. Graduate Student Regional Research Conference, University of Louisville

OUTREACH PRESENTATIONS

"Failure is not an option." Newcomer Academy Shawnee High School in Louisville, KY	**2013-Present**
"Failure is not an option." Newcomer Academy JCPS Gheens Academy in Louisville, KY	**2013-Present**
"Failure is not an option." Newcomer Academy Phoenix School in Louisville, KY	**2013-Present**
"Failure is not an option." Oldham County High School Buckner, KY	**2019**
"Failure is not an option." Seneca High School in Louisville, KY	**2016-2018**
"Inspired by Science." Goldsmith Elementary School in Louisville, KY	**2015**
"Inspired by Science." Camp Taylor Elementary School in Louisville, KY	**2014**

COMMUNITY SERVICE/OUTREACH

Voluntary one-on-one conference with ESL students, Louisville, KY
2013-Present
Talks on how to adapt to a new country, language, and culture
Prepare them for the transition to a regular school
Talks about the importance of academic achievement, strong leadership, and community service

Voluntary Agricultural work
June 2013- July 2013
Holguin, Cuba
Collaborated in the Agricultural Program picking up and distributing crops, such as tomatoes, squash, corn, and potatoes. Involved in activities such as painting, decorating shelters, taking away the fungus from plants, feeding and caring animals, planting trees, and sanitation of the water

Childcare assistant teacher (80 hours)
June 2012 – July 2012
Wesley House Community Service Louisville, KY

Conducted activities such as, diapering children, feeding children, caring for children during naptime, and maintain hygienic conditions
Stimulated children through didactic games
Elaborated and Created teaching's materials

Tutor for Elementary students
2012- 2013
Goldsmith Elementary School Louisville, KY
Instructed students about correct spelling, decoding and pronunciation of sounds
Implemented continuous reading strategy for students Evaluated students' learning skills

RESEARCH PUBLICATIONS

Submitted Bao, L., Perez Martinez, S., Ren, J., Nguyen, M., Slawomir Slusarczyk, A., Thole, J.M., S., Huang, J., Fujita, T., and Running, M.P (2022). Cellular function of ROP GTPase prenylation is important for multicellularity in the moss *Physcomitrium patens*. Submitted to *Development*.

Published White, A.J., Perez Martinez, S., and Running, M.P. (2021). The Effects of PPAL-1 in Arabidopsis Gamete Development. *The Cardinal Edge* 1(1),11. DOI: 10.18297/tce/vol1/iss1/11

Manuscripts for Submission

Perez Martinez, S., Bao, L., and Running, M.P. The biological and developmental roles of PPAL in the moss *Physcomitrium Patens*

Perez Martinez, S. and Running, M.P. PpPPAL is needed to sense and respond to the available nutrient and energy status and to mediate glucose and hormone signaling in *Physcomitrium Patens*

Perez Martinez, S. and Running, M.P. Characterization of novel moss biomass, Physcomitrium Patens, as a candidate biomass feedstock for biofuel production

HONOR AND AWARDS

A&S McSweeny Fellowships Scholar (Full tuition plus Stipend)   **2020-present**

American Society of Plant Biologist (ASPB) Award	**October 2018- Present**
Undergraduate Mentored Research Grant Award	**2018-2019**
STEM GTA Academy Certificate	**July 23-July 27, 2018**
Outstanding Poster Presentation Certificate at GSRRC	**March 2018**
Three Minute Thesis Presentation Certificate at GSRRC	**March 2018**
Member of the National Society of Collegiate Scholars	**February 2014-Present**
Gates Millennium Scholar (10 years of full tuition &living expenses funding)	**June 2013- Present**
Migrant Network Coalition Scholarship Recipient (Amount: $300)	**June 2013- 2017**
Louis Edward Nicklies Scholarship Recipient (Amount: $750)	**July 2013- 2017**
Congressional Hispanic Caucus Institute Scholar	**2013-Present**
Member of the Latin American and Hispanic Student Organization	**August 2013-2017**
Louisville Urban Charles T Steele Scholarship Recipient (Amount: $ 1000)	**May 2013- 2017**
Recognition for volunteering at the English Language Learner Program	**2013-Present**
Jefferson County Board of Education Recognition	**May 2013**
Recognition for volunteering at Wesley House Community Center	**2012**
Certificate of Achievement: Brown-Forman INSPIRE Program	**June 2011- August 2011**
Certificate of Achievement: National Honors Society	**August 2011**